Characterization of Amyloid-β and Other Proteins Related to Alzheimer's Disease, their Role in Neurodegeneration and Biomarker Discovery

INAUGURALDISSERTATION

zur

Erlangung der Würde eines Doktors der Philosophie

vorgelegt der

Philosophisch-Naturwissenschaftlichen Fakultät

der Universität Basel

von

Andreas Güntert

aus

Böckten, Baselland

Basel 2006

Genehmigt von der Philosophisch-Naturwissenschaftlichen Fakultät

auf Antrag der Herren
Prof. Dr. M. Rüegg, Prof. Dr. Y.-A. Barde und Dr. B. Bohrmann.

Basel, den 4. Juli 2006

Prof. Dr. sc. techn. Hans-Jakob Wirz
Dekan

… to all my friends

ACKNOWLEDGEMENTS

The present investigation was carried out at F. Hoffmann-La Roche Ltd., Pharma Discovery Research Basel, Department Neuroscience, which made it possible for me to interact with various excellent scientists in the field. During my work, I encountered numerous people who provided essential help and supported me along the work in various ways. The interaction with you was stimulating and fun! Unfortunately it is not possible to mention you all by name.

However, I would like to specifically thank

- Dr. Bernd Bohrmann, project leader in Alzheimer's disease research and my supervisor - for your guidance, support, valuable advice and extensive discussions which made this thesis possible; for sharing your comprehensive knowledge and experience in the field with me.

- Professors Markus Rüegg and Yves-Alain Barde - for being my University mentors, faculty representatives and for your stimulating advice and discussions.

- Dr. Heinz Döbeli and Dr. Bernd Müller - for your ability to inspire, your encouragement and support and educating me in various ways.

- Dr. Christian Czech and Dr. Rodolfo Gasser - for fruitful discussions, general advice and sharing your experience.

- Françoise Gerber, Krisztina Oroszlan, Claudia Richardson, Fabienne Göpfert, Nicole Soder, Christian Miess, Daniel Röder and Jürg Messer - for your expertise, experimental support, your patience and enthusiastic participation.

- All other friends and colleagues at Roche - for your friendship, help, stimulating discussions and for sharing your experience and interests in all aspects of life.

- Simone Rudin - for making this work worthwhile and for the many hours of happiness together.

- Serge Corpataux, Bernhard Kohli and Steven Knecht - for all our discussions, support and your friendship.

- Pascal Beck, Jonas Köpfer and Pascal Geiger - for your ability to make me laugh and keep a reasonable life-work-balance; your deep friendship.

- Professor Theodor Güntert in his function as my advisor - for skilful guidance, endless discussions, critical review of any possible text or manuscript and for support in any kind of way one could think of.

- My parents, Theodor and Regina, and my little brother, Stefan - for all your love, fantastic support, for all our talks and sharing the good and the bad. Most importantly, for giving me the feeling of being something special.

TABLE OF CONTENTS

MANUSCRIPTS DISCUSSED

This thesis is based on the following manuscripts, either published and submitted or prepared for submission and referred to in the text by their Roman numerals [I – IV].

I. Pascal Rüfenacht, Andreas Güntert, Bernd Bohrmann, Axel Ducret and Heinz Döbeli
"Quantification of the Aβ peptide in Alzheimer's plaques by laser dissection microscopy combined with mass spectrometry"
J. Mass Spectrom. **40** (2005), 193 – 201

II. Andreas Güntert, Heinz Döbeli and Bernd Bohrmann
"High sensitivity analysis of Aβ composition in amyloid deposits from human and PS2APP mouse brain"
Neuroscience, in press

III. Andreas Güntert, Céline Adessi, Heinz Döbeli and Bernd Bohrmann
"Studying the role of pyroglutamate in Alzheimer's disease"
manuscript *prepared for submission*

IV. Andreas Güntert, Bernd Müller, Christian Miess, Nikos Berntenis, Françoise Gerber, Jürg Messer, Kristina, Oroszlan and Bernd Bohrmann
"Altered protein levels in Alzheimer's disease: a proteomic characterization"
submitted to *Neurobiology of Disease*

PATENT APPLICATIONS SUBMITTED

The findings in the present doctoral thesis led to a number of patent applications describing potentially useful biomarkers in Alzheimer's disease.

Authors:

Güntert A., Berntenis N., Bohrmann B., Miess C., Müller B.

European Application Numbers:

EP 06115015.7:	Cell adhesion and neurite outgrowth proteins as biomarker for Alzheimer's disease
EP 06115026.4:	Enzymes as biomarker for Alzheimer's disease
EP 06115035.5:	Cytoskeleton proteins as biomarker for Alzheimer's disease
EP 06115017.3:	Synaptic proteins as biomarker for Alzheimer's disease
EP 06115034.8:	Matrin-3 as biomarker for Alzheimer's disease
EP 06115041.3:	Transgelin-3 as biomarker for Alzheimer's disease
EP 06115043.9:	Programmed Cell Death Protein 8 as biomarker for Alzheimer's disease

ABBREVIATIONS

The following abbreviations are used in this thesis:

AD	-	Alzheimer's disease
Aβ	-	Amyloid beta peptide
APP	-	Amyloid precursor protein
BACE	-	Beta site APP cleaving enzyme
PS1 / 2	-	Presenilin 1 / 2
N3pE-42	-	Pyroglutamate 3 - 42
FAD	-	Familial Alzheimer's disease
CAA	-	Cerebral amyloid angiopathy
PA	-	Pathological aging
DS	-	Down Syndrome (Trisomy 21)
PHFs	-	Paired helical filaments
NFTs	-	Neurofibrillary tangles
CSF	-	Cerebrospinal fluid
CNS	-	Central nervous system
PS2APP	-	Employed double-transgenic mouse model with mutations in PS2 and APP genes
NSAIDs	-	Non-steroidal anti-inflammatory drugs
COX	-	Cyclooxygenase
ROS	-	Reactive oxygen species
CAMs	-	Cell adhesion molecules
MAP	-	Microtubule-associated protein
GFAP	-	Glial fibrillary acidic protein
PAD	-	Protein arginine deiminase
Hsp	-	Heat shock protein
LDM	-	Laser dissection microscopy
Lys-C	-	Lysyl endopeptidase
TCA cycle	-	Tricarboxylic acid cycle

PDH	-	Pyruvatedehydrogenase
MOMeNT	-	Microdissection of membrane-mounted native tissue
MS	-	Mass spectrometry
TOF	-	Time of flight
MALDI	-	Matrix assisted laser desorption ionization
SELDI	-	Surface enhanced laser desorption ionization
HPLC	-	High performance liquid chromatography
6-GuHe	-	6-guanidohexanoic acid – N-hydroxysuccinimide
LC/MS/MS	-	Liquid chromatography coupled with tandem mass spectrometry
SDS-PAGE	-	Sodium dodecyl sulfate polyacrylamide gel electrophoresis
MMSE	-	Mini Mental State Examination
ADAS-cog	-	Alzheimer's Disease Assessment Scale - cognitive subscale

SUMMARY

Studies were performed to identify factors explaining the difference in the neurodegeneration seen in Alzheimer's disease (AD) and in transgenic mice. A high level of neuronal loss is typically associated with AD, whereas in transgenic mice, this feature is only weakly displayed. Furthermore, the studies aimed at determining proteins occurring at altered levels in AD brains which could be involved in pathogenic mechanisms underlying the disease. The results of these investigations could help to identify Aβ variants and other proteins affecting the degree of neurodegeneration and would hopefully contribute to the development of biomarkers and new drug targets in AD.

Using laser dissection microscopy in combination with MALDI-TOF MS and urea-based Western blotting, the Aβ composition in morphologically differentiated plaque types from three different sources could be investigated: human brains from AD patients, pathologically aging (PA) individuals – i.e. individuals who form amyloid plaques, but suffer of no cognitive impairment - and from double-transgenic PS2APP mice. Diffuse plaques are found in human AD and PA, as well as in PS2APP transgenic mice and were previously suggested to be the initially occurring plaque type. We detected almost exclusively Aβ 42 in diffuse plaques. This Aβ variant was shown to be prone to aggregation. Furthermore, no differences in the Aβ species composition between diffuse plaques from AD and PA individuals were detected. Cored plaques, the main plaque type in AD, contain also predominantly Aβ 42, whereas compact plaques, which sporadically occur in human but are found more frequently in PS2APP mice, consist of Aβ 40. This has implications on the putative evolutionary path of plaque formation: Due to the Aβ composition of the respective plaque types, a sequential maturation of diffuse plaques over compact to cored plaques can be excluded. Our data support the concept that diffuse plaques are the initially occurring plaque type and develop independently to compact or cored plaques. The Aβ composition of vascular amyloid was also investigated. Here, we detected high amounts of Aβ 40, which is consistent with previous findings using C-terminal specific antibodies.

Aβ in human plaques and to a considerably lesser extent in plaques from PS2APP mice is N-terminally truncated. The investigation of different Braak stages revealed an increasing amount of N-terminally truncated Aβ variants accompanying disease progression, indicative for

a successive modification by exoproteases upon deposition. Consistently low levels of N-terminally truncated Aβ forms were detected in diffuse plaques, which further support the view of diffuse plaques being at the beginning of the plaque maturation process. The major N-terminally truncated Aβ variant detected by MALDI-TOF MS in human cored plaques was pyroglutamate 3-40 / 42. To corroborate these findings, Western blotting and immuno-histochemistry were applied and the existence of pyroglutamate in all types of plaques in human AD and PS2APP transgenic mice was shown.

The rate of aggregation of an Aβ variant is likely to be important for initial deposition of amyloid into plaques. To test the aggregation and toxicity properties of pyroglutamate 3-42, *in vitro* experiments were performed on PC12 and hippocampal cell lines comparing synthetic pyroglutamate 3-42 with Aβ 1-42. These experiments showed a considerably lower rate of aggregation for synthetic pyroglutamate 3-42 when compared to Aβ 1-42. Our experiments suggest that pyroglutamate 3-40 / 42 alone is probably not a critical seed for plaque formation. The cytotoxicity of Aβ peptides is correlated with the aggregation state. Synthetic pyroglutamate 3-42 *in vitro* showed a significantly reduced toxicity when compared to Aβ 1-42.

Cross-linking of Aβ fibrils in plaques was investigated with solubility experiments. It was found that Aβ in human plaques is cross-linked to a higher extent than Aβ in plaques from PS2APP transgenic mice. A higher degree of cross-linking in human Aβ was also indicated by our MALDI-TOF MS analysis. The high level of cross-linking may result in a hampered clearance of Aβ from the brain in AD patients. Taken together, enhanced levels of post-translational modifications in human plaques, i.e. cross-linking and N-terminal truncation of Aβ peptides, may lead to their reduced clearance from the brain.

The methodology used in our experiments allowed to discriminate between oxidized and reduced Aβ species. Diffuse plaques in PA were shown to contain a large proportion of oxidized Aβ, which could indicate a protective response in these brains and which would explain the lack of clinical symptoms in these individuals.

To determine, whether the amyloid load in plaques may contribute to the high level of neuronal loss observed in AD as opposed to transgenic PS2APP mice, ^{15}N-labeled Aβ 1-42 was used and the quantitative amyloid load in plaques from human AD and PS2APP mice was compared by MALDI-TOF MS. Roughly comparable amounts of Aβ in both species were found.

Therefore, we conclude that a dose-effect of Aβ alone can not account for the higher level of neurodegeneration observed in AD patients than in PS2APP mice.

Using LC/MS/MS the identification of additional proteins involved or affected in the pathogenesis of AD was aimed at. A comparison of the proteome in AD brain with control tissue was based on the analysis of over 2000 proteins. Proteins generally accepted to be related to AD like Aβ, apolipoprotein E, heat shock protein 90, glial fibrillary acidic protein (GFAP) and tau were detected at increased levels in AD. Numerous proteins previously tentatively implicated with the disease were identified at aberrant levels in AD. We found proteins indicative for an enhanced susceptibility to oxidative stress (e.g. decrease of peroxiredoxin 5), an impaired glucose metabolism (decrease of enzymes involved in citrate cycle), cytoskeletal derangement (e.g. decrease in alpha-internexin), synaptic dysfunction (e.g. decrease in presynaptic density protein-95, syntaxin-1A and synaptotagmin-1), an activation of the ubiquitin proteasome system (increase in ubiquitin), deficits in the neuritic network (decrease of various cell adhesion molecules) and membrane trafficking (e.g. decrease in AP-180), as well as altered levels of enzymes involved in the hyperphosphorylation of tau (e.g. decrease in phosphatase-2A).

Most notably, we detected 18 new proteins previously not associated with the disease, which occurred at altered levels in AD. These are the synaptic proteins synaptogyrin-1 and -3, myelin associated glycoprotein, myelin oligodendrocyte glycoprotein, contactin-1, contactin-2, neurexin IV and claudin-11 involved in cell adhesion, the chaperone protein Hsp 75, plectin 1, ankyrin, α-adducin and microtubule-associated protein RP/EB family member 3 as structural cytoskeletal proteins, peroxiredoxin 5 and microsomal glutathione S-transferase 3 for the protection against oxidative stress and programmed cell death protein 8, matrin-3 and transgelin-3, whose functions are not known. The findings obtained by LC/MS/MS were confirmed by immunohistochemistry and Western blotting for selected proteins, thereby providing a first validation of some of the proteins found at aberrant levels in AD. Interestingly, we were able to authenticate decreased levels of syntaxin-1A and reticulon-1 and increased synaptogyrin-1 levels in AD using confocal microscopy.

The identification of proteins involved in the processes finally leading to neurodegeneration and cognitive deficits associated with AD could lead to the development of biological markers for the disease. Such biomarker candidates found at altered levels in AD brain tissue could possibly be reflected in the cerebrospinal fluid (CSF) and eventually in the periphery and may be explored for their value as drug targets or markers for diagnosis, disease progression

or even responsiveness to treatment. The results from our studies indicate pathways which appear promising in such a quest.

INTRODUCTION

Molecular background on Alzheimer's Disease

Alois Alzheimer, a Bavarian psychiatrist, described at a meeting in 1906 a clinicopathological syndrome, which has emerged as the most common type of dementia in the elderly today. Alzheimer's original patient, a woman referred to as Auguste D., exemplified several cardinal features of the disorder that are valid in patients nowadays: progressive memory impairment, disordered cognitive function, altered behavior including paranoia, delusions and loss of social appropriateness, as well as a progressive decline in language function. The neuro-pathological investigation of the brain showed the cerebral cortex to be considerably shrinked (Figure 1).

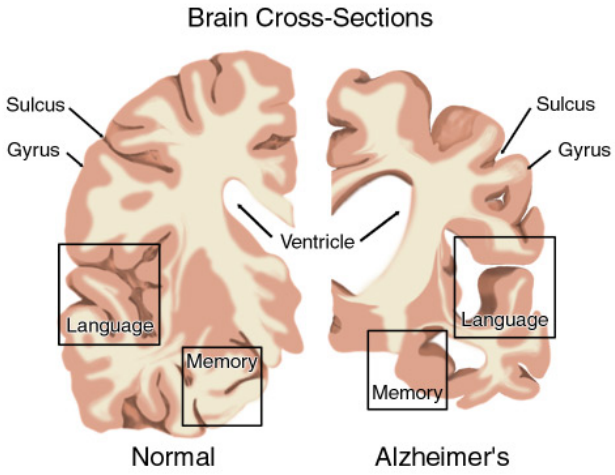

Figure 1. Cross-section of the brain from a normal individual (left) and from an AD patient (right). In Alzheimer's disease, there is an overall shrinkage of brain tissue. The sulci are noticeably widened and shrinkage of the gyri can be observed. In addition, the ventricles, or chambers within the brain that contain CSF, are noticeably enlarged.
Source: http://www.ahaf.org/alzdis/about/BrainAlzheimer.htm

Alzheimer noted two further abnormalities in the brain. The one being senile plaques, a structure previously described in the brain of elderly people. The other abnormality was neurofibrillary tangles (NFTs) in histological material from her cerebral cortex, a fiber structure of the nerve

cells. The nerve tangling had not been previously described, and it was mainly this abnormality that defined the new disease. For many decades after Alzheimer's original description, little progress in defining the pathogenesis of Alzheimer's disease (AD) occurred. With the advent of electron microscopy in the 1960s, the two lesions originally described by Alzheimer then became subject to intensive research; although considerable progress in the understanding of the disease has been made in recent years, these key changes are still under investigation today.

Senile plaques are extracellular deposits of the amyloid-β peptide (Aβ) (Glenner et al., 1984), which is formed after a sequential cleavage of the amyloid precursor protein (APP), a membrane-spanning glycoprotein (Kang et al., 1987, Tanzi et al., 1987), by β- and γ-secretases. β-secretase is a type I transmembrane glycosylated aspartyl protease, whereas the γ-secretase complex consists of at least four proteins, including presenilin-1 and -2 (Nunan and Small, 2000, Haass, 2004). The normal functions of APP are not fully understood, but increasing evidence suggests that it has important roles in regulating neuronal survival, neurite outgrowth, synaptic plasticity and cell adhesion (Mattson, 1997). Due to heterogeneous cleavage sites of γ-secretase on APP, a series of Aβ peptides, including the major variants Aβ 1-40 and Aβ 1-42, are produced and deposited in senile plaques principally in a filamentous form as amyloid fibrils. The two Aβ peptides differ in their neurotoxicity, solubility and their tendency to undergo fibrillogenesis, with Aβ 1-42 being more toxic and more prone to aggregation (Jarrett et al., 1993, El-Agnaf et al., 2000). Senile plaques are associated with axonal and dendritic injury and are generally found in large numbers in the limbic and association cortices. Several genes have been implicated in AD in humans, most notably those encoding APP and its processing proteases, which cause early-onset familial AD (FAD) when mutated (Selkoe, 2001a). In addition, the ε4 allele of apolipoprotein E was identified as a genetic risk factor for AD, increasing the risk of developing the disease considerably (Tanzi et al., 1996). An excellent source of current information on genetic variants associated with AD provides the AlzGene website (www.alzforum.org/res/com/gen/alzgene/default.asp). The identification of genes involved in AD ultimately allowed the development of transgenic mouse models, harboring various mutations in these genes. A mouse model that reflects all aspects of AD has not yet been produced, but some transgenic mouse lines provide highly useful phenotype(s) reproducing AD relevant features (McGowan et al., 2006).

Based upon the two diagnostic features displayed in AD brains, the amyloid cascade hypothesis and a model of neurodegenerative tauopathies were developed and provide a framework for the study of AD pathogenesis. Soon after the discovery of mutations in the APP gene in FAD, the amyloid cascade hypothesis was proposed (Hardy and Higgins, 1992, Selkoe, 2001a, Hardy, 2006). Basically, this hypothesis states that altered APP expression/proteolytic processing or changes in Aβ stability/aggregation result in a chronic imbalance between Aβ production and clearance. Gradual accumulation of aggregated Aβ initiates a complex, multistep process that includes gliosis, inflammatory changes, neuritic/synaptic change, neurofibrillary tangles, reduction in neurotransmitters and finally neurodegeneration and neuronal cell death. Central to this hypothesis is the observation that the vast majority of mutations causing FAD increase the amount of fibrillogenic Aβ 42. In addition, transgenic mouse models expressing pathogenic mutations of APP and presenilin-1 have increased levels of Aβ and amyloid plaques (Hsiao et al., 1996). Furthermore, individuals with trisomy 21 have 3 copies of APP and develop advanced AD usually within the fourth decade of life (Mann, 1988).

NFTs are intraneuronal lesions primarily composed of paired helical filaments (PHFs), which consist of hyperphosphorylated protein tau. It is known that normal tau binds and stabilizes microtubules thereby maintaining the network of microtubules that are essential for axonal transport in neurons. Moreover, the phosphorylation of tau prevents the binding of tau to microtubules. Neurodegenerative tauopathies suggest that the conversion of normal tau into hyperphosphorylated tau results in a loss of tau function, which leads to a depolymerization of microtubules, thereby impairing axonal transport followed by neuronal dysfunction and neurodegeneration (Lee and Trojanowski, 1992, Iqbal et al., 2005, Lee et al., 2005). The distribution of neurofibrillary tangles spreads as the severity of Alzheimer's disease increases and it has been proposed that the concomitant loss of synaptic density is likely to have a more immediate relationship to dementia in Alzheimer's disease than does amyloid accumulation. However, Thal and colleagues showed that Aβ deposition in the brain follows a distinct sequence in which the regions are hierarchically involved and that phases of Aβ deposition are very predictive and correlative to disease progression of AD (Thal et al., 2002). Because brains from cognitively normal, pathologically aged individuals were found to display an extensive amyloidosis without concomitant tau pathology, it could be suggested that NFTs are ultimately responsible to induce the cognitive deficits. On the other hand, studies with transgenic mice

showed that Aβ immunotherapy reduced not only extracellular amyloid plaques, but most notably lead to the clearance of early tau pathology. It was shown that Aβ deposits were cleared first and subsequently reemerged prior to the tau pathology, indicative of a kind of hierarchical and direct relationship between Aβ and tau (Oddo et al., 2004). The explicit relation between Aβ deposition and tau pathology is not clear yet, but tau aggregation has many consequences for the neuron and is probably the final common cause of neurodegeneration in AD, and in the other tauopathies such as frontal lobe dementia and progressive supranuclear palsy. However, the molecular mechanism leading from Aβ accumulation with plaque deposition to tau accumulation and neurodegeneration with cognitive deficits are not fully elucidated at the molecular level.

A more recent hypothesis suggests that soluble oligomers are the toxic species with a substantial impact on synaptic function and neurodegeneration. A growing number of *in vitro* and *in vivo* studies suggest that soluble oligomeric peptides with high β-sheet content are toxic to neuronal cells and cause their dysfunction and death. According to this hypothesis, the sequestering of soluble Aβ into amyloid fibrils and the deposition in plaques may present a protective response of the brain that delays neurodegeneration (Watson et al., 2005). Recently, soluble Aβ-oligomers of 56 kD were detected in Tg2576 mice and were shown to contribute to cognitive deficits associated with AD (Lesne et al., 2006).

Additionally, emerging evidence indicates that intraneuronal Aβ plays a pathophysiological role in the progression of the disease (Tseng et al., 2004). It has been shown in a triple transgenic mouse model that the first pathological manifestation is the accumulation of intraneuronal Aβ (Billings et al., 2005) and that a progressive decrease in the intraneuronal Aβ pool goes along with an increase in extracellular plaque load (Oddo et al., 2006). Therefore, intraneuronal Aβ may serve as a source for some of the extracellular amyloid deposits. However, there is no doubt that extracellular Aβ accumulation in form of neuritic plaques contributes to AD pathology and induces a microglia-mediated chronic inflammation with devastating consequences.

The co-incidence of amyloid plaques with AD poses the question, whether plaques are the cause or a consequence of the disease. The fact that Aβ was shown to be toxic *in vitro* supports the view of a causative role. Therefore, the observed neuronal cell death in AD may be the destructive effect of plaque-related Aβ on the adjacent neuronal cell bodies or processes such

as dendrites or synapses. It was shown that Aβ peptides undergo extensive N- and C-terminal truncation, occur in oxidized forms and are subject to post-translational modifications. Enhanced Aβ synthesis rates coupled with decreased degradative enzyme production (Selkoe, 2001b) and posttranslational modifications that slow down or inhibit proteolysis like pyroglutaminated or cross-linked Aβ peptides, may all enhance amyloid deposit formation and subsequent neurodegeneration, although the degree of neuronal and synaptic losses not always correlates with the amyloid plaque burden (Walsh et al., 2002). Transgenic mice lack the extensive neurodegeneration associated with AD (King and Arendash, 2002, Higgins and Jacobsen, 2003, Hu et al., 2003). Considering the low level of neuron loss observed in many of the transgenic AD models, the question arises whether differences in the plaque amyloid load, in plaque-comprising Aβ variants, its oxidation state or post-translational modifications of Aβ in plaques can be detected in AD and may ultimately be responsible for the differing level of neurodegeneration observed.

Not much is known about the events leading to deposition and formation of senile plaques. Several plaque types are described and different ways of their formation were proposed (Armstrong, 1998). The hypothesis of a sequential evolution and time-dependent modification of plaques stems from the immunohistochemical evidence that fibrillogenic Aβ 1-42 is the main Aβ component in early diffuse plaques in AD and Down Syndrome (DS) (Iwatsubo et al., 1994, Iwatsubo et al., 1995). A further accumulation and aggregation of secreted Aβ may then result in mature amyloid plaques of various shapes, which represent different stages in the life history of senile plaques. Another theory suggests that different types of amyloid plaques, e.g. compact and cored plaques, form independently and not sequentially. The process of plaque formation and evolution is not solved yet, even though evidence (Armstrong, 1998) hints to an independent and not sequential plaque development. A specific combination of proteinous factors, like different Aβ variants, modifications or other plaque associated proteins, possibly influence and determine the evolution of diffuse plaques to the respective matured plaque types. It is known, that apart from Aβ, several other proteins were described to be associated with amyloid plaques. Among them, apolipoprotein E is the best characterized and its involvement in fibrillization and plaque formation was demonstrated (Wisniewski et al., 1994, Dickson et al., 1997). The elucidation of plaque development is important and is likely to reveal steps in the maturation process, which can serve as drug targets and may be influenced to slow down the disease progress.

Secondary to the deposition of amyloid in plaques and the formation of NFTs, various other biochemical processes occur during the onset and the progression of the disease. Various proteomic attempts have been undertaken to elucidate the pathways affected by the disease (Schonberger et al., 2001, Tsuji et al., 2002); several genetic approaches were also taken (Loring et al., 2001, Ho et al., 2005). The abnormally expressed proteins / genes that were found are in principle indicative for neurodegeneration and nerve cell loss, an inflammation response of the brain, oxidative stress and an impaired glucose metabolism. For a better understanding of the disease and improved therapeutic modalities it is necessary to reveal the proteins and processes involved, because through this knowledge reliable biomarkers and effective disease modifying drugs can be generated.

Biomarkers for Alzheimer's disease

AD is a common disease but a definitive diagnosis can still only be made by a postmortem assessment of brain neuropathology. Hence the necessity of a biological marker for AD is obvious (Lovestone, 2006). Such a marker should meet several criteria as outlined by the Ronald and Nancy Reagan Research Institute and the NIA Working Group report (1998). According to these specifications, a biomarker is "a characteristic that is objectively measured and evaluated as an indicator of normal biological processes, pathogenic processes, or pharmacological responses to a therapeutic intervention."

It is difficult to follow AD progression or monitor response to treatment and to date, no pre-symptomatic biomarker for AD is available. By the time AD is clinically apparent, the disease is already well-established, limiting the possible effectiveness of any therapeutic intervention designed to slow progression by reducing pathological processes (see chapter 'Development of therapeutic agents for Alzheimer's disease' below). The diagnosis of AD is currently based on cognitive tests and behavioral analysis. Thus, the MMSE (Mini Mental State Examination) and the ADAS-cog (Alzheimer's Disease Assessment Scale - cognitive subscale) remain the most widely used measures of cognitive change and drug trial efficacy in clinical practice. Both MMSE and ADAS-cog, and all similar memory measures, are subject to learning effects and critical in utility if they are used repeatedly in a patient. Both clinical practice and clinical trials would be much enhanced by a quantitative biomarker usable for diagnosis or

disease progression. A biomarker is clearly needed also for drug development, be it in drug discovery and in preclinical or in early to late phase clinical development.

Considerable progress in the search for a biomarker has been made with markers derived from the well known pathological lesions using a variety of techniques to investigate biochemical changes in the cerebrospinal fluid (CSF), blood and other tissues and fluids. The most promising sources for biomarkers in AD are the CSF or blood plasma, because compared to brain tissue, these fluids are more easily accessible and, in case of CSF, in close contact with the central nervous system, where the key biochemical changes take place. Several biomarkers were suggested like CSF total-tau (Andreasen et al., 1998) and phospho-tau (Parnetti et al., 2001) levels, CSF Aβ 1-42 levels (Andreasen and Blennow, 2002) or a combination thereof (Andreasen et al., 2003). In addition, numerous proteins expressed at aberrant levels in AD were identified (Vercauteren et al., 2004). However, a considerable amount of work is required to progress any of these putative markers to the point where they may be useful as surrogates for diagnostics and monitoring disease modification trials.

Therapeutic approaches for treatment of Alzheimer's disease

Due to the prevalence of AD today and the prospect of a rapidly growing disease population due to increased life expectancy, there is an unmet medical need for therapeutic interventions. To date, no treatment approach has been clinically proven to modify the disease process in a way that significantly slows or prevents its progression. However, at the present time, there are some pharmacological agents that may ameliorate or temporarily suppress certain symptoms. Acetylcholine esterase inhibitors like tacrine, donezepil, rivastigmine and galanthamine may cause a delay of the decline (Doody, 2003), but a clear demonstration that these drugs significantly affect the disease course itself is not obtained. Currently, several strategies for the development of a disease modifying agent are pushed forward:

Inhibition of β-secretase – β-secretase, often referred to as BACE (beta-site APP cleaving enzyme) is an attractive target for therapies aiming at modifying the course of AD, as this enzyme initiates and is the rate limiting step in the formation of Aβ (Vassar, 2001). The molecular sequence and crystal structure of the key protease have been identified (Hong et al.,

2000) and the development of specific β-secretase inhibitors is being actively pursued (John, 2006). The observation that BACE1 knockout mice do not generate any Aβ (Roberds et al., 2001), supports the validity of the target. Importantly, these mice appear to be healthy, with no obvious neurological and behavioral abnormalities. However, up to now the compounds found to inhibit β-secretase are either not specific enough or are too large for crossing the blood brain barrier after their peripheral administration.

Inhibition of γ-secretase – The screening of compound libraries revealed a substantial number of compounds of different structural classes that appeared to inhibit the activity of γ-secretase (Dewachter and Van Leuven, 2002). One of the problems that emerged was the similar proteolytic processing of APP and the Notch receptors and the associated difficulty to reduce Aβ production without significantly interfering with the functions of Notch signaling in adults. Notch functions include a variety of cell fate decisions necessary for the proper differentiation of several cells.

A different approach to avoid amyloidogenic Aβ 1-42 is to shift the cleavage specificity of γ-secretase away from position 42, without altering overall Aβ levels. It was suggested that certain members of the non-steroidal anti-inflammatory class of drugs (NSAIDs), may induce such a shift if administered at appropriate doses (Townsend and Pratico, 2005). NSAIDs are also used to interfere with the chronic inflammatory reaction that takes place in AD. The best-characterized action of NSAIDs is the inhibition of cyclooxygenase (COX) (Hoozemans et al., 2003). However, the doses of NSAIDs used to date are very high and more work is needed to determine whether chronic NSAID administration could have true therapeutic benefit.

Immunological approach – The immunological strategy involves either a classical vaccination with Aβ in order for the host immune system to generate anti-Aβ antibodies or providing antibodies passively. In both cases, the primary function of the antibodies is binding to its target, i.e. Aβ, thereby enhancing the clearance and/or preventing the deposition of Aβ in plaques. Active immunization with Aβ 1-42 was initially shown to be able in clearing pre-existing Aβ deposits and also in preventing the development of new Aβ plaques and associated neuropathology in transgenic mouse models of AD (Schenk et al., 1999). Furthermore, the reduction in Aβ burden is accompanied by improved cognitive performance.

Several hypotheses how anti-Aβ antibodies may work therapeutically are discussed. It was suggested, that the antibody could enter the brain and bind to Aβ plaques (Bard et al., 2000) and/or shifts the CNS - plasma Aβ equilibrium by acting as peripheral sink (DeMattos et al., 2001).

The approaches currently undertaken for drug discovery in AD follow predominantly the concept of the amyloid cascade hypothesis. The overall aim of the attempts is to lower the amyloid brain burden, either by modifying APP processing enzymes or by directly targeting amyloid plaques in the brain. For this reason, a deeper understanding of Aβ variants deposited in plaques – one topic of this thesis – is of considerable interest and is fundamental for the development of amyloid targeting drugs. Since preclinical drug development relies on animal models, the knowledge of the comparative Aβ plaque composition in AD and the investigated PS2APP transgenic mice is of special importance. Substantial differences in the nature and amount of Aβ peptides could affect the translation of preclinical data into the clinics. This is especially relevant for immunotherapeutic approaches which utilize the binding of antibodies to amyloid plaques and a detailed knowledge of occurring Aβ variants is essential. The observed difference in the degree of neuronal cell loss between AD patients and transgenic animal models, which is extensive in AD, but limited in transgenic mice, offers to study Aβ plaque composition and identify Aβ modifications, which might impact on neurodegeneration in AD. Identification of proteins other than Aβ involved in biochemical processes affected by AD, might further enrich this knowledge and could reveal biological markers and drug targets unrelated to Aβ.

AIMS OF THE INVESTIGATION

The key aims of this thesis were to determine proteomic factors involved in neurodegeneration. Aβ variants including post-translational modifications were determined in AD and double-transgenic PS2APP mice, in order to possibly explain the observed differences in neuronal cell loss in human patients and the transgenic animals. By investigation of proteins beyond Aβ it was expected to get insight into additional pathways involved in disease progression in AD brains opening the possibility to identify biomarkers and new drug targets.

Four specific steps were taken; each step is described in a stand-alone manuscript (*one published [I], two submitted [II, IV] and one prepared for submission [III]):*

- Quantification of the amyloid load in plaques from AD and PS2APP mice and a detailed physico-chemical analysis of Aβ in deposited amyloid plaques [**I**]

- Identification of early, disease-relevant Aβ species in AD with impact on neurodegeneration and comparison to PS2APP mice and pathological aging individuals [**II**]

- Identification of pyroglutamate as a component of senile plaques in AD and PS2APP mice, and *in vitro* aggregation and toxicity studies with synthetic N3pE-42 [**III**]

- Proteomic comparison of AD and control brain tissue: Determination of affected biochemical pathways and identification of potential biomarkers [**IV**]

METHODOLOGY AND TOOLS

Detailed information concerning patients, animals, material and methods is given in the individual papers. In the following an overview spanning across all four approaches of the experimental work is presented.

Human brain tissue and transgenic mice

Human brain tissue from eight different individuals was used [I-IV]. The brain tissue was collected approximately two hours postmortem and was immediately frozen at -80°C. Brains were neuropathologically staged according to Braak (Braak and Braak, 1991). The age of the patients ranged from 77 to 89 years, five female and three male patients were used for investigation. The available brain tissue bank allowed to investigate AD brains with different Braak stages from IV to VI and to compare with controls and pathological aging (PA) individuals. Individuals with Braak stages V and VI showed heavy, with Braak stages IV and PA cases moderate plaque load. Individuals with Braak stage II were used as controls and did not exhibit amyloid plaque pathology. Differences in the amyloid composition of plaques from different Braak stages could hence be correlated to disease progression.

Additionally, brain tissue from six PS2APP double-transgenic mice (Richards et al., 2003) at an age of 8 and 20 months was employed [I-III]. PS2APP mice overexpress mutant forms of human presenilin 2 (N141I) and human APP (K670N, M671L). The animals develop an age-related cognitive decline associated with severe cerebral amyloidosis. Additionally, an inflammation response in discrete brain regions, and behavioral changes, evaluated by the Morris water maze and active avoidance tests, were observed. Neuronal cell loss in transgenic mice in general is observed only to a small extent, but the employed transgenic PS2APP mouse model exhibits many of the features typical for AD and was therefore considered as a suitable tool to investigate the role of amyloid and plaques in AD.

Histochemistry

Frozen brain tissue was used and sections of 10 - 30 μm from AD and PA individuals, as well as from PS2APP mice were cut with a cryostat microtome. Subsequently, the brain sections were stained with different antibodies at a concentration of 1 – 10 μg/ml.

Using anti-Aβ antibody and thioflavine S, vascular amyloid, diffuse plaques, compact plaques and cored plaques could be distinguished according to their morphology and staining properties [I-II]. These different plaque types were isolated using laser dissection microscopy and the Aβ composition thereof was determined using MALDI-TOF MS and urea-based Western blotting. In addition, using a pyroglutamate specific antibody, the localization of pyroglutamate in plaques from human AD brains and PS2APP mice was traced [III].

Antibodies against proteins other than Aβ and identified at aberrant levels by LC/MS/MS were used to reveal co-localization of the respective proteins with amyloid-plaques and reactive astrocytes or to determine an abundance difference between AD and control tissue [IV].

Laser dissection microscopy

Laser dissection microscopy (LDM) is the non-contact laser microdissection of membrane-mounted native tissue (MOMeNT). The method allows the isolation of a microscopic area with high precision (Simone et al., 1998), whereas the surrounding tissue remains intact and the excised area retains its morphological structure. LDM can be used to obtain a highly homogenous sample set, e.g. the accumulation of specific cell or plaque types, and enhances the opportunities for the molecular analysis of pathological processes significantly. The usefulness of LDM in AD was shown for the isolation of thousands of plaques and subsequent analysis by mass spectrometry (Liao et al., 2004, Miravalle et al., 2005). Within this thesis, LDM was employed to isolate specifically different types of amyloid plaques or vascular amyloid after (immuno-) histological differentiation [I-III] for subsequent analysis by MALDI-TOF MS or urea-based Western blotting. The methods of analysis were refined to maximize sensitivity. Highest possible sensitivity was aimed in order to allow characterization of minute amounts of homogeneous plaque types, rather than averaging the senile plaque load by the analysis of brain

homogenates. Depending on the isolated plaque type, the species and the method of further analysis, different numbers of amyloid plaques were required: required plaque numbers ranged from as little as one single PS2APP compact plaque to 10-20 human cored and diffuse plaques for analysis by urea-based Western blotting, whereas 30 PS2APP compact plaques, 50 cored plaques and 100 diffuse plaques from human AD were needed to surpass the detection limit of the MALDI-TOF mass spectrometer.

Western blotting

Conventional SDS-PAGE and Western blotting was modified according to Ida and colleagues (Ida et al., 1996) to enhance sensitivity. The method was used to determine solubility differences between human and PS2APP mouse plaques [I], quantify plaque derived Aβ in human and PS2APP mice [I], in the sample preparation procedure for LC/MS/MS to separate brain proteins [IV], as well as to compare protein levels between AD and control tissue [IV].

High sensitivity urea-based Western blotting allowed the separation of full length Aβ peptides, e.g. Aβ 1-40 and Aβ 1-42, at a detection limit of 1-2 fmol (Klafki et al., 1996, Wiltfang et al., 1997) [II-III]. Additionally, it enabled to discriminate between the oxidized and reduced forms of Aβ 40 and 42.

MALDI-TOF MS

MALDI-TOF MS measurements [I-III] were performed on a Bruker UltraFlex TOF / TOF mass spectrometer in reflector mode using standard operating parameters. Peptide sequencing by tandem mass spectrometry [I] was performed on the same instrument operated in the LIFT mode according to the manufacturer's standard operating parameters.

Analysis of plaque constituting Aβ variants was done using a protocol that includes endoproteinase Lys-C digestion of Aβ peptides. The cleavage of Aβ by Lys-C generates three fragments, whereas the C-terminal fragment could not be detected probably due to its hydrophobicity. For detection of the C-terminal Aβ fragment, an ionization modifier, 6-

guanidohexanoic acid – N-hydroxysuccinimide (6-GuHe), was developed. 6-GuHe enabled identification of the C-terminal fragments and discriminating of oxidized and reduced forms [II]. The digestion with Lys-C was performed for enhanced sensitivity and the resulting peptides could be detected with a sensitivity of ~ 200 - 300 fmol.

The use of ^{15}N-labeled Aβ 1-42 allowed quantification of plaque derived Aβ in human and PS2APP mice in a highly accurate manner [I].

LC/MS/MS

Liquid chromatography combined with tandem mass spectrometry is a technique that couples solute separation by HPLC, with detection of column effluent by mass spectrometry. This allows the analysis of thousands of proteins from a complex protein mixture even at concentrations in the femto- or sub-femtomolar range. The LC/MS/MS technique was demonstrated to be suitable for proteomic characterization in various fields, like cancer research (Baker et al., 2005, Gagne et al., 2005), glycoproteomic analysis (Hashii et al., 2005, Wuhrer et al., 2005) or AD (Liao et al., 2004). In our studies, LC/MS/MS was used for the comparison of protein levels in grey matter from severe AD and control tissue [IV]. More than 2000 proteins from less than 1 mg brain tissue were identified and compared in a semi-quantitative manner. Numerous proteins with significantly altered levels in AD were detected and identified using the HumanGP protein library. Among known AD-related proteins like Aβ, tau, GFAP, ubiquitin and apolipoprotein E, a total of 18 new proteins were detected which previously had not been associated with the disease.

SELDI-TOF MS

This technology is suitable to perform mass spectrometric analysis of protein mixtures retained on chromatographic chip surfaces. Preactivated surfaces allow coupling of antibodies to the spot surfaces, generating user-defined arrays. The skills of handling the chips were acquired in the laboratory of Prof. Dr. med. Jens Wiltfang in Erlangen, Germany and aimed to specifically analyzing full-length Aβ isolated from laser dissected plaques. The analysis of synthetic Aβ and

PS2APP mouse brain homogenates of 20 month old mice was done for setting up the methodology. Brain homogenates contain large amounts of Aβ and several C-terminal truncated Aβ forms were detected (Figure 2). However, even though we were able to detect the main Aβ species in vascular amyloid and cored amyloid plaques, namely Aβ 1-40 and Aβ 1-42, it was not possible to identify N-terminally and other C-terminally truncated Aβ species due to sensitivity limitations. It is likely, that the sample preparation procedure, which included formic acid treatment, interfered with the binding of Aβ to its antibody on the chip surface.

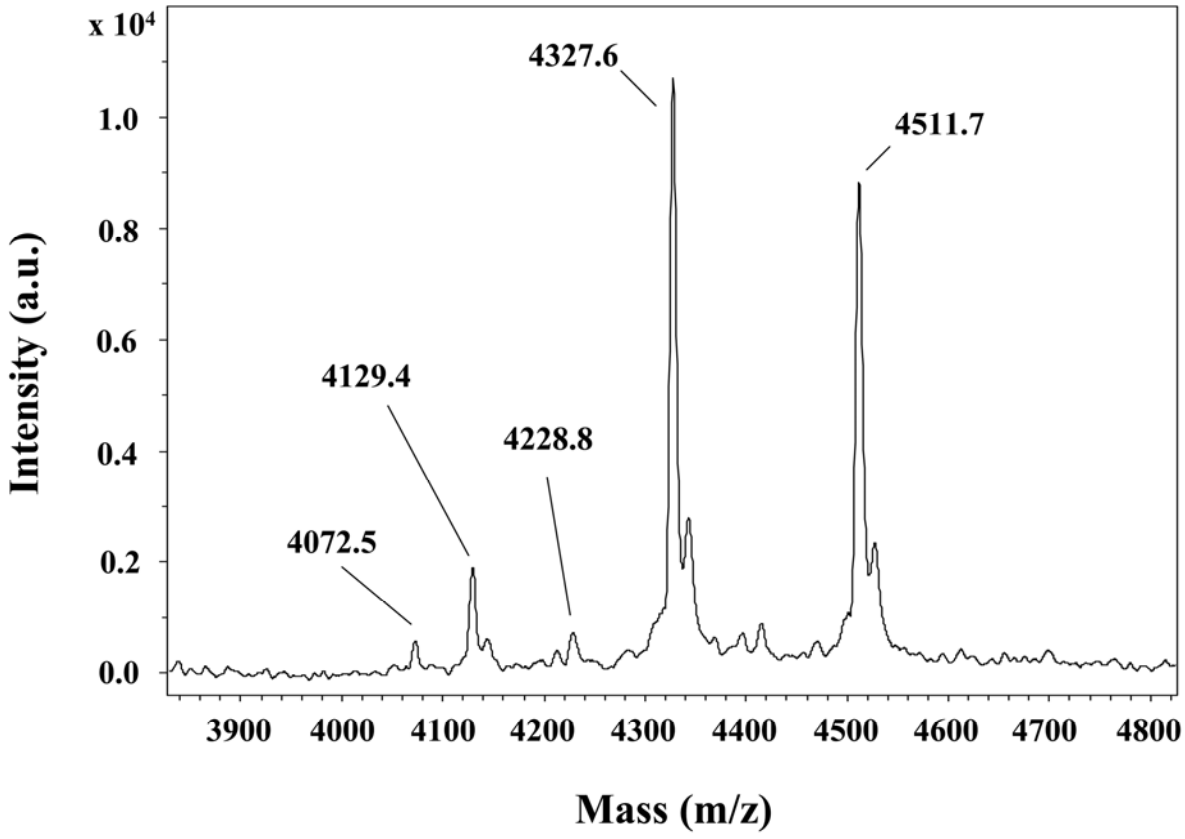

Figure 2. SELDI-TOF MS analysis of PS2APP transgenic mouse brain homogenates.
Using an Aβ specific antibody, a series of Aβ peptides were detected, including Aβ 1-37 (m/z 4072.5), Aβ 1-38 (m/z 4129.4), Aβ 1-39 (m/z 4228.8), Aβ 1-40 (m/z 4327.6) and Aβ 1-42 (m/z 4511.7). The successful analysis of brain homogenates indicates the potential of the method. However, the analysis of laser dissected plaques did not reveal N-terminal and C-terminal truncated Aβ variants due to sensitivity limitations.

OVERALL RESULTS AND DISCUSSION

The present set of studies clarified two complementary aspects of protein characterization, providing insight into various processes that contribute to neurodegeneration and loss of cognitive functions observed in AD. On the one hand, an amyloid-based approach was undertaken to determine Aβ variants and post-translational modifications of Aβ and to characterize and quantify the amyloid load of plaques in AD and in PS2APP transgenic mice. The aim was to identify Aβ species responsible for the high level of neuron loss observed in AD contrasting to the low level of neurodegeneration observed transgenic models in general. A characterization of plaques observed in pathological aging was additionally made, as individuals with these changes do exhibit amyloid plaques, but show no cognitive deficits.

As an alternative approach on the other hand, we identified proteins other than Aβ that occur at altered levels in AD and which might impact additionally on neurodegeneration. Such proteins could present potential biomarkers in AD and might be useful in the diagnosis or monitoring the progression of the disease or help in increasing the efficiency of developing new pharmacological treatment modalities for AD.

Aβ variants, posttranslational modifications of Aβ and amyloid load in plaques from human AD brains, PA individuals and transgenic PS2APP mice [I-III]

The investigation of the amount and nature of Aβ variants in plaques of PS2APP mice and AD / PA revealed substantial differences in the Aβ composition and degree of posttranslational modification in plaques of human AD patients and the transgenic PS2APP mouse model.

The main plaque types occurring in human AD patients are cored and diffuse plaques, whereas a large number of compact plaques was found in PS2APP mice. Vascular amyloid was frequently detected in human AD, but only sporadically in the PS2APP transgenic mouse model. The Aβ composition in the various plaque types is different: Cored plaques consist mainly of Aβ 42, whereas compact plaques, which can sporadically be found also in human, and vascular

amyloid contain mostly Aβ 40. Aβ 42 was shown previously to be prone to more extensive aggregation than Aβ 40 (Jarrett et al., 1993). We detected Aβ 1-42 as the main Aβ component in diffuse plaques.

Diffuse plaques are commonly accepted to be the initial plaque type occurring in AD (Selkoe, 2001a); they are also found in PS2APP mice, although here they show already at this maturation stage structural differences when investigated by immuno-electron microscopy. Diffuse plaques can also be found in brains of cognitively normal PA cases (Thal et al., 2004). A characterization of diffuse deposits using MALDI-TOF MS and urea-based Western blotting revealed no difference in the main Aβ component in PA and AD subjects. However, diffuse plaques in PA individuals showed a higher degree of oxidized methionine 35 than cored plaques in AD. It was demonstrated that oxidized Aβ shows a reduced toxicity (Clementi et al., 2004). This could indicate a protective response of the brain and would explain the absence of clinical symptoms typical for AD in PA individuals, although they carry considerable diffuse plaque load in the neocortex.

The evolution of different plaque types is subject to speculations (Armstrong, 1998); the present study provides important information for clarification. Considering the short life span of mice contrasting with the progression of the disease in humans over several decades, it might be suggested that compact plaques represent an intermediate plaque type, which develop over time to cored plaques. However, taking our data into account, this is very unlikely to be the case since compact plaques consist of Aβ 40 and cored plaques mainly of Aβ 42; hence transformation of compact to cored plaques would require a posttranslational attachment of amino acids. Our data support the following evolutionary sequence: plaque maturation starts with diffuse plaques, which then independently evolve either to typical cored or compact plaques. Various factors, like plaque associated proteins, kinetics of Aβ deposition and clearance or posttranslational modifications then would lead to divergent processes resulting in the species dependent frequency of different plaque types observed in AD and PS2APP mice. An overview of the different plaque types detected can be seen in Figure 3.

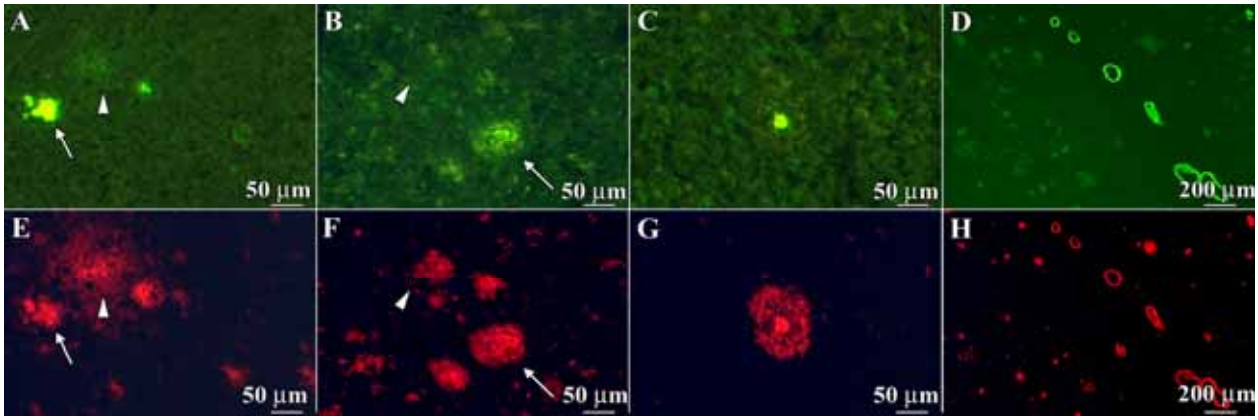

Figure 3. Histology of human and PS2APP transgenic mouse brain sections.
Brain sections from PS2APP mice (A, E) and from human AD (B-D, F-H) specimen were doublestained with thioflavine S and Aβ antibody in order to differentiate between the different plaque types. Arrowheads indicate diffuse plaques, arrows highlight compact plaques. A typical example of a cored plaque is given in C and G. Human vascular amyloid can be seen in D and H.

Aβ peptides in plaques undergo extensive N-terminal truncation in AD (Mori et al., 1992, Miller et al., 1993, Sergeant et al., 2003, Miravalle et al., 2005), a process which is reported to a considerably smaller extent in some transgenic mouse models (Kuo et al., 2001). This likely impacts on the evolution of plaques and might contribute to the level of neurotoxicity of Aβ. It was therefore of interest to investigate and compare N-terminal truncated Aβ forms of plaques from AD and PS2APP mice with our method, using MALDI-TOF MS in combination with laser dissection microscopy (Rüfenacht et al., 2005). Because brains from patients at various Braak stages were available, a correlation of N-terminal truncation with disease severity could be evaluated. We detected a progressive increase in N-terminally truncated Aβ species in human cored plaques correlating with disease progression in AD, indicative for a successive truncation of Aβ by an exoprotease upon deposition. Accordingly, lower levels of N-terminally truncated Aβ variants were detected in plaques from PS2APP mice, reflective for the shorter time of disease course. We identified pyroglutamate 3-40 /42 (N3pE-40 / 42) as the major N-terminal truncated Aβ species in human cored plaques by MALDI-TOF MS (Figure 4) and were able to confirm its abundance by immunohistochemistry and urea-based Western blotting using an N3pE-42 specific antibody. Although diffuse plaques in AD show only low levels of N-terminal truncation, N3pE-40 / 42 could also be identified by mass spectrometry. It was described earlier, that N3pE-40 / 42 could be a likely seed for plaque deposition (Saido et al., 1995, Saido, 2000). This is not supported by our data. We detected only small amounts of N3pE-40 / 42 in diffuse

plaques (i.e. the precursor stage of cored plaques) and the aggregation and toxicity properties of synthetic pyroglutamate 3-40 / 42 studied *in vitro* do not support the idea of an involvement of pyroglutamate in initial disease stages. Pyroglutamate, however, contributes to the amyloid load in the brain through its resistance to most of the aminopeptidases and hence the amount of N3pE-40/ 42 present in the brain is indicative for disease progression.

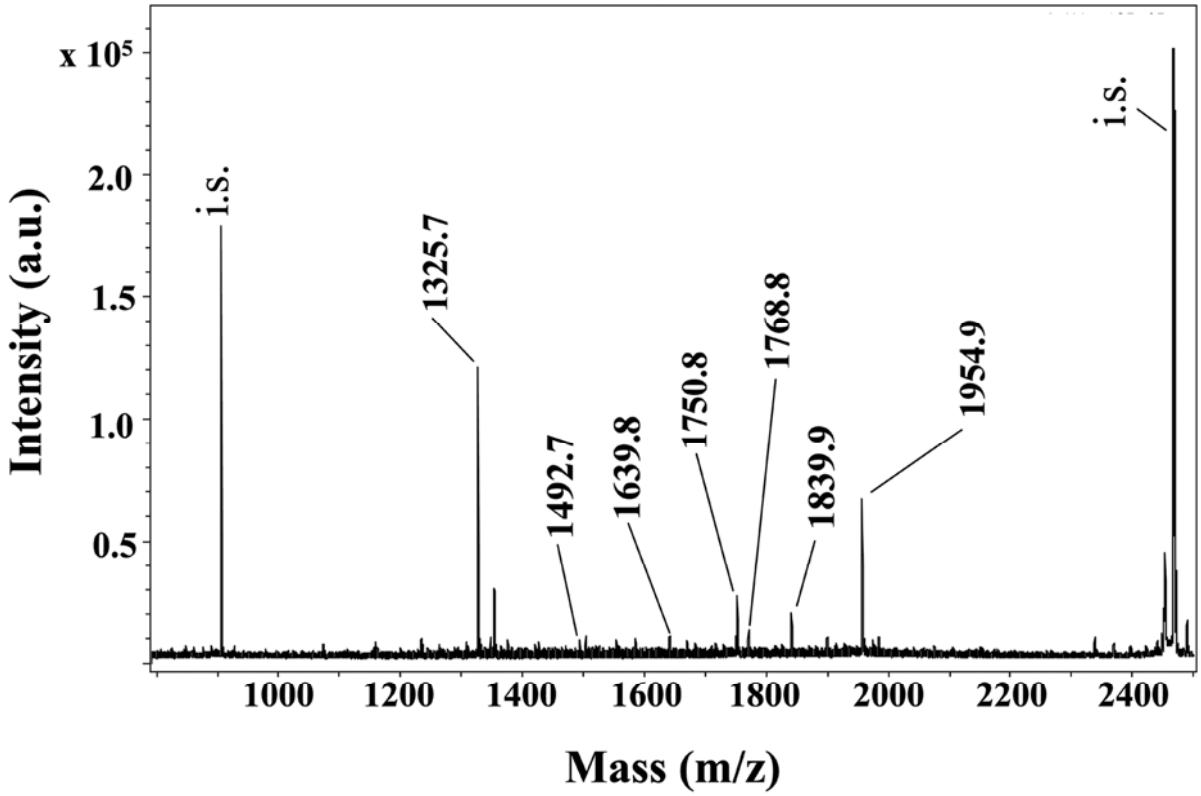

Figure 4. N-terminal truncation of Aβ derived from 30 human cored plaques and detected by MALDI-TOF MS.
Typically, N-terminal Aβ peaks corresponding to Aβ 1-16 (1954.9), 2-16 (1839.9), 3-16 (1768.8), N3pE-16 (1750.8), 4-16 (1639.8) and 5-16 (1492.7) were observed. Pyroglutamate 3-16 was detected as the major N-terminal truncated Aβ variant. m/z 1325.7 corresponds to the Aβ fragment 17-28. i.s., internal standard.

As was described earlier, Aβ present in homogenized senile plaques are crosslinked to a higher extent in AD than in transgenic mice (Kuo et al., 2001). We found, that human plaques require strong hydrolyzation conditions, namely formic acid for solubilization, whereas PS2APP mouse plaques could be solubilized in SDS-containing buffer already. Furthermore, our mass spectrometric data support the hypothesis of a high level of crosslinking in human plaques.

Enhanced stability of Aβ deposits through crosslinkage in AD is likely to contribute to a hampered clearance of Aβ from the brain and therefore has consequences for immunotherapeutical approaches used for the treatment of AD.

The Aβ peptide was described to be neurotoxic and a difference in the amyloid load in plaques from AD and PS2APP mice consequently would explain different degrees of neuronal cell death in AD and PS2APP transgenic animals. The quantification of the amyloid load, however, revealed a roughly comparable amount of Aβ present in human and PS2APP mouse plaques by mass spectrometry. A dose-effect of Aβ alone therefore can not explain the observed difference of neurodegeneration in transgenic PS2APP mice and man.

In summary, the different levels of neuronal cell death observed in AD and PS2APP mouse models is probably an interplay of various factors. Beside genetic and kinetic differences that most likely play a role, we focused on the analysis of Aβ and detected enhanced N-terminal truncation of Aβ, indications for a higher degree of crosslinking of Aβ fibrils and the occurrence of different main plaque types with dissimilar constituting Aβ variants in AD, which might contribute to the different levels of neuronal cell loss observed in PS2APP mice and AD. Furthermore, our results suggest that oxidation events on the Aβ peptide in the brain may significantly influence the degree of nerve cell loss and cognitive symptoms. The amyloid load in plaques per se cannot account for neurodegenerative differences.

Identification of proteins involved in pathogenic processes of AD and potential biomarkers [IV]

Apart from the above mentioned Aβ-related factors likely to influence neurodegeneration in AD, the proteomic background of human AD patients can provide more insight. Therefore, we compared protein levels from human AD and control tissue to detect and quantify altered protein levels and possibly to thereby identify proteins hitherto not implicated in mechanisms leading from the deposition of Aβ and tau to nerve cell loss and cognitive failure. We found that various processes are affected by the disease. Our method using LC/MS/MS allowed to detect more than 2000 proteins in AD brain tissue and we identified altered levels of numerous proteins. These are proteins which are known to be involved in the deposition of Aβ and the hyperphosphorylation

of tau, or are indicative of an aberrant energy metabolism, an enhanced susceptibility to oxidative damage, an inflammatory response, cytoskeletal impairment, disease related deficits in cell adhesion molecules**,** impaired membrane trafficking and a synaptic impairment in AD. Beyond that, 18 proteins previously not implicated with the disease were detected at aberrant levels in AD and selected proteins were confirmed by immunohistochemistry and Western blotting.

The diversity of involved pathways reflects many of currently discussed mechanisms contributing to the development of nerve cell loss and synaptic failure in AD. Several proteins identified at altered levels in this study could be causatively linked or be a stand-alone phenomenological observation – but all are indicators of a malfunction of various processes in AD. A direct connection between different pathways is difficult to establish and many questions are still open; however, the following thoughts are an attempt to combine several puzzle stones to a more coherent picture.

It can be suggested, that an inflammatory response with the activation of microglia and astrocytes is induced upon deposition of Aβ into plaques. In AD, activated microglia congregate around amyloid plaques and degenerating neurons, and may produce toxins and inflammatory cytokines that contribute to the neurodegenerative process. In addition to activation of microglia, the innate immune response includes engagement of the classical complement cascade and induction of chemokines and pentraxins. These inflammatory changes may be an important mediator, together with the neurotoxic Aβ aggregates, of subsequent neuronal injury and synaptic dysfunction seen in the brains of AD patients. The effects of Aβ accumulation and the concomitant inflammatory response may give rise to oxidative stress with an excessive generation of free radicals and peroxidative injury to proteins, lipids and other macromolecules. Mitochondria are the primary source of cellular oxidants and therefore a prime target of cumulative oxidative damage. A damage of mitochondrial proteins and DNA is likely to decrease their functionality and activity and contributes to the observed aberrant energy metabolism by decreased levels of metabolic enzymes. Removal of reactive oxygen species (ROS) eventually requires their chemical reduction; a functional deficiency in the tricarboxylic acid (TCA) cycle is likely to lead to reduced production of the electrons (NADH equivalents), which are needed for the chemical reduction of ROS. Oxidative stress can damage the pyruvatedehydrogenase (PDH) complex, which in turn leads to an accumulation of pyruvate or lactate. Most importantly, a decreased activity of the PDH complex results in a shortage of the

neurotransmitter acetylcholine, another characteristic of AD, by an inadequate supply of acetyl-CoA. A shortage of energy caused by an impaired TCA cycle in turn has widespread consequences, since synaptic vesicle exocytosis and axonal transport is dependent on the hydrolysis of ATP. An additional effect of Aβ induced oxidative stress is the disturbance of the ionic homeostasis in surrounding neuronal cells by an impairment of pump activities. This could lead to an excessive calcium accumulation, which might affect the activity of calcium-regulated relevant kinases and phosphatases that could subsequently contribute to the hyperphosphorylation of tau. The loss of tau function upon hyperphosphorylation in principle can be compensated by the other two neuronal microtubule-associated proteins MAP 1A / 1B and MAP 2, which have similar functions. A decrease in MAP levels - as observed in our study - indicates an impairment of this compensation mechanism. The breakdown of the microtubule network in the affected neurons contributes to general cytoskeletal impairment and compromises axonal transport, leading to retrograde degeneration which, in turn, results in neuronal dysfunction and dementia. Impaired membrane trafficking was reflected by reduced levels of several proteins with a known function in clathrin-mediated synaptic vesicle recycling. Reduced levels of such proteins could affect the control of synaptic vesicle endocytosis and the synaptic terminals of these neurons would become incapable of supplying adequate synaptic vesicles. These defects could lead to functional disruption of synapses, resulting in impaired communications between neurons – an essential determinant of learning and memory. Neurotrophic factors, like nerve growth factor or brain-derived neurotrophic factor, are secreted by cells in a neuron's target field, and act by protecting the neuron from apoptosis. Altered clathrin-mediated endocytosis could also play a role in impaired neurotrophic factor uptake and consequently in impaired signaling cascades, which may contribute to the pathogenesis of Alzheimer's disease. The interplay of various pathways finally results in the high level of neurodegeneration seen in AD and to the observed clinical symptoms like cognitive failure and behavioral alterations.

A group of proteins not included in the above mentioned framework of AD are the cell adhesion molecules (CAMs). Various proteins in AD, involved either in neurite outgrowth or cell adhesion, were detected at decreased levels in this study, indicative for an impaired neuritic network. Synapses are highly specialized structures designed to guarantee precise and efficient communication between neurons and their target cells, and numerous proteins are involved in the

Table 1

Protein	Ratio AD / control tissue	Reference	Reported (De-)regulation
cell adhesion / neurite outgrowth			
Thy-1 membrane glycoprotein	0.65	Leifer et al. 1992	↓
Myelin-associated glycoprotein	0.59	-	
Claudin-11	0.45	-	
Neurexin IV	0.41	-	
Myelin oligodendrocyte glycoprotein	0.38	-	
Contactin 1	0.7	-	
Contactin 2	0.28	-	
chaperones			
Hsp 27	1.59	Renkawek et al., 1993	↑
Hsp 75	1.48	-	
Hsp 90	1.43	Anthony et al., 2003	↑
Hsp 60	0.68	Yoo et al., 2001	↓
T-complex protein 1	0.46	Schuller et al., 2000	↓
cytoskeleton			
Microtubule-associated protein tau	2.36	Mandelkow et al., 1994	↑
Plectin 1	1.3	-	
Ankyrin 2	0.69	-	
Alpha-internexin	0.64	Dickson et al., 2005	n.d.
Alpha adducin	0.59	-	
Microtubule-associated protein 1B	0.51	Hasegawa et al., 1990	n.d.
Microtubule-associated protein RP/EB family member 3	0.19	-	
inflammation			
GFAP	4.45	Styren et al., 1998	↑
Vimentin	1.44	Porchet et al., 2003	↑
Complement C3	only AD	McGeer et al., 1989	↑
Complement C4	only AD	McGeer et al., 1989	↑
glucose metabolism			
Isocitrate dehydrogenase	0.7	Hoyer, 1991	↓
Succinyl-CoA ligase	0.65	Hoyer, 1991	↓
Malate dehydrogenase, cytoplasmic	0.55	Hoyer, 1991	↓
Malate dehydrogenase, mitochondrial	0.51	Hoyer, 1991	↓
Succinate dehydrogenase	0.51	Hoyer, 1991	↓
Phosphofructokinase 1	0.49	Hoyer, 1991	↓

Table 1 (continued)

hyperphosphorylation of tau			
Mitogen-activated protein kinase 3 (ERK 1)	only AD	Pei et al., 2002	↑
Mitogen-activated protein kinase 1 (ERK 2)	0.86	Pei et al., 2002	↑
Serine/threonine protein phosphatase 2A	0.45	Gong et al., 1995	n.d.
citrullination of proteins			
Protein-arginine deiminase type II	1.45	Ishigami et al., 2005	↑
oxidative stress			
Peroxiredoxin 5	0.61	-	
Microsomal glutathione S-transferase 3	0.47	-	
Superoxide dismutase [Mn]	decreased	Krapfenbauer et al., 2003	↔
synaptic proteins			
Synaptogyrin-1	1.73	-	
Synaptogyrin-3	increased	-	
Synaptotagmin-1	0.62	Yoo et al., 2001	↓
Nogo protein	0.54	Strittmatter et al., 2002	n.d.
Reticulon-1	0.53	Yan et al., 2004	n.d.
Syntaxin-1A (HPC-1)	0.32	Minger et al., 2001	↓
Presynaptic density protein 95 (PSD-95)	0.3	Gylys et al., 2004	↓
membrane trafficking			
Clathrin coat assembly protein AP180	0.58	Yao et al., 1999	↓
proteolysis			
Ubiquitin	1.92	Iqbal et al. 1997	↑
others			
Amyloid Beta	only AD	Glenner & Wong, 1984	↑
Apolipoprotein E	2.33	Strittmatter et al., 1993	↑
Alpha-1-antichymotrypsin (ACT)	only AD	Abraham et al., 1988	↑
Matrin-3	0.49	-	
Major prion protein	0.43	Lantos et al., 2005	↓
Transgelin-3 (Neuronal protein NP25)	0.4	-	
Programmed cell death protein 8	0.34	-	

Table 1. Proteins detected at altered levels in AD.
The ratio is indicative for the protein abundance in AD compared to control tissue. Proteins only present in AD are indicated. 'Increased' refers to protein level for proteins detected in only one of the control samples; 'decreased' indicates the protein level for proteins detected in only one of the AD cases. Arrows indicate change in protein levels found in AD in the respective references. The complete table and references can be seen in [IV]. n.d., not determined

formation of synaptic connections (Ruegg, 2001). CAMs play a prominent role at all stages of synapse assembly, from contact initiation to stabilization (Gerrow and El-Husseini, 2006). A breakdown in the organization of CAMs and activation of their signal transduction mechanisms is likely to contribute to neuronal dysfunction and failure as seen in AD. In addition, a decrease in protein levels of molecules involved in axonal guidance may further negatively influence the process of synapse formation in AD.

Table 1, excerpted from a more complete compilation in [IV], lists some of the proteins detected at altered levels in the brain of AD cases.

The identification of the proteins involved in the molecular pathogenesis of AD is a requirement for a better understanding of the disease and for the eventual development of a biological marker, be it for diagnosis, for monitoring the progression of the disease or for assessing the effects of putative new pharmacological agents developed for AD. In our study, we identified numerous proteins with altered levels in AD. Proteins with changed levels in postmortem AD brains may present potential biomarkers, but are only useful if the protein or fragments thereof are measurable in the CSF and most preferentially also in the periphery. The brain clearly resembles the adequate target and a suitable starting point in the search for novel biomarkers of AD. However, biomarker candidates need further investigation and confirmation, but most importantly the brain pathology needs to be reflected in easier accessible tissues or fluids, like CSF or blood.

Discovery of a biomarker from altered brain protein levels needs to be rationalized in relation to AD and the molecular pathways involved. As an example, we detected decreased levels of six enzymes involved in the citrate cycle. A decreased glucose breakdown may possibly lead to the accumulation of intermediate products like pyruvate or α-ketoglutarate, which may be secreted and eventually be detected in urine or blood more sensitively than the responsible enzymes alone. Oxidative stress resulting in ROS might be another event triggering the occurrence of a therapeutic or diagnostic useful biomarker. Even though we might not be able to measure differences in the single oxidative stress related proteins, we eventually might be able to detect an accumulation of lipid peroxidation products or a secretion of damaged mitochondrial proteins upon oxidative stress induced nerve cell death into peripheral fluids. Schwemmer and colleagues have suggested earlier, that urinary nitrotyrosine levels may serve as a biomarker to

detect changes in oxidant stress (Schwemmer et al., 2000). Nitrotyrosine is formed by nitration of tyrosine residues via peroxynitrite (van der Vliet et al., 1995), a reactive oxygen species previously described to occur in AD and to interfere with key enzymes of the TCA cycle (Bolanos et al., 1997). Nitrotyrosine may therefore also serve as a biological marker for AD related oxidative stress.

However, the difficulty in using proteins or intermediate products from the glycolytic pathway as well as oxidative-stress related enzymes and products is their limited specificity. A decrease in the degradation of glucose and increased oxidative stress are processes that can occur under a variety of (patho-) physiological conditions unrelated to AD. The incidence of for example nitrotyrosine in urine is thus not necessarily related to AD-related oxidative stress. For this reason, proteins involved in such ubiquitous pathways could only be important as biological markers in an overall quantitative manner. Since the brain is relatively small compared to the rest of the body and separated by the blood brain barrier, significant changes in the brain levels of such a non-specific putative biomarker are possibly attenuated and cannot be detected easily in peripheral fluids. A biomarker in AD needs to have a high specificity for the discrimination from other diseases. Optimally suited for such a surrogate marker would be an AD-specific protein or metabolite, or a modification, which is uniquely related to the pathogenesis of AD, is not part of another biochemical pathway and does not occur in the periphery and also in other types of dementia. In our studies, we identified several synaptic proteins, e.g. syntaxin-1A and synaptotagmin-1, occurring at decreased levels in AD brain compared to healthy control tissue. This could on one hand be indicative for AD triggered neuronal loss and on the other hand could reflect a synaptic impairment associated with AD. In contrast to these observations, we detected increased levels of synaptogyrin-1 and -3 in AD, a protein which is known to be associated with presynaptic vesicles in neuronal cells. Many synaptic proteins, including synaptogyrin-1 and -3, are brain specific. Altered synaptic brain protein levels as detected in our study might be reflected in CSF and eventually be detected in the periphery and would thus present ideal biomarkers for AD.

We detected elevated levels of protein-arginine deiminase 2 (PAD 2) in AD, catalyzing the citrullination of proteins. Citrullination refers to the process of deimination, which changes the basic character of arginine to a neutral peptidyl citrulline (Gyorgy et al., 2006). This process could change the structure of a protein to a more open configuration (Tarcsa et al., 1996). The abnormal accumulation of citrullinated proteins, especially GFAP and vimentin, was observed in

AD (Ishigami et al., 2005) and it was suggested, that citrullination promotes the disassembly process of these intermediate filament proteins (Gyorgy et al., 2006). The degradation of citrullinated proteins is possibly impaired, as the action of specific proteases is disturbed, which may explain in turn the observed accumulation. Because citrulline is not a natural amino acid, it is possible that the accumulation of proteins harboring a citrulline triggers an innate immune response of the brain in AD. Formed auto-antibodies may then eventually be detectable in the serum of AD patients and might serve as useful marker for AD. This is exactly what has been found in rheumatic arthritis, where auto-antibodies against citrullinated proteins are built and serve as specific and predictive markers for the disease (Aho et al., 1994).

Proteomic information obtained from the investigation of brain tissue is important and useful in the discovery of a biomarker for this devastating disease. The characterization of postmortem brains can reveal altered levels of a multitude of proteins implicated in various pathogenic pathways of AD. A consideration of formation and clearance pathway(s) of such proteins or of the formed (intermediate) products, significantly increases the probability of identifying a specific and useful marker in more easily accessible fluids. A modified approach to translate the findings from postmortem brain to a useful biomarker is to look for metabolic peptide fragments of the identified proteins. It can be speculated, that early events leading to neurodegeneration and apoptotic or senescent cells in AD would lead to the degradation of numerous proteins. For example, neuron specific cytoskeletal proteins occur abundantly in the brain; neurodegeneration and cell loss would likely result in the release of degraded portions of such structural proteins, which may eventually be detected in the CSF or in the periphery.

In summary, studies, such as the ones performed in the present thesis, giving insight into the nature of affected pathways or processes in AD are an indispensable pre-condition for the successful identification and development of biomarker candidates, which can be found in peripheral fluids.

CONCLUDING REMARKS AND FUTURE PERSPECTIVES

The present investigation on a detailed analysis of the amyloid-β protein in plaques regarding the nature and extent of N-terminal truncation, plaque comprising Aβ variants, amyloid plaque load, main plaque types and cross-linking of fibrils cannot answer all questions regarding the role of Aβ in the neurodegenerative process of AD. However, they give insight into the molecular composition of specific amyloid plaque types and help to more clearly outline the missing links. A comparison of plaque constituting Aβ variants in AD and PS2APP transgenic mice is essential in preclinical drug development (e.g. immunization approach), where PS2APP mouse models are used in evaluating drug efficiency. Our methodology enabled to investigate specific plaque types, thus presenting an advantage over the analysis of brain homogenates, which average the senile plaque load. This allowed getting more insight into the course of plaque evolution and the process of N-terminal truncation.

Even though our study indicates a high level of oxidized Aβ in diffuse plaques, especially in PA cases, the mechanism of protection by met-35 oxidation on the pathogenesis of AD is still an unresolved mystery. Since oxidation of met-35 was described to influence toxicity and aggregation properties of Aβ, the correlation of oxidation status in plaques from different Braak stages or brain regions with the degree of neurodegeneration, might present an essential step in the elucidation of plaque-specific impact on neurodegeneration in AD. A clarification of the role of oxidized Aβ in AD might further complement the understanding of the disease.

To further gain clarity on the process of neurodegeneration, the specific analysis of neuritic plaques is likely to reveal important additional information. Neuritic plaques are amyloid depositions associated with dystrophic neurites containing tau. In the present studies, we analyzed morphologically differentiated plaque types, i.e. cored, compact or diffuse plaques. Only a subset of plaques from the different types is neuritic and a further differentiation and investigation revealing their Aβ composition, extent of N-terminal truncation and oxidation status may further contribute to determine the role of plaques in AD. The approach used in our studies could potentially be very valuable also for the analysis of amyloid plaques in specific brain regions. Thal and colleagues described a hierarchical involvement of distinct areas of the brain in Aβ deposition (Thal et al., 2002, Thal et al., 2006). An analysis of amyloid plaques in

different brain regions, e.g. plaques from areas affected early in the disease process is a further step in identifying disease relevant Aβ variants. Additionally, an analysis of plaques from different FAD mutations could be aimed at. It is not known to date how different mutations in the APP, PS1 or PS2 genes affect the nature of deposited Aβ species. It was reported, that the arctic mutation facilitates senile plaque formation in transgenic mice (Lord et al., 2006). A detailed analysis of plaque constituting Aβ variants would therefore be highly informative and might reveal Aβ variants affecting the plaque deposition process. Other FAD mutations exhibit different features and a characterization of the deposited Aβ variants holds promise to give important insight into the impact of Aβ species to the pathogenesis of AD.

Another field of application includes transgenic mouse models. Numerous transgenic mouse models with different genetic backgrounds were described (McGowan et al., 2006). A comparative analysis and characterization of Aβ deposited either intraneuronally or in amyloid plaques is important in the definition of the relevance of any transgenic mouse model used as preclinical tool to evaluate drug efficiency.

Our studies also provided insight into alteration of levels of proteins other than Aβ in AD and allow for overview of various processes involved in the pathogenesis of the disease. Although this work can be regarded as exploratory, because the number of patients investigated was limited, the results are promising new and contribute to a more thorough understanding of the disease. The identification of new proteins involved in AD triggered a follow-up study. The results will be evaluated with a larger number of patients in an approach currently performed at Roche. Inclusion of different Braak stages for analysis is expected to substantiate findings, because this would allow for the detection of proteins changing their levels as a function of severity of disease. Since we detected various proteins previously unknown to be related to AD, their specific function and role in the pathogenesis of AD needs to be determined for the derivation of biological markers or new drug targets. Knockout mice are used in a variety of ways. They allow to test the specific functions of particular gene products and to observe the processes that these particular genes could regulate. A knock-out of genes identified in this approach alone or in combination with the already available transgenic AD mouse models might reveal more information of how a protein occurring at altered levels in AD contributes to the etiopathology of the disease. As mentioned above, the translation of the findings of proteins detected at altered levels in AD to biological markers measurable in the periphery can happen in

various ways. Future approaches could include a closer investigation of the proteome of CSF or peripheral fluids with respect to the candidates detected during this study. Can these proteins, metabolic fragments thereof or auto-antibodies generated against abnormal protein accumulations be detected? Are they specific for AD and do their changes correlate with disease progression? The technologies to answer these questions are SELDI-TOF MS, MALDI-TOF MS, LC/MS/MS and 2D-gel electrophoresis, i.e. those technologies successfully applied, at least in part, already in the present studies.

A project build upon the present work and to identify biomarkers in AD would preferentially be divided into two phases. During the first phase the identification of biological markers that correlate with cognitive decline could be aimed at. Using human plasma samples collected over a period of time, would allow for a longitudinal study, monitoring specific changes in protein composition as a function of disease progression. Plasma samples of two patient groups could be analyzed using 2D-gel electrophoresis: cases with slow or no cognitive decline could be compared to individuals with a more rapidly progressing disease phenomenology, determined by MMSE scores. Changes in protein expression levels might then be measured and followed over time. With the help of bioinformatics, the data could be evaluated and a set of putative biomarkers for disease progression from these subject sample sets could be established.

In a second phase, the markers identified in the first phase should be validated with complementary methods, e.g. Western blot or ELISA. For this reason, a second plasma sample set is analyzed to determine if these markers might serve as surrogates of symptomatic change. Hopefully, such investigations might complement therapeutic assessment in clinical trials and could speed up the development of new drugs.

REFERENCES

1998. Consensus report of the Working Group on: "Molecular and Biochemical Markers of Alzheimer's Disease". The Ronald and Nancy Reagan Research Institute of the Alzheimer's Association and the National Institute on Aging Working Group. Neurobiol Aging. 19, 109-116.

Aho, K., Palusuo, T. and Kurki, P., 1994. Marker antibodies of rheumatoid arthritis: diagnostic and pathogenetic implications. Semin Arthritis Rheum. 23, 379-387.

Andreasen, N. and Blennow, K., 2002. Beta-amyloid (Abeta) protein in cerebrospinal fluid as a biomarker for Alzheimer's disease. Peptides. 23, 1205-1214.

Andreasen, N., Sjogren, M. and Blennow, K., 2003. CSF markers for Alzheimer's disease: total tau, phospho-tau and Abeta42. World J Biol Psychiatry. 4, 147-155.

Andreasen, N., Vanmechelen, E., Van de Voorde, A., Davidsson, P., Hesse, C., Tarvonen, S., Raiha, I., Sourander, L., Winblad, B. and Blennow, K., 1998. Cerebrospinal fluid tau protein as a biochemical marker for Alzheimer's disease: a community based follow up study. J Neurol Neurosurg Psychiatry. 64, 298-305.

Armstrong, R. A., 1998. Beta-amyloid plaques: stages in life history or independent origin? Dement Geriatr Cogn Disord. 9, 227-238.

Baker, H., Patel, V., Molinolo, A. A., Shillitoe, E. J., Ensley, J. F., Yoo, G. H., Meneses-Garcia, A., Myers, J. N., El-Naggar, A. K., Gutkind, J. S. and Hancock, W. S., 2005. Proteome-wide analysis of head and neck squamous cell carcinomas using laser-capture microdissection and tandem mass spectrometry. Oral Oncol. 41, 183-199.

Bard, F., Cannon, C., Barbour, R., Burke, R. L., Games, D., Grajeda, H., Guido, T., Hu, K., Huang, J., Johnson-Wood, K., Khan, K., Kholodenko, D., Lee, M., Lieberburg, I., Motter, R., Nguyen, M., Soriano, F., Vasquez, N., Weiss, K., Welch, B., Seubert, P., Schenk, D. and Yednock, T., 2000. Peripherally administered antibodies against amyloid beta-peptide enter the central nervous system and reduce pathology in a mouse model of Alzheimer disease. Nat Med. 6, 916-919.

Billings, L. M., Oddo, S., Green, K. N., McGaugh, J. L. and LaFerla, F. M., 2005. Intraneuronal Abeta causes the onset of early Alzheimer's disease-related cognitive deficits in transgenic mice. Neuron. 45, 675-688.

Bolanos, J. P., Almeida, A., Stewart, V., Peuchen, S., Land, J. M., Clark, J. B. and Heales, S. J., 1997. Nitric oxide-mediated mitochondrial damage in the brain: mechanisms and implications for neurodegenerative diseases. J Neurochem. 68, 2227-2240.

Braak, H. and Braak, E., 1991. Neuropathological stageing of Alzheimer-related changes. Acta Neuropathol (Berl). 82, 239-259.

Clementi, M. E., Martorana, G. E., Pezzotti, M., Giardina, B. and Misiti, F., 2004. Methionine 35 oxidation reduces toxic effects of the amyloid beta-protein fragment (31-35) on human red blood cell. Int J Biochem Cell Biol. 36, 2066-2076.

DeMattos, R. B., Bales, K. R., Cummins, D. J., Dodart, J. C., Paul, S. M. and Holtzman, D. M., 2001. Peripheral anti-A beta antibody alters CNS and plasma A beta clearance and decreases brain A beta burden in a mouse model of Alzheimer's disease. Proc Natl Acad Sci U S A. 98, 8850-8855.

Dewachter, I. and Van Leuven, F., 2002. Secretases as targets for the treatment of Alzheimer's disease: the prospects. Lancet Neurol. 1, 409-416.

Dickson, T. C., Saunders, H. L. and Vickers, J. C., 1997. Relationship between apolipoprotein E and the amyloid deposits and dystrophic neurites of Alzheimer's disease. Neuropathol Appl Neurobiol. 23, 483-491.

Doody, R. S., 2003. Current treatments for Alzheimer's disease: cholinesterase inhibitors. J Clin Psychiatry. 64 Suppl 9, 11-17.

El-Agnaf, O. M., Mahil, D. S., Patel, B. P. and Austen, B. M., 2000. Oligomerization and toxicity of beta-amyloid-42 implicated in Alzheimer's disease. Biochem Biophys Res Commun. 273, 1003-1007.

Gagne, J. P., Gagne, P., Hunter, J. M., Bonicalzi, M. E., Lemay, J. F., Kelly, I., Le Page, C., Provencher, D., Mes-Masson, A. M., Droit, A., Bourgais, D. and Poirier, G. G., 2005. Proteome profiling of human epithelial ovarian cancer cell line TOV-112D. Mol Cell Biochem. 275, 25-55.

Gerrow, K. and El-Husseini, A., 2006. Cell adhesion molecules at the synapse. Front Biosci. 11, 2400-2419.

Glenner, G. G., Wong, C. W., Quaranta, V. and Eanes, E. D., 1984. The amyloid deposits in Alzheimer's disease: their nature and pathogenesis. Appl Pathol. 2, 357-369.

Gyorgy, B., Toth, E., Tarcsa, E., Falus, A. and Buzas, E. I., 2006. Citrullination: A posttranslational modification in health and disease. Int J Biochem Cell Biol.

Haass, C., 2004. Take five-BACE and the gamma-secretase quartet conduct Alzheimer's amyloid beta-peptide generation. Embo J. 23, 483-488.

Hardy, J., 2006. Has the amyloid cascade hypothesis for Alzheimer's disease been proved? Curr Alzheimer Res. 3, 71-73.

Hardy, J. A. and Higgins, G. A., 1992. Alzheimer's disease: the amyloid cascade hypothesis. Science. 256, 184-185.

Hashii, N., Kawasaki, N., Itoh, S., Hyuga, M., Kawanishi, T. and Hayakawa, T., 2005. Glycomic/glycoproteomic analysis by liquid chromatography/mass spectrometry: analysis of glycan structural alteration in cells. Proteomics. 5, 4665-4672.

Higgins, G. A. and Jacobsen, H., 2003. Transgenic mouse models of Alzheimer's disease: phenotype and application. Behav Pharmacol. 14, 419-438.

Ho, L., Sharma, N., Blackman, L., Festa, E., Reddy, G. and Pasinetti, G. M., 2005. From proteomics to biomarker discovery in Alzheimer's disease. Brain Res Brain Res Rev. 48, 360-369.

Hong, L., Koelsch, G., Lin, X., Wu, S., Terzyan, S., Ghosh, A. K., Zhang, X. C. and Tang, J., 2000. Structure of the protease domain of memapsin 2 (beta-secretase) complexed with inhibitor. Science. 290, 150-153.

Hoozemans, J. J., Veerhuis, R., Rozemuller, A. J. and Eikelenboom, P., 2003. Non-steroidal anti-inflammatory drugs and cyclooxygenase in Alzheimer's disease. Curr Drug Targets. 4, 461-468.

Hsiao, K., Chapman, P., Nilsen, S., Eckman, C., Harigaya, Y., Younkin, S., Yang, F. and Cole, G., 1996. Correlative memory deficits, Abeta elevation, and amyloid plaques in transgenic mice. Science. 274, 99-102.

Hu, L., Wong, T. P., Cote, S. L., Bell, K. F. and Cuello, A. C., 2003. The impact of Abeta-plaques on cortical cholinergic and non-cholinergic presynaptic boutons in alzheimer's disease-like transgenic mice. Neuroscience. 121, 421-432.

Ida, N., Hartmann, T., Pantel, J., Schroder, J., Zerfass, R., Forstl, H., Sandbrink, R., Masters, C. L. and Beyreuther, K., 1996. Analysis of heterogeneous A4 peptides in human cerebrospinal fluid and blood by a newly developed sensitive Western blot assay. J Biol Chem. 271, 22908-22914.

Iqbal, K., Alonso Adel, C., Chen, S., Chohan, M. O., El-Akkad, E., Gong, C. X., Khatoon, S., Li, B., Liu, F., Rahman, A., Tanimukai, H. and Grundke-Iqbal, I., 2005. Tau pathology in Alzheimer disease and other tauopathies. Biochim Biophys Acta. 1739, 198-210.

Ishigami, A., Ohsawa, T., Hiratsuka, M., Taguchi, H., Kobayashi, S., Saito, Y., Murayama, S., Asaga, H., Toda, T., Kimura, N. and Maruyama, N., 2005. Abnormal accumulation of citrullinated proteins catalyzed by peptidylarginine deiminase in hippocampal extracts from patients with Alzheimer's disease. J Neurosci Res. 80, 120-128.

Iwatsubo, T., Mann, D. M., Odaka, A., Suzuki, N. and Ihara, Y., 1995. Amyloid beta protein (A beta) deposition: A beta 42(43) precedes A beta 40 in Down syndrome. Ann Neurol. 37, 294-299.

Iwatsubo, T., Odaka, A., Suzuki, N., Mizusawa, H., Nukina, N. and Ihara, Y., 1994. Visualization of A beta 42(43) and A beta 40 in senile plaques with end-specific A beta monoclonals: evidence that an initially deposited species is A beta 42(43). Neuron. 13, 45-53.

Jarrett, J. T., Berger, E. P. and Lansbury, P. T., Jr., 1993. The carboxy terminus of the beta amyloid protein is critical for the seeding of amyloid formation: implications for the pathogenesis of Alzheimer's disease. Biochemistry. 32, 4693-4697.

John, V., 2006. Human beta-secretase (BACE) and BACE Inhibitors: Progress Report. Curr Top Med Chem. 6, 569-578.

Kang, J., Lemaire, H. G., Unterbeck, A., Salbaum, J. M., Masters, C. L., Grzeschik, K. H., Multhaup, G., Beyreuther, K. and Muller-Hill, B., 1987. The precursor of Alzheimer's disease amyloid A4 protein resembles a cell-surface receptor. Nature. 325, 733-736.

King, D. L. and Arendash, G. W., 2002. Maintained synaptophysin immunoreactivity in Tg2576 transgenic mice during aging: correlations with cognitive impairment. Brain Res. 926, 58-68.

Klafki, H. W., Wiltfang, J. and Staufenbiel, M., 1996. Electrophoretic separation of betaA4 peptides (1-40) and (1-42). Anal Biochem. 237, 24-29.

Kuo, Y. M., Kokjohn, T. A., Beach, T. G., Sue, L. I., Brune, D., Lopez, J. C., Kalback, W. M., Abramowski, D., Sturchler-Pierrat, C., Staufenbiel, M. and Roher, A. E., 2001. Comparative analysis of amyloid-beta chemical structure and amyloid plaque morphology of transgenic mouse and Alzheimer's disease brains. J Biol Chem. 276, 12991-12998.

Lee, V. M., Kenyon, T. K. and Trojanowski, J. Q., 2005. Transgenic animal models of tauopathies. Biochim Biophys Acta. 1739, 251-259.

Lee, V. M. and Trojanowski, J. Q., 1992. The disordered neuronal cytoskeleton in Alzheimer's disease. Curr Opin Neurobiol. 2, 653-656.

Lesne, S., Koh, M. T., Kotilinek, L., Kayed, R., Glabe, C. G., Yang, A., Gallagher, M. and Ashe, K. H., 2006. A specific amyloid-beta protein assembly in the brain impairs memory. Nature. 440, 352-357.

Liao, L., Cheng, D., Wang, J., Duong, D. M., Losik, T. G., Gearing, M., Rees, H. D., Lah, J. J., Levey, A. I. and Peng, J., 2004. Proteomic characterization of postmortem amyloid plaques isolated by laser capture microdissection. J Biol Chem. 279, 37061-37068.

Lord, A., Kalimo, H., Eckman, C., Zhang, X. Q., Lannfelt, L. and Nilsson, L. N., 2006. The Arctic Alzheimer mutation facilitates early intraneuronal Abeta aggregation and senile plaque formation in transgenic mice. Neurobiol Aging. 27, 67-77.

Loring, J. F., Wen, X., Lee, J. M., Seilhamer, J. and Somogyi, R., 2001. A gene expression profile of Alzheimer's disease. DNA Cell Biol. 20, 683-695.

Lovestone, S., 2006. Biomarkers in Alzheimer's disease. J Nutr Health Aging. 10, 118-122.

Mann, D. M., 1988. Alzheimer's disease and Down's syndrome. Histopathology. 13, 125-137.

Mattson, M. P., 1997. Cellular actions of beta-amyloid precursor protein and its soluble and fibrillogenic derivatives. Physiol Rev. 77, 1081-1132.

McGowan, E., Eriksen, J. and Hutton, M., 2006. A decade of modeling Alzheimer's disease in transgenic mice. Trends Genet.

Miller, D. L., Papayannopoulos, I. A., Styles, J., Bobin, S. A., Lin, Y. Y., Biemann, K. and Iqbal, K., 1993. Peptide compositions of the cerebrovascular and senile plaque core amyloid deposits of Alzheimer's disease. Arch Biochem Biophys. 301, 41-52.

Miravalle, L., Calero, M., Takao, M., Roher, A. E., Ghetti, B. and Vidal, R., 2005. Amino-terminally truncated Abeta peptide species are the main component of cotton wool plaques. Biochemistry. 44, 10810-10821.

Mori, H., Takio, K., Ogawara, M. and Selkoe, D. J., 1992. Mass spectrometry of purified amyloid beta protein in Alzheimer's disease. J Biol Chem. 267, 17082-17086.

Nunan, J. and Small, D. H., 2000. Regulation of APP cleavage by alpha-, beta- and gamma-secretases. FEBS Lett. 483, 6-10.

Oddo, S., Billings, L., Kesslak, J. P., Cribbs, D. H. and LaFerla, F. M., 2004. Abeta immunotherapy leads to clearance of early, but not late, hyperphosphorylated tau aggregates via the proteasome. Neuron. 43, 321-332.

Oddo, S., Caccamo, A., Smith, I. F., Green, K. N. and LaFerla, F. M., 2006. A dynamic relationship between intracellular and extracellular pools of Abeta. Am J Pathol. 168, 184-194.

Parnetti, L., Lanari, A., Amici, S., Gallai, V., Vanmechelen, E. and Hulstaert, F., 2001. CSF phosphorylated tau is a possible marker for discriminating Alzheimer's disease from dementia with Lewy bodies. Phospho-Tau International Study Group. Neurol Sci. 22, 77-78.

Richards, J. G., Higgins, G. A., Ouagazzal, A. M., Ozmen, L., Kew, J. N., Bohrmann, B., Malherbe, P., Brockhaus, M., Loetscher, H., Czech, C., Huber, G., Bluethmann, H., Jacobsen, H. and Kemp, J. A., 2003. PS2APP transgenic mice, coexpressing hPS2mut and hAPPswe, show age-related cognitive deficits associated with discrete brain amyloid deposition and inflammation. J Neurosci. 23, 8989-9003.

Roberds, S. L., Anderson, J., Basi, G., Bienkowski, M. J., Branstetter, D. G., Chen, K. S., Freedman, S. B., Frigon, N. L., Games, D., Hu, K., Johnson-Wood, K., Kappenman, K. E., Kawabe, T. T., Kola, I., Kuehn, R., Lee, M., Liu, W., Motter, R., Nichols, N. F., Power, M., Robertson, D. W., Schenk, D., Schoor, M., Shopp, G. M., Shuck, M. E., Sinha, S., Svensson, K. A., Tatsuno, G., Tintrup, H., Wijsman, J., Wright, S. and McConlogue, L., 2001. BACE knockout mice are healthy despite lacking the primary beta-secretase activity in brain: implications for Alzheimer's disease therapeutics. Hum Mol Genet. 10, 1317-1324.

Ruegg, M. A., 2001. Molecules involved in the formation of synaptic connections in muscle and brain. Matrix Biol. 20, 3-12.

Rüfenacht, P., Güntert, A., Bohrmann, B., Ducret, A. and Döbeli, H., 2005. Quantification of the A beta peptide in Alzheimer's plaques by laser dissection microscopy combined with mass spectrometry. J Mass Spectrom. 40, 193-201.

Saido, T. C., 2000. Involvement of polyglutamine endolysis followed by pyroglutamate formation in the pathogenesis of triplet repeat/polyglutamine-expansion diseases. Med Hypotheses. 54, 427-429.

Saido, T. C., Iwatsubo, T., Mann, D. M., Shimada, H., Ihara, Y. and Kawashima, S., 1995. Dominant and differential deposition of distinct beta-amyloid peptide species, A beta N3(pE), in senile plaques. Neuron. 14, 457-466.

Schenk, D., Barbour, R., Dunn, W., Gordon, G., Grajeda, H., Guido, T., Hu, K., Huang, J., Johnson-Wood, K., Khan, K., Kholodenko, D., Lee, M., Liao, Z., Lieberburg, I., Motter, R., Mutter, L., Soriano, F., Shopp, G., Vasquez, N., Vandevert, C., Walker, S., Wogulis, M., Yednock, T., Games, D. and Seubert, P., 1999. Immunization with amyloid-beta attenuates Alzheimer-disease-like pathology in the PDAPP mouse. Nature. 400, 173-177.

Schonberger, S. J., Edgar, P. F., Kydd, R., Faull, R. L. and Cooper, G. J., 2001. Proteomic analysis of the brain in Alzheimer's disease: molecular phenotype of a complex disease process. Proteomics. 1, 1519-1528.

Schwemmer, M., Fink, B., Kockerbauer, R. and Bassenge, E., 2000. How urine analysis reflects oxidative stress--nitrotyrosine as a potential marker. Clin Chim Acta. 297, 207-216.

Selkoe, D. J., 2001a. Alzheimer's disease: genes, proteins, and therapy. Physiol Rev. 81, 741-766.

Selkoe, D. J., 2001b. Clearing the brain's amyloid cobwebs. Neuron. 32, 177-180.

Sergeant, N., Bombois, S., Ghestem, A., Drobecq, H., Kostanjevecki, V., Missiaen, C., Wattez, A., David, J. P., Vanmechelen, E., Sergheraert, C. and Delacourte, A., 2003. Truncated beta-amyloid peptide species in pre-clinical Alzheimer's disease as new targets for the vaccination approach. J Neurochem. 85, 1581-1591.

Simone, N. L., Bonner, R. F., Gillespie, J. W., Emmert-Buck, M. R. and Liotta, L. A., 1998. Laser-capture microdissection: opening the microscopic frontier to molecular analysis. Trends Genet. 14, 272-276.

Tanzi, R. E., Gusella, J. F., Watkins, P. C., Bruns, G. A., St George-Hyslop, P., Van Keuren, M. L., Patterson, D., Pagan, S., Kurnit, D. M. and Neve, R. L., 1987. Amyloid beta protein gene: cDNA, mRNA distribution, and genetic linkage near the Alzheimer locus. Science. 235, 880-884.

Tanzi, R. E., Kovacs, D. M., Kim, T. W., Moir, R. D., Guenette, S. Y. and Wasco, W., 1996. The gene defects responsible for familial Alzheimer's disease. Neurobiol Dis. 3, 159-168.

Tarcsa, E., Marekov, L. N., Mei, G., Melino, G., Lee, S. C. and Steinert, P. M., 1996. Protein unfolding by peptidylarginine deiminase. Substrate specificity and structural relationships of the natural substrates trichohyalin and filaggrin. J Biol Chem. 271, 30709-30716.

Thal, D. R., Capetillo-Zarate, E., Del Tredici, K. and Braak, H., 2006. The development of amyloid beta protein deposits in the aged brain. Sci Aging Knowledge Environ. 2006, re1.

Thal, D. R., Del Tredici, K. and Braak, H., 2004. Neurodegeneration in normal brain aging and disease. Sci Aging Knowledge Environ. 2004, pe26.

Thal, D. R., Rub, U., Orantes, M. and Braak, H., 2002. Phases of A beta-deposition in the human brain and its relevance for the development of AD. Neurology. 58, 1791-1800.

Townsend, K. P. and Pratico, D., 2005. Novel therapeutic opportunities for Alzheimer's disease: focus on nonsteroidal anti-inflammatory drugs. Faseb J. 19, 1592-1601.

Tseng, B. P., Kitazawa, M. and LaFerla, F. M., 2004. Amyloid beta-peptide: the inside story. Curr Alzheimer Res. 1, 231-239.

Tsuji, T., Shiozaki, A., Kohno, R., Yoshizato, K. and Shimohama, S., 2002. Proteomic profiling and neurodegeneration in Alzheimer's disease. Neurochem Res. 27, 1245-1253.

van der Vliet, A., Eiserich, J. P., O'Neill, C. A., Halliwell, B. and Cross, C. E., 1995. Tyrosine modification by reactive nitrogen species: a closer look. Arch Biochem Biophys. 319, 341-349.

Vassar, R., 2001. The beta-secretase, BACE: a prime drug target for Alzheimer's disease. J Mol Neurosci. 17, 157-170.

Vercauteren, F. G., Bergeron, J. J., Vandesande, F., Arckens, L. and Quirion, R., 2004. Proteomic approaches in brain research and neuropharmacology. Eur J Pharmacol. 500, 385-398.

Walsh, D. M., Klyubin, I., Fadeeva, J. V., Rowan, M. J. and Selkoe, D. J., 2002. Amyloid-beta oligomers: their production, toxicity and therapeutic inhibition. Biochem Soc Trans. 30, 552-557.

Watson, D., Castano, E., Kokjohn, T. A., Kuo, Y. M., Lyubchenko, Y., Pinsky, D., Connolly, E. S., Jr., Esh, C., Luehrs, D. C., Stine, W. B., Rowse, L. M., Emmerling, M. R. and Roher, A. E., 2005. Physicochemical characteristics of soluble oligomeric Abeta and their pathologic role in Alzheimer's disease. Neurol Res. 27, 869-881.

Wiltfang, J., Smirnov, A., Schnierstein, B., Kelemen, G., Matthies, U., Klafki, H. W., Staufenbiel, M., Huther, G., Ruther, E. and Kornhuber, J., 1997. Improved electrophoretic separation and immunoblotting of beta-amyloid (A beta) peptides 1-40, 1-42, and 1-43. Electrophoresis. 18, 527-532.

Wisniewski, T., Castano, E. M., Golabek, A., Vogel, T. and Frangione, B., 1994. Acceleration of Alzheimer's fibril formation by apolipoprotein E in vitro. Am J Pathol. 145, 1030-1035.

Wuhrer, M., Deelder, A. M. and Hokke, C. H., 2005. Protein glycosylation analysis by liquid chromatography-mass spectrometry. J Chromatogr B Analyt Technol Biomed Life Sci. 825, 124-133.

APPENDIX I

Quantification of the Aβ Peptide in Alzheimer's Plaques by Laser Dissection Microscopy Combined with Mass Spectrometry

by

Pascal Rüfenacht[1], Andreas Güntert[1], Bernd Bohrmann, Axel Ducret and Heinz Döbeli

[1]equal contribution to this work

published in *Journal of Mass Spectrometry*

JOURNAL OF MASS SPECTROMETRY
J. Mass Spectrom. 2005; **40**: 193–201
Published online in Wiley InterScience (www.interscience.wiley.com). DOI: 10.1002/jms.739

JMS

Quantification of the Aβ peptide in Alzheimer's plaques by laser dissection microscopy combined with mass spectrometry

Pascal Rüfenacht,[1†] Andreas Güntert,[1†] Bernd Bohrmann,[1] Axel Ducret[2] and Heinz Döbeli[1]*

[1] Pharma Research Basel, F. Hoffmann-La Roche Ltd, Grenzacherstrasse 124, CH-4070 Basel, Switzerland
[2] Roche Center for Medical Genomics, F. Hoffmann-La Roche Ltd, Grenzacherstrasse 124, CH-4070 Basel, Switzerland

Received 22 March 2004; Accepted 29 June 2004

The accumulation and aggregation of the beta-amyloid peptide (Aβ) in the brain represents a key factor in the pathogenesis of Alzheimer's disease (AD). Many of the transgenic mouse models for AD exhibit an amyloid pathology with neuritic plaques but they typically vary by the type and abundance of plaques identified in their brains and by the onset and severity of cognitive impairment. Thus, an important consideration in the characterization of AD transgenic mouse models should be the quantitative evaluation of the amyloid load in the brain together with a detailed physico-chemical analysis of Aβ from the deposited plaques. Here we present an analytical procedure to collect single amyloid plaques from anatomically defined brain regions by laser dissection microscopy that can be quantitatively assessed in their Aβ isoforms composition by matrix-assisted laser desorption/ionization time-of-flight mass spectrometry. Quantification was achieved by stable isotope dilution using calibrated ^{15}N-labeled Aβ standards that were spiked in the sample immediately after laser dissection. Using this method, we found that the amyloid loads in brain plaques isolated from the transgenic AD mouse model PS2APP or from human were similar. Total Aβ composition was estimated at ∼50–100 fmol per excised plaque disc, as confirmed by immunoblot analysis. N-Terminal truncated Aβ isoforms were identified in both transgene and human amyloid plaques but with significantly elevated levels in human samples.

KEYWORDS: Alzheimer's disease; Aβ peptide; laser dissection microscopy; matrix-assisted laser desorption/ionization time-of-flight mass spectrometry

INTRODUCTION

Alzheimer's disease (AD),[1] the most common form of dementia in humans, is histopathologically characterized by the intracellular aggregation of hyperphosphorylated tau protein in neurofibrillary tangles and by the extracellular accumulation of Aβ peptides in neuritic amyloid plaques, in particular in limbic and association cortices.[1] Cleavage of the amyloid precursor protein (APP) by the β- and γ-secretases releases both the $A\beta_{1-40}$ and $A\beta_{1-42}$ peptides, the latter being far more prone to aggregation, leading to Aβ deposition in the brain in the form of insoluble fibrils that can be visualized *in situ* by congo red and thioflavin S stains or by immunohistochemistry.[2,3] Plaque formation is thought to represent a dynamic process and the relative frequency of morphologically different plaque depositions changes during the progression of AD. Diffuse plaques are mostly prevalent in the preclinical stages whereas compact plaques are increasingly observed as the disease progresses to clinical dementia.[3,4] The apparent causal neurotoxicity of the amyloid plaques and the observation that early-onset familial forms of AD are characterized by the enhanced production of the secreted Aβ peptides have led to the amyloid hypothesis, which postulates that the Aβ peptide is a key factor in the pathogenesis of AD.[5] However, a molecular mechanism linking the accumulation of plaques with the memory loss characteristic for this disease has yet to be established.

Numerous transgenic mouse models, overexpressing the mutated human APP either alone or together with mutations of human presenilins known to affect the processing of APP, have been reported to mimic amyloidosis and plaque deposition with neuronal damage.[6–8] Recently, a triple transgenic mouse has been developed that exhibits tau pathological features and thereby displays most of the critical aspects of AD pathology.[9] In the frame of the amyloid hypothesis, Aβ appears to be causally involved in the aetiology of AD. Thus, an important consideration in the characterization of AD transgenic mouse models is the quantitative evaluation of the amyloid load in the brain together with a detailed physico-chemical analysis of Aβ from the deposited plaques. Plaque quality is currently best

*Correspondence to: Heinz Döbeli, Pharma Research Basel, F. Hoffmann-La Roche Ltd, Grenzacherstrasse 124, CH-4070 Basel, Switzerland. E-mail: heinz.doebeli@roche.com
†These authors contributed equally to this work.

investigated *in situ* by immunochemistry[10] or fluorescence staining[11] and by the propensity of amyloid plaques to be dissolved in conventional urea-containing sodium dodecyl sulfate (SDS) buffers.[12] Aβ composition has typically been relying on the availability of well-characterized antibodies directed against various epitopes of Aβ or by the use of urea-based SDS polyacrylamide gel electrophoresis (PAGE) analysis, for separation of the multiple Aβ isoforms, followed by immunodetection.[13] In addition, Stoeckli *et al.*[14] recently presented a new analytical method that allows the direct mass spectrometric evaluation of plaques from mouse brain thin sections. However, most of aforementioned techniques do not provide accurate quantification data as losses that occurred at the sample preparation levels are typically not considered.

In this paper, we present an alternative analytical approach based on the sectioning of the amyloid plaques by laser microdissection, the addition of a stable isotope-labeled Aβ internal standard and the detailed, quantitative analysis of the amyloid content of plaques by matrix-assisted laser desorption/ionization time-of-flight mass spectrometry (MALDI-TOFMS). The method was first cross-validated using the transgenic AD mouse PS2APP,[15] comparing the mass spectrometric method with a sensitive western blot analysis. Its usefulness was then demonstrated in showing significant quantitative differences in Aβ composition between amyloid plaques isolated from the transgenic AD mouse and from human. In particular, we believe that the ability to detect quantitative and qualitative differences from plaques collected according to their distinct staining properties within the same brain section represents an important asset to understand better the molecular basis of amyloid plaque formation.

EXPERIMENTAL

Amyloid peptide standards

^{15}N-Aβ_{1-42} (M35M$_{ox}$) peptide was produced by recombinant DNA technology using *E. coli* fed with [^{15}N]ammonium chloride.[16,17] Synthetic Aβ_{1-42} and Aβ_{p3-42} (Glu at position 3 converted to pyroglutamic acid) peptides were purchased from Bachem. The integrity of each Aβ species was checked by electrospray mass spectrometry and the exact concentration of the Aβ peptides' stock solutions, dissolved in 50% formic acid and used for spiking, were determined by amino acid analysis (Dr P. Hunziker, Protein Analysis Unit, University of Zürich, Switzerland).

Collection and preparation of brain slices

All animal experiments were performed in full accordance with the guidelines issued by the Swiss Veterinary Office. Twenty-month-old double-transgenic PS2APP mice[15] were obtained from Dr H. Bluethmann (F. Hoffmann-La Roche). Mice were killed either by cervical dislocation or by decapitation after anaesthesia with halothane. The skull pan was opened with scissors and the brain was removed and divided into hemispheres before freezing in dry-ice.

Human cortical brain tissue (kindly provided by Professor R. Fall, New Zealand) was collected from a single patient. The tissue was collected 2 h after death and immediately frozen at −80 °C.

Brain tissue sections of 10 μm thickness were excised from cortical areas using a Model CM3050 S cryostat microtome (Leica Microsystems). These slices were placed on a glass cover-slip and stored until staining at −20 °C. Cover-slips used for laser dissection microscopy were coated with a 1.35 μm thick polyethylene foil (LPC-MOMenT-Object slides, 8150, PALM Robot Microbeam).

Staining of brain thin sections

Prior to the staining procedures, brain tissue slices were rehydrated for 5 min with phosphate-buffered saline (PBS; 6 mM phosphate buffer, pH 7.4, 85 mM NaCl) and fixed on a glass slide by applying ice-cold 70% acetone for ∼1 min.

Sections visualized by immunostaining were washed twice for 2 min with 1 ml of PBS containing protease inhibitors (one protease inhibitor cocktail tablet (Catalog No. 1 836 145) per 50 ml; Roche Diagnostics) and unspecific binding sites were blocked for 15 min with 500 μl of PBS containing 1% BSA (bovine serum albumin fraction 5; Roche) and 1% ovalbumin (ovalbumin from hen egg white; Fluka). The slices were then incubated for 30 min at room temperature with 200 μl of a 3 μg ml^{-1} primary antibody BAP-2 solution (specific for the Aβ peptide epitope amino acids 2–8, kindly provided by Dr M Brockhaus, F. Hoffmann-La Roche). The samples were then washed three times for 5 min with 500 μl of PBS containing 1% BSA. Detection was performed using an Alexa Fluor 488-conjugated secondary antibody (goat anti-mouse antibody diluted 1 : 200 in PBS containing 1% BSA; Molecular Probes) applied for 30 min at room temperature. The preparations were then washed once for 5 min with 1 ml of PBS and once for 2 min with doubly distilled water before being air-dried and stored at −20 °C until further usage.

Congo red staining was performed using the diagnostic amyloid stain kit HT60 (Accustain Amyloid Stain, Congo Red, Sigma Diagnostics).

Thioflavin S was applied as a 1% solution for 3–5 min followed by a wash step with 70% ethanol for 3–5 min.

Plaque excision by laser dissection and ^{15}N-Aβ peptide spiking

Laser dissection microscopy was performed according to Schütze and Lahr.[18] An inverse fluorescence microscope (Axiovert 135; Carl Zeiss) was attached to a pulsed nitrogen laser (337 nm, PALM Robot MicroBeam) with beamsplitters to allow simultaneous visualization of the sample and laser dissection. Laser dissection was performed in a two-step process comprising cold ablation, an excision process based on a restricted photodecomposition process without heating[19] and laser pressure catapulting for contamination-free harvesting. Samples were visualized using the 10- or 20-fold objectives. Settings for laser focus and energy were re-optimized for each slide.

Immunostained mouse or human cortex sections were first air-dried for ∼30 min before individual amyloid plaques were excised by laser ablation. A single laser pulse of increased energy, with its focal plane slightly below the

sample, induced the transport of the excised material directly into the cap of a 500 µl Eppendorf tube held above the line of laser fire. By repeating this procedure several times, the excised material could be accumulated in a single cap filled with ~25 µl of liquid (either NuPAGE SDS Sample Buffer (Invitrogen) containing 8 M urea for SDS–PAGE or 70% formic acid or water for MALDI-TOFMS) for better adhesion of the material. After collection, the liquid was spun down at 15 500 *g* into the tube. The cap containing the plaques was then additionally rinsed twice with 30 µl of buffer, spun down and all fractions were pooled.

Amyloid plaque preparations analyzed by mass spectrometry were typically spiked with the ^{15}N-Aβ peptide internal standard immediately after laser dissection. Based on iterative cycles of experiments, 45 or 60 fmol of [^{15}N]Aβ peptide per dissected human or mouse plaque, respectively, were added to the samples to generate mass spectra profiles exhibiting the preferred 1:1 Aβ peak ratio between endogenous material and internal standard.

SDS–PAGE and western blots

The dried samples obtained after dissolution of the plaques in formic acid were neutralized with 50 µl of 1% (v/v) pyridine–water solution, dried again and then taken up in 25 µl of SDS sample buffer containing 8 M urea. Samples were analyzed on a 12% Bis-Tris NuPage SDS-PAGE system according to the manufacturer's recommendations (Invitrogen). Western blotting was performed according to Ida *et al*.[20] using Hybond-C extra, RPN303E nitrocellulose membrane (Amersham). Binding of Aβ to the membrane was enhanced by heating the blotted membrane for 3 min in a microwave oven (900 W) in PBS. Enhanced chemiluminescence detection of Aβ was performed with the monoclonal WO-2 as primary antibody (kindly provided by Dr K. Beyreuther, Heidelberg, Germany) and a horseradish peroxidase-labeled secondary antibody (Amersham).

Dissolution, endoproteinase Lys-C digestion and ZipTip desalting

Samples were incubated in 90 µl of 70% (v/v) formic acid–water solution overnight at room temperature, after which they were subjected to sonication (3 × 3 min in a water-bath at room temperature with intermediate vortex mixing). Dissolution of plaques with 1,1,1,3,3,3-hexafluoroi-2-propanol was not as effective as with formic acid. The formic acid was then evaporated in an evacuated centrifuge and the residue was dissolved in 10 µl of unbuffered 10 mM NH_4HCO_3 solution and digested with 15 ng of endoproteinase Lys-C (Wako) for 2 h at 20 °C. The resulting peptide fragments were adsorbed on a 0.6 µl RP-18 matrix ZipTip pipette tip (Millipore), desalted with 5% (v/v) methanol–water containing 0.1% (v/v) trifluoroacetic acid and eluted with 2.5 µl of 60% (v/v) acetonitrile–water containing 0.1% (v/v) trifluoroacetic acid.

Mass spectrometry

Mass spectrometric analysis of amyloid plaques was perfomed in triplicate using three consecutive dilutions to circumvent possible signal suppression due to salt contamination and poor crystallization conditions. The 2.5 µl of eluate was mixed with 2.5 µl of a α-cyano-4-hydroxycinnamic acid solution (Sigma; 5 mg ml^{-1} in 50% (v/v) acetonitrile–water) containing bradikynin and adrenocorticotropic hormone (ACTH 18–39) as internal standards and 1 µl thereof was spotted on a standard stainless-steel Bruker MALDI 384-target plate (Bruker Daltonics). The remaining solution (4 µl) was diluted with 6 µl of the matrix solution and 6 µl of the 60% (v/v) acetonitrile–water containing 0.1% (v/v) trifluoroacetic acid solution (generating a 1:4 dilution) and 1 µl thereof was spotted on the MALDI target. The resulting solution (15 µl) was then further diluted with 30 µl of the matrix solution and 30 µl of the 60% (v/v) acetonitrile–water containing 0.1% (v/v) trifluoroacetic acid solution (generating a 1:12 dilution) and 1 µl thereof was also spotted on the MALDI target.

All measurements were performed on a Bruker UltraFlex Tof/Tof mass spectrometer in reflector mode using standard operating parameters. To reduce signal variability due to sample preparation heterogeneity, spectra were acquired in the automatic acquisition mode in 10 cycles of 20 shots each using a different spot location after a maximum of four cycles. A 20-shot spectrum was accepted for averaging by Bruker's fuzzy logic evaluation software if the signal-to-noise ratio of the highest peak between m/z 1200 and 2100 was >4 and its resolution >3000.

Peptide sequencing by tandem mass spectrometry was performed on the same instrument operated in the LIFT mode according to the manufacturer's standard operating parameters. Tandem mass spectra were analyzed using the Mascot search algorithm (http://www.matrixscience.com/).

Mass spectrometric quantification of Aβ

Quantification of the Aβ content in amyloid plaques was achieved by directly measuring the most intense peaks-height ratios $A\beta_{1-16}/^{15}$N-$A\beta_{1-16}$ and $A\beta_{17-28}/^{15}$N-$A\beta_{17-28}$, assuming 98% labeling of the ^{15}N-peptides as judged from the isotopic envelope (Fig. 1(a)). The concentration range for which a linear relationship could be validated was tested using various amounts of ^{14}N-Aβ and ^{15}N-Aβ synthetic peptides mixed in various ratios and analyzed by mass spectrometry as described above (Fig. 1(b)). Spectra were accepted for quantification if the following analytical criteria were met: the signals for $A\beta_{1-16}$, ^{15}N-$A\beta_{1-16}$, $A\beta_{17-28}$ and ^{15}N-$A\beta_{17-28}$ had to exceed a signal-to-noise ratio of 4 and the ratio $A\beta_{17-28}/^{15}$N-$A\beta_{17-28}$ had to be within the range 3:7 to 7:3. In addition, mass spectra that were obviously contaminated with foreign peaks (e.g. keratins) were excluded from the quantification process.

For simplification, the three mass spectra obtained from one amyloid preparation (undiluted and 1:4 and 1:12 dilution, see above) were considered as three independent measurements, that is, every valid mass spectrum generated from experiments performed with a given number of plaques was equally weighted for quantification purposes.

Quantification was performed by using the intensity of the highest peak of the corresponding peak pattern. Compared with the integration of the area of the entire peak pattern, the amount of $A\beta_{1-16}$ is underestimated by 1.9% and that of $A\beta_{17-28}$ by 4.6%.

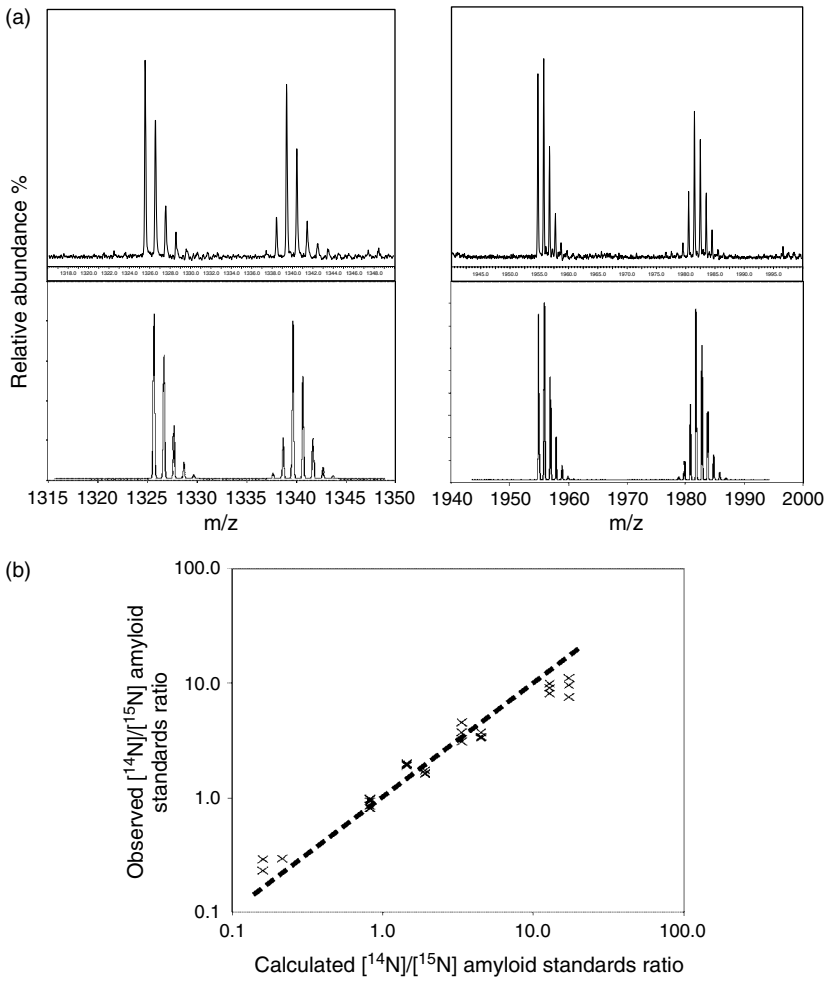

Figure 1. Quantification by mass spectrometry. (A) Observed (upper panels) and calculated (lower panels) isotopic ratio for two amyloid peptides, Aβ_{17-28} (*m/z* 1325.7 and 1339.7) and Aβ_{1-16} (*m/z* 1954.8 and 1981.8) for ^{14}N- and ^{15}N-labeled peptides, respectively. The calculation is based on a ^{15}N labeling degree of 98%. For quantification, the intensities of the highest peaks were measured and put into relation to the height of the standard. (B) Linearity of signal. Known amounts of ^{14}N-Aβ and ^{15}N-Aβ were mixed and processed according to the protocol. The data given in this figure represent the mixtures of synthetic Aβ_{1-42}, which was compared with two different ^{15}N-Aβ_{1-42} lots. One of the standards was predominantly monomeric; the second one, which derived from the first lot, was allowed for aggregation.

RESULTS

Assay principle

Quantitative Aβ peptide analysis from Alzheimer plaques was achieved by combining laser dissection microscopy with mass spectrometry using an internal standard (Fig. 2). Selected amyloid plaques were dissected from brain cryosections by laser dissection and were transferred into a test-tube by laser catapulting. The plaques were treated overnight in 70% formic acid to solubilize the amyloid fibrils and, after removal of the acid by evaporation, the dissolved Aβ peptides were subjected to proteolysis using the endoproteinase LysC. The generated fragments, in particular the N-terminal peptide Aβ_{1-16} and the middle fragment Aβ_{17-29}, have been demonstrated to be detected with a 100-fold higher sensitivity than the full-length Aβ_{1-40} or Aβ_{1-42} peptides.[21] The preparations were then concentrated and desalted using ZipTips before being spotted on the MALDI target. This last step was important to enhance sensitivity and to prevent spectral overlap of the main sodium adduct with the internal standards, which would have made an accurate quantification difficult. Quantification of the endogenous Aβ peptide was performed using a known amount of ^{15}N-Aβ peptide[16] directly added to the dissected plaque samples. Since endogenous and ^{15}N-Aβ peptides do not differ chemically from each other, except for the presence of the ^{15}N heavy isotope in the standard, all experimental losses were assumed to be equally reflected on both Aβ species, thus allowing absolute quantification by comparing peak ratios.

Identification of endogenous Aβ

The MALDI-TOFMS profiles obtained from amyloid plaques were virtually free from non-Aβ components (Fig. 3). The most dominant peaks were accounted by the two N-terminal fragments, Aβ_{1-16} and Aβ_{17-28} (*m/z* 1954.8 and 1325.7, respectively), accompanied by their respective internal standards (*m/z* 1981.8 and 1339.7, respectively). The identity of each of those fragments was further substantiated by sequencing using tandem mass spectrometry (Fig. 4). The C-terminal fragments Aβ_{29-40} or Aβ_{29-42} were not detected using these

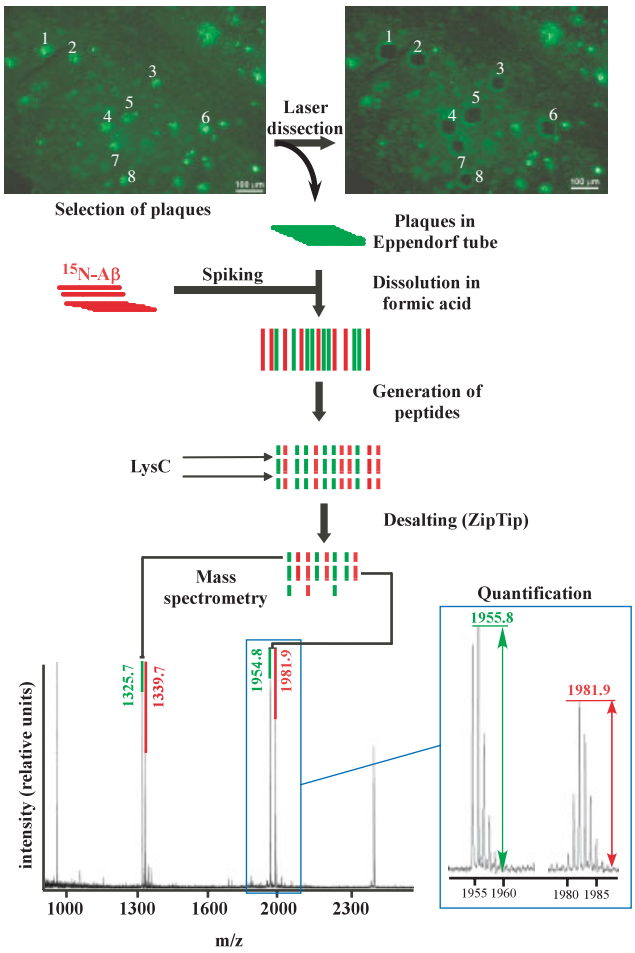

Figure 2. Analytical procedure. The procedure's starting material was a thin section of a brain slice containing the structures of interest. Plaques were selected, excised under the microscope by a laser beam and transferred into a test-tube. The preparations obtained were spiked with an appropriate amount of ^{15}N-Aβ internal standard and the plaques were dissolved in formic acid. The Aβ peptides were then subjected to endoproteinase Lys-C digestion and the generated fragments were concentrated and desalted using a ZipTip pipette tip before mass spectrometric analysis. Quantification was achieved by comparing the peak-height ratio for each observed Aβ fragment with the added ^{15}N-Aβ internal standard.

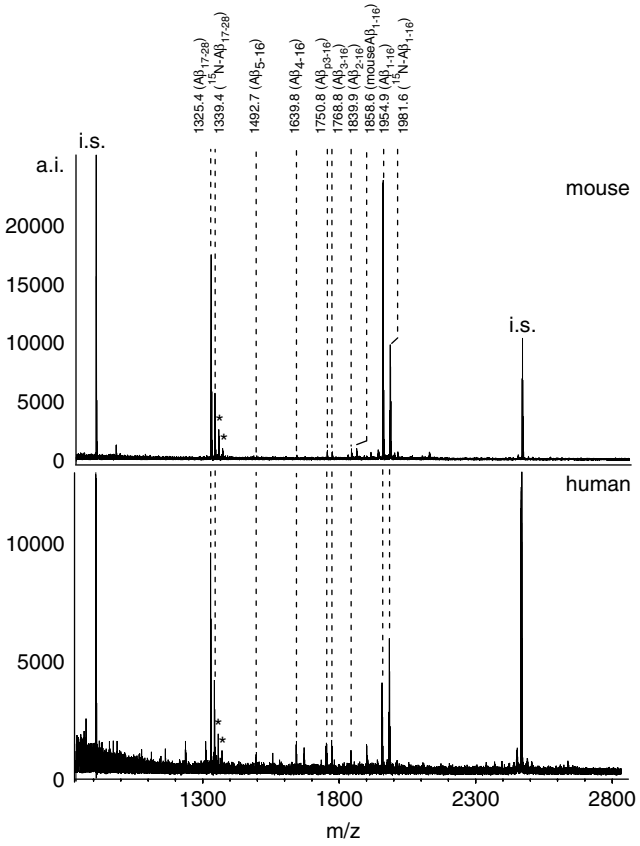

Figure 3. Mass spectrometric profiles from mouse and human amyloid plaques. The profiles were generated with 30 mouse plaques spiked with 1.8 pmol of ^{15}N-Aβ (upper panel) and 30 human plaques spiked with 1.35 pmol of ^{15}N-Aβ (lower panel). Typical for human plaques is the deficit of the N-terminal fragment Aβ_{1-16}, reflected by the inversed peak proportions (see also Table 1), which is indicative of the higher degree of N-terminal truncations. Occasionally, in the mouse specimen the endogenous Aβ_{1-16} fragment bearing mutations at three positions could be observed. i.s., internal standard; asterisks, formylation products.

conditions. These hydrophobic peptides were poorly ionized during the MALDI process and they may have been only partially recovered from the ZipTip desalting step. Further, we identified several additional peaks that corresponded by mass to the additional N-terminal fragments Aβ_{2-16} (m/z 1839.9), Aβ_{3-16} (m/z 1768.8), Aβ_{p3-16} (Glu$_3$ converted to pyroglutamic acid; m/z 1750.8), Aβ_{4-16} (m/z 1639.8) and Aβ_{5-16} (m/z 1492.7). The identity of Aβ_{p3-16} was also confirmed by tandem mass spectrometric analysis (Fig. 4). The corresponding ^{15}N-labeled fragments were not observed even if the spiked Aβ internal standard was applied to the brain slice before laser microdissection. This finding strongly suggests that the observed N-terminal Aβ peptide heterogeneities were already present in the amyloid plaque at the sampling time and that they were not generated, among others, during laser ablation, dissolution with formic acid or mass spectrometric analysis. Finally, in the analysis of amyloid plaques dissected from mouse brain tissue, a tiny peak at mass m/z 1858.9 potentially corresponding to the endogenous rodent Aβ_{1-16} fragment was also detected (Fig. 3), in agreement with the findings of Pype *et al.*[22]

Sensitivity and quantification

Quantification of the human Aβ peptide was achieved by comparing the peak height of the two Aβ ^{14}N-labeled fragments' most intense peaks generated from the endogenous material (at m/z 1325.7 and 1955.9) with the peak height of the corresponding Aβ fragments' ^{15}N monoisotopic peak generated from the added internal standard (at m/z 1339.7 and 1981.8; Fig. 2). These measurements were repeated numerous times over a wide range of conditions to ensure accurate statistics (Table 1). The mass spectral profiles from which these measurements were derived had to fulfil the following criteria to be accepted for this purpose. The signal-to-noise ratio of the four peaks of interest had to exceed four and the

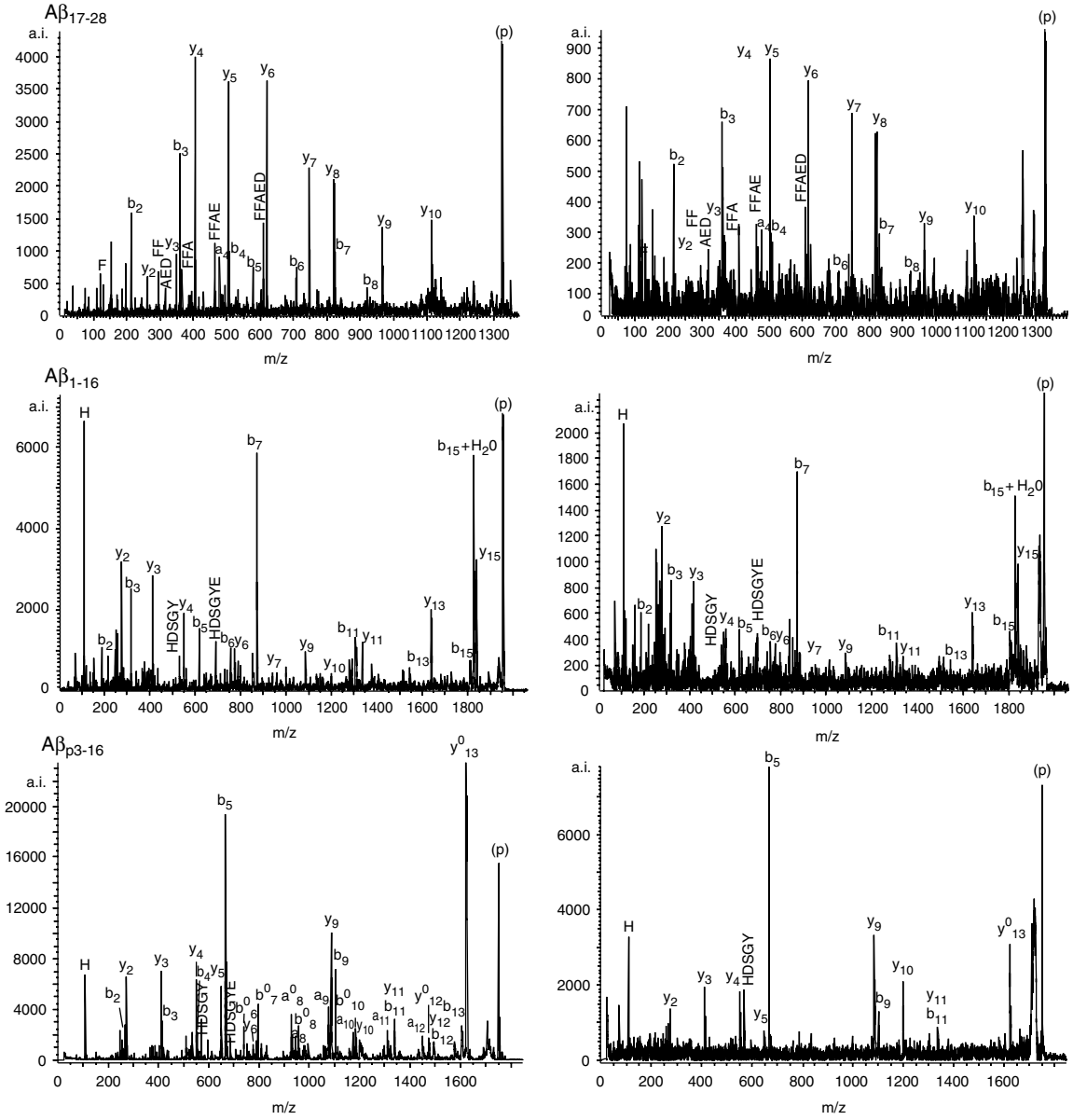

Figure 4. Tandem mass spectrometric analysis of three Aβ fragments. Aβ_{17-28} (upper panel), Aβ_{1-16} (middle panel) and Aβ_{p3-16} (lower panel) were derived either from standards (left panels) or from amyloid plaques (right panels). The most abundant fragments are labeled.

^{14}N-Aβ_{17-28}/^{15}N-Aβ_{17-28} peak-height ratio had to be within the range 3 : 7 to 7 : 3. Not surprisingly, the likelihood of obtaining a suitable mass spectral profile decreased as a decreasing number of plaques were analyzed. Using these criteria, we found roughly equivalent amounts of Aβ amyloid peptide per excised plaque in both brain specimens (87 ± 29 fmol in mouse tissue and 61 ± 26 fmol in human tissue, calculated from the Aβ_{17-28} fragment).

Differences between human and mouse amyloid plaques

Interestingly, in both tissues, the measured amount of the Aβ_{1-16} peptide was reproducibly lower than that of the corresponding Aβ_{17-28} fragment. In mouse, the Aβ_{1-16}/Aβ_{17-28} ratio was 77% whereas in human it was only 51%. In the latter, this deficit could clearly be correlated with the increased presence of truncated N-terminal Aβ peptides.[23] Their relative distribution in mouse and human is shown in Fig. 5. Whereas most of the N-terminal peptide's truncations appeared to be limited to the first two amino acids in mouse, additional species in higher abundance were present in human, including Aβ_{4-16}, Aβ_{5-16} and Aβ_{p3-16}. Their increased presence in human can be observed as a 'right-shifted' distribution compared with what was observed in the mouse (Fig. 5). It is noteworthy that none of those derivatives could be detected with the ^{15}N-labeled internal standard, strongly indicating that these N-terminal truncated Aβ peptides were not artefactual.

The sensitivity and the dynamic range of the method were compared with a high-sensitivity western blot.[20] A selected number of plaques were excised by laser dissection, dissolved with formic acid, dried down in a Speed-Vac and neutralized with pyridine, before being resuspended in an SDS-PAGE sample buffer containing 8 M urea. After

Table 1. Quantitation of Aβ peptide in mouse and human amyloid plaques[a]

Origin of Plaques	Plaques per experiment	Number of experiments	Number of MS profiles	Number of quantifiable MS profiles	$A\beta_{17-28}$ fmol/plaque	$A\beta_{1-16}$ fmol/plaque	Ratio $A\beta_{1-16}/A\beta_{17-28}$
mouse	1	15	42	16 (38%)	59	54	0.92
mouse	2	8	22	1 (4%)	104	23	0.22
mouse	5	2	6	4 (67%)	60	55	0.92
mouse	10	4	12	11 (92%)	72	61	0.85
mouse	15	1	3	1 (33%)	73	45	0.62
mouse	16	2	6	5 (83%)	50	34	0.68
mouse	25	2	6	6 (100%)	131	107	0.82
mouse	30	2	6	6 (100%)	136	126	0.93
mouse	36	2	6	6 (100%)	112	96	0.86
mouse	49	2	6	6 (100%)	75	68	0.91
Average over all experiments		40		62	87 +/− 29	67 +/− 31	0.77
human	1	6	15	0	—	—	—
human	2	2	5	0	—	—	—
human	3	10	29	7 (24%)	75	40	0.53
human	5	5	15	5 (33%)	71	41	0.57
human	9	6	18	5 (28%)	76	62	0.82
human	10	2	6	4 (67%)	111	52	0.47
human	15	2	6	1 (17%)	73	23	0.31
human	25	2	6	3 (50%)	36	22	0.60
human	30	10	30	13 (43%)	21	10	0.49
human	36	2	6	5 (83%)	35	18	0.51
human	49	3	9	5 (56%)	52	15	0.29
Average over all experiments		50		48	61 +/− 26	31 +/− 17	0.51

[a] The Aβ peptide contents in human cortex (from one case) and mouse amyloid plaques (from three different mouse brains all with an age of 20 months) were calculated as described in the Experimental section. The column 'Quantifiable MS profiles' represents those mass spectral profiles fulfilling the quantification criteria defined in the section 'Mass spectrometric quantification of Aβ'. The fmol/plaque values indicated here represent only the fraction of the excised plaque that was enclosed in the analyzed 10 μm thin section. The true Aβ content could be extrapolated if amyloid plaques were assumed to have a spherical character. Depending on the plaque's true diameter, the amounts indicated in the table should be multiplied several fold.

electrophoresis, samples were blotted on to a nitrocellulose membrane and probed with an Aβ peptide-specific antibody (data not shown). The plaques' amyloid content was estimated by applying known amounts of a calibrated amyloid solution to the same gel. The average amount of Aβ peptide found per plaque and the limit of detection were of the same order of magnitude for both methods. However, quantification by the mass spectrometric method was considerably more accurate owing to the presence of an internal standard compensating for the experimental losses.

DISCUSSION

To our knowledge, this is the first published report describing a procedure to quantify directly the Aβ content from individual plaques by mass spectrometry. This method, by maintaining the sample's topological information, also differentiates itself from other mass spectrometry-based analyses requiring brain tissue homogenization[23,26] or pooling of cell supernatants[24,25] An alternative approach allowing the direct investigation of Aβ peptide by imaging mass spectrometry has been presented by Stoeckli *et al*.[14] Using brain tissue sections from the APP23 transgenic AD mouse, they were able to demonstrate the presence of several C-terminal variants such as $A\beta_{1-37}$, $A\beta_{1-38}$, $A\beta_{1-39}$, $A\beta_{1-40}$, $A\beta_{1-42}$ and $A\beta_{1-42ox}$. However, in the absence of a suitable internal standard, the plaques' Aβ peptide content was only measured in a relative fashion.

Since reasonable mass spectral profiles can be obtained from a few hundred picograms of Aβ peptide, it is now possible to compare plaques selected according to morphological or topological criteria. In this respect, it has become evident to us that human and humanized mouse plaques differ in several aspects. Under the microscope, amyloid plaques from mouse tissue showed a virtually identical staining with Congo red, thioflavin or anti-Aβ antibodies whereas most plaques from human tissue were reliably detected only by immunostaining. Mouse plaques were readily dissolved in an 8 M urea-containing SDS buffer whereas the dissolution of human plaques required the harsher formic acid treatment. Finally, the mouse and the human plaques clearly differ in their levels of N-terminal heterogeneity, both in amount and in complexity. These findings all independently suggest that experimental

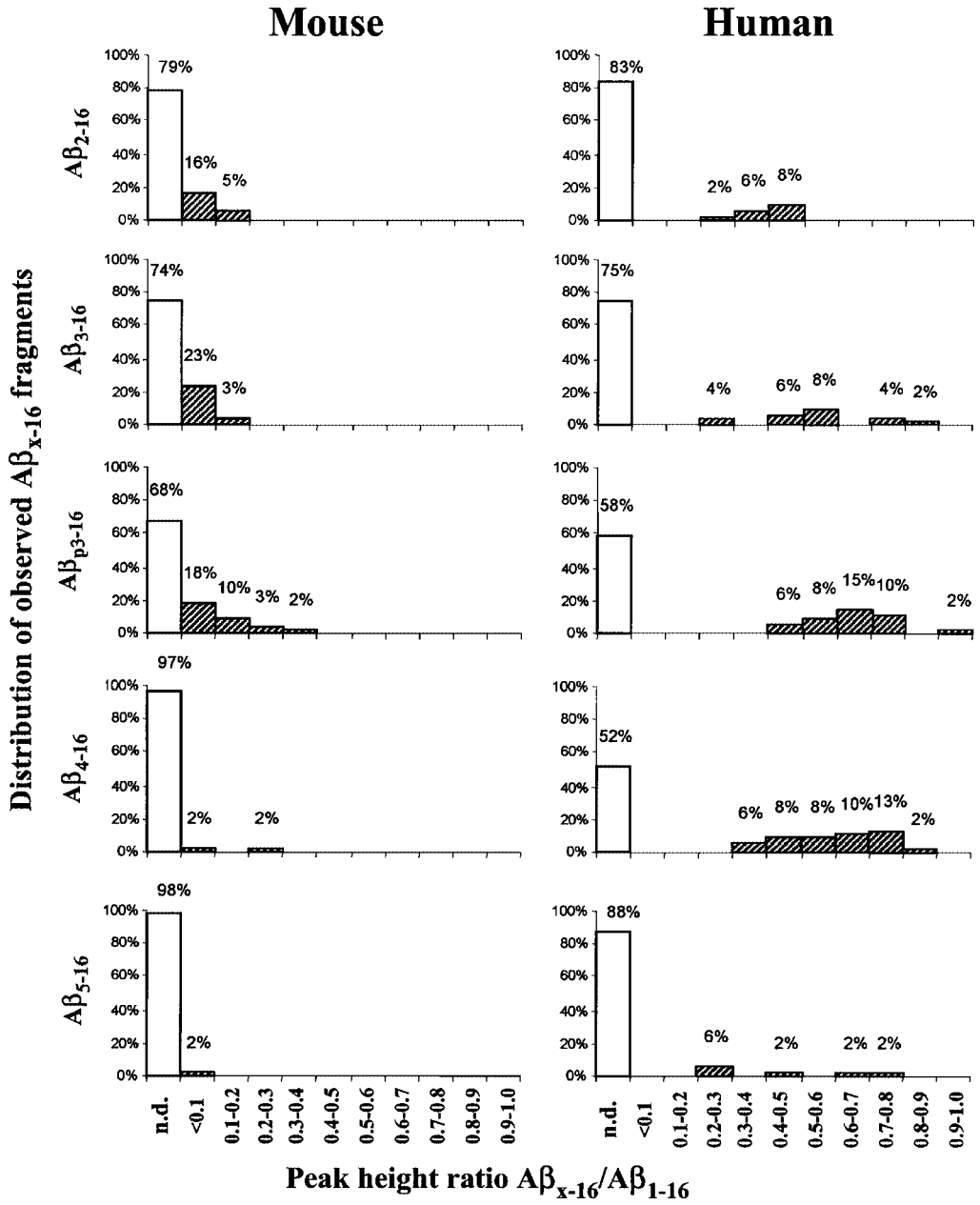

Figure 5. Distribution of truncated N-terminal Aβ peptides in human and mouse amyloid plaques. The histograms show an evaluation of mass spectrometric profiles derived from 48 human plaque samples (from one brain specimen) and 62 mouse plaque samples (from three different mice). The height of the hatched bars in the histogram indicates the percentage of mass spectrometric experiments in which an Aβ species was detected at the indicated ratio. The empty bars represent the fraction of those profiles, where no truncated Aβ versions could be observed. The larger number of N-terminal truncated peptides found in human is observed as a right-hand shift compared with what is observed in the mouse.

evidences derived from humanized mouse plaques may not necessarily directly apply to human plaques.

The abundance and integrity of two main N-terminal peptides were effectively assessed by the analytical procedure, in agreement with the identification of N-terminal Aβ variants reported for brain extracts of the insoluble Aβ compartment of AD patients[25] and transgenic mice carrying the London APP mutant.[22] However, the small fragment $A\beta_{11-16}$[22] and the main C-terminal fragments $A\beta_{29-40}$ and $A\beta_{29-42}$ were not detected using the described instrumental set-up. We were nevertheless able, using a procedure omitting the digestion and the desalting steps but otherwise similar to the one described above, to detect the full-length $A\beta_{1-40}$ and $A\beta_{1-42}$ amyloid peptides, albeit at a much lower sensitivity than the individual digested peptides (data not shown). We were surprised that only a few non-Aβ-derived peaks were detected in the mass spectral profiles. While the Aβ peptide represents the main component of senile plaques, many more proteins have been detected by immunological methods and the list of these proteins is still growing.[27] This may be due to the vast excess of Aβ in the plaques, the fixation procedure of the sample on the glass slide prior to laser dissection, the tailoring of the fragmentation of Aβ to optimize ionization and/or ionization suppression resulting

in the quenching of signals from minor components. A preliminary attempt to analyze digested plaques components by liquid chromatography/electrospray mass spectrometry revealed two additional proteins, cystatin A and ubiquitin, thus indicating that the presented method, *per se*, is suitable for characterizing further plaque proteins. (During the review process, we became aware of an on-line publication which contains a list of 488 proteins identified in amyloid plaques by mass spectrometry.[28])

Acknowledgements

We thank Daniela Matscheko for performing some initial experiments, Nicole Soder for producing ^{15}N-Aβ, Françoise Gerber for help in tissue staining and thin sectioning, Arno Friedlein for verifying the Aβ fragments by tandem mass spectrometry and Christian Czech for critical help in establishing the high-sensitivity western blot assays.

REFERENCES

1. Selkoe DJ. Alzheimer's disease: genes, proteins, and therapy. *Physiol. Rev.* 2001; **81**: 741.
2. Dickson TC, Vickers JC. The morphological phenotype of beta-amyloid plaques and associated neuritic changes in Alzheimer's disease. *Neuroscience* 2001; **105**: 99.
3. Yamaguchi H, Hirai S, Morimatsu M, Shoji M, Ihara Y. A variety of cerebral amyloid deposits in the brains of the Alzheimer-type dementia demonstrated by beta protein immunostaining. *Acta Neuropathol.* 1988; **76**: 541.
4. Thal DR, Rüb U, Schultz C, Sassin I, Ghebremedhin E, Del Tredici K, Braak E, Braak H. Sequence of A beta-protein deposition in the human medial temporal lobe. *J. Neuropathol. Exp. Neurol.* 2000; **59**: 733.
5. Hardy J, Selkoe DJ. The amyloid hypothesis of Alzheimer's disease: progress and problems on the road to therapeutics. *Science* 2002; **297**: 353.
6. Price DL, Sisodia SS. Mutant genes in familial Alzheimer's disease and transgenic models. *Annu. Rev. Neurosci.* 1998; **21**: 479.
7. Higgins GA, Jacobsen H. Transgenic mouse models of Alzheimer's disease: phenotype and application. *Behav. Pharmacol.* 2003; **14**: 419.
8. Morgan D. Learning and memory deficits in APP transgenic mouse models of amyloid deposition. *Neurochem. Res.* 2003; **28**: 1029.
9. Oddo S, Caccamo A, Kitazawa M, Tseng BP, LaFerla FM. Amyloid deposition precedes tangle formation in a triple transgenic model of Alzheimer's disease. *Neurobiol. Aging* 2003; **24**: 1063.
10. Hanzel DK, Trojanowski JQ, Johnston RF, Loring JF. High-throughput quantitative histological analysis of Alzheimer's disease pathology using a confocal digital microscanner. *Nat. Biotechol.* 1999; **17**: 53.
11. Styren SD, Hamilton RL, Styren GC, Klunk WE. X-34, a fluorescent derivative of congo red: a novel histochemical stain for Alzheimer's disease pathology. *J. Histochem. Cytochem.* 2000; **48**: 1223.
12. Kuo YM, Kokjohn TA, Beach TG, Sue LI, Brune D, Lopez JC, Kalback WM, Abramowski D, Sturchler-Pierrat C, Staufenbiel M, Roher AE. Comparative analysis of amyloid-β chemical structure and amyloid plaque morphology of transgenic mouse and Alzheimer's disease brains. *J. Biol. Chem.* 2001; **276**: 12 991.
13. Wiltfang J, Smirnov A, Schnierstein B, Kelemen G, Matthies U, Klafki HW, Staufenbiel M, Hüther G, Rüther E, Kornhuber J. Improved electrophoretic separation and immunoblotting of beta-amyloid (Ab) peptides 1–40, 1–42 and 1–43. *Electrophoresis* 1997; **18**: 527.
14. Stoeckli M, Staab D, Staufenbiel M, Wiederhold KH, Signor L. Molecular imaging of amyloid β peptides in mouse brain sections using mass spectrometry. *Anal. Biochem.* 2002; **311**: 33.
15. Richards JG, Higgins GA, Ouagazzal AM, Ozmen L, Kew JNC, Bohrmann B,Malherbe P, Brockhaus M, Loetscher H, Czech C, Huber G, Bluethmann H, acobsen H, Kemp JA. PS2APP transgenic mice, coexpressing hAPPswe andhPS2mut, show age-related discrete brain amyloid deposition and inflammationassociated with cognitive deficits. *J. Neurosci.* 2003; **23**: 8989.
16. Riek R, Güntert P, Döbeli H, Wipf B, Wüthrich K. NMR studies in aqueous solution fail to identify significant conformational differences between the monomeric forms of two Alzheimer peptides with widely different plaque- competence, Aβ(1–40)ox and Aβ (1–42)ox. *Eur. J. Biochem.* 2001; **268**: 5930.
17. Döbeli H, Draeger N, Huber G, Jakob P, Schmidt D, Seilheimer B, Stüber D, Wipf B, Zulauf M. A biotechnolocal method provides accesss to aggregation competent monomeric Alzheimer's 1–42 residue amyloid peptide. *Biotechnology* 1995; **13**: 988.
18. Schütze K, Lahr G. Identification of expressed genes by laser-mediated manipulation of single cells. *Nat. Biotechnol.* 1998; **16**: 737.
19. Srinivasan R. Ablation of polymers and biological tissue by ultraviolet lasers. *Science* 1986; **234**: 559.
20. Ida N, Hartmann T, Pantel J, Schroder J, Zerfass R, Forstl H, Sandbrink R, Masters CL, Beyreuther K. Analysis of Heterogenous βA4 peptides in human cerebrospinal fluid and blood by a newly developed sensitive western blot assay. *J. Biol. Chem.* 1996; **271**: 22 908.
21. Grüninger-Leitch F, Berndt P, Langen H, Nelboeck P, Döbeli H. Identification of β-secretase-like activity using a mass spectrometry-based assay system. *Nat. Biotechnol.* 2000; **18**: 66.
22. Pype S, Moechars D, Dillen L, Mercken M. Characterization of amyloid beta peptides from brain extracts of transgenic mice overexpressing the London mutant of human amyloid precursor protein. *J. Neurochem.* 2003; **84**: 602.
23. Naslund J, Schierhorn A, Hellman U, Lannfelt L, Roses AD, Tjernberg LO, Silberring J, Gandy SE, Winblad B, Greengard P, Nordstedt C, Terenius L. Relative abundance of Alzheimer A beta amyloid peptide variants in Alzheimer disease and normal aging. *Proc. Natl. Acad. Sci. USA* 1994; **91**: 8378.
24. Wang R, Sweeney D, Gandy SE, Sisodia SS. The profile of soluble amyloid β protein in cultured cell media. *J. Biol. Chem.* 1996; **271**: 31 894.
25. Huse JT, Liu K, Pijak DS, Carlin D, Lee VM, Doms RW. Secretase processing in the trans-Golgi network preferentially generates truncated amyloid species that accumulate in Alzheimer's disease brain. *J. Biol. Chem.* 2002; **277**: 16 278.
26. Sergeant N, Bombois S, Ghestem A, Drobecq H, Kostanjevecki V, Missiaen C, Wattez A, David JP, Vanmechelen E, Sergheraert C, Delacourte A. Truncated beta-amyloid peptide species in pre-clinical Alzheimer's disease as new targets for the vaccination approach. *J. Neurochem.* 2003; **85**: 1581.
27. Hashimoto T, Wakabayashi T, Watanabe A, Kowa H, Hosoda R, Nakamura A, Kanazawa I, Arai T, Takio K, Mann DM, Iwatsubo T. CLAC: a novel Alzheimer amyloid plaque component derived from transmembrane precursor, CLAC-P/collagen type XXV. *EMBO J.* 2002; **21**: 1524.
28. Liao L, Cheng D, Wang J, Duong DM, Losik TG, Gearing M, Rees HD, Lah JJ, Levey AI, and Peng J. Proteomic characterization of postmortem amyloid plaques isolated by laser capture microdissection. *JBC Papers in Press* **25**: June 2004; Manuscript M403672200.

APPENDIX II

High Sensitivity Analysis of Aβ Composition in Amyloid Deposits from Human and PS2APP Mouse Brain

by

Andreas Güntert, Heinz Döbeli and Bernd Bohrman

***Neuroscience,* in press**

High Sensitivity Analysis of Aβ Composition in Amyloid Deposits from Human and PS2APP Mouse Brain

Andreas Güntert[a], Heinz Döbeli[a] and Bernd Bohrmann[a]*

[a]Pharma Research Basel, F. Hoffmann - La Roche Ltd, Grenzacherstrasse 124, CH-4070 Basel, Switzerland

*corresponding author: Tel: +41-61-688-8369; Fax.: +41-61-688-1720.
E-mail address: bernd.bohrmann@roche.com

Key words: mass spectrometry, pathological aging, pyroglutamate, ultrastructure, laser dissection microscopy, Alzheimer's disease

Cortical amyloid-beta (Aβ) deposition is considered essential in Alzheimer's disease (AD) and is also detectable in nondemented individuals with pathologic aging (PA). The present work presents a detailed analysis of the Aβ composition in various plaque types from human AD and PA cases, compared to plaque Aβ isolated from PS2APP mice. To determine minute amounts of Aβ from 30 to 50 laser dissected amyloid deposits, we used a highly sensitive mass spectrometry procedure after restriction protease Lys-C digestion. This approach allowed the analysis of the amino-terminus and, including a novel ionization modifier, for the first time the carboxy-terminus of Aβ at a detection limit of ~200 fmoles. In addition, full length Aβ 40/42 and pyroglutamate 3-42 was analyzed using a highly sensitive urea-based Western blot procedure. Generally, Aβ fragments were less accessible in human deposits, indicative for more posttranslational modifications. Thioflavine S positive cored plaques in AD were found to contain predominantly Aβ 42, whereas thioflavine S positive compact plaques and vascular amyloid consist mostly of Aβ 40. Diffuse plaques from AD and PA, as well as from PS2APP mice are composed predominantly of Aβ 1-42. Despite biochemical similarities in human and PS2APP mice, immuno-electron microscopy revealed an extensive extracellular matrix associated to Aβ fibrils in AD, specifically in diffuse plaques. Amino-terminal truncations of Aβ, especially pyroglutamate 3-40/42, are more frequently found in human plaques. In cored plaques we measured an increase of N-terminal truncations of ~20% between Braak stage IV to VI. In contrast, diffuse plaques of AD and PA cases, show consistently only low levels of amino-terminal truncations. Our data support the concept that diffuse plaques represent initial Aβ deposits but indicate a structural difference for Aβ depositions in human AD compared to PS2APP mice already at the stage of diffuse plaque formation.

Manuscript [II],
Neuroscience, in press

INTRODUCTION

Alzheimer's disease (AD) is characterized by a wide array of neuropsychiatric alterations, the most dominant being memory loss. Pathologically, AD brains show extracellular protein deposits of amyloid-β (Aβ) in different types of senile plaques and intraneuronal bundles of paired helical filaments (PHF) of phosphorylated tau protein, referred to as neurofibrillary tangles.

Aβ peptides are the main protein component of plaques (Glenner et al., 1984) and derive from a proteolytic cleavage of the amyloid precursor protein (APP), a membrane-spanning glycoprotein (Kang et al., 1987, Tanzi et al., 1987). Aβ peptides are secreted upon sequential cleavage of APP by β-secretase, a type I transmembrane glycosylated aspartyl protease, and γ-secretase, a large protein complex that includes at least four proteins (Nunan and Small, 2002, Haass, 2004). Due to heterogeneous γ-secretase cleavage sites, a series of Aβ peptides, including the major species Aβ 1-40 and Aβ 1-42, are produced.

AD occurs predominantly as a sporadic, age-dependent disease, but several inherited variants were also identified. Gene mutations which cause an early onset familial AD (FAD) are known and all these mutations lead to an increased secretion of Aβ, especially Aβ 42. Therefore, it is tempting to assume that the pathogenesis in AD is strongly related to an accumulation of Aβ (Selkoe, 1991, Hardy and Higgins, 1992). Aβ 1-42 is considered crucial in β-amyloidogenesis (Jarrett et al., 1993) being the initially deposited Aβ variant (Iwatsubo et al., 1994, Iwatsubo et al., 1995). In addition to the C-terminal heterogeneity of Aβ peptides, a variety of N-terminal truncated Aβ 40/42 species are reported (Miller et al., 1993, Sergeant et al., 2003, Miravalle et al., 2005, Rufenacht et al., 2005).

Aβ deposits can also be found in a remarkable number of cognitively normal PA individuals. These deposits primarily occur as diffuse amyloid depositions, with a different distribution (predominantly in cortical regions) compared to AD patients brains (Thal et al., 2004).

To investigate the role of Aβ in AD, a variety of transgenic mouse strains have been developed that utilize mutant human APP and presenilin 1 and 2 mutations. Several transgene mouse models that exhibit AD-like phenotypes, especially amyloid deposits, astroglial activation, synaptic loss and dysfunction, memory deficits and finally neurodegeneration are described (McGowan et al., 2006). However, the available AD mouse models only partially display the human pathophysiology and the morphological appearance of plaques from human brain are different from those observed in some transgenic mice (Masliah et al., 1996, Kuo et al., 2001). Recently, triple transgenic mice harbouring three mutant genes, i.e. APP, presenilin 1 and tau, have been developed (Oddo et al., 2003).

Considering the low level of neuron loss observed in many of the transgenic AD models (King and Arendash, 2002, Hu et al., 2003), other factors beside full length Aβ 40 and Aβ 42 may account for the massive neurodegeneration observed in AD patients. We have previously quantified by mass spectrometry the Aβ content in plaques from AD patients and PS2APP double transgenic mice (Richards et al., 2003) using ^{15}N-labeled amyloid peptide as a reference (Rufenacht et al., 2005). As the amount of Aβ in plaques from PS2APP mice exceeds the Aβ amount in human, we could exclude a simple dose-effect for the low degree of neurodegeneration.

So far, the composition and Aβ content of human senile plaques was examined either by the use of C-terminal end-specific antibodies (Harigaya et al., 2005) and by the analysis of brain homogenates (Mori et al., 1992, Miller et al., 1993, Sergeant et al., 2003), . Here, we used a method which allows the isolation of single plaques from brain thin sections using laser dissection microscopy (Schutze and Lahr, 1998). This enabled to collect small numbers of morphologically defined plaque types and vascular amyloid of vessels with cerebral amyloid angiopathy (CAA) and analyze their Aβ composition by mass spectrometry and urea-based Western blot assay. We compared different types of senile plaques isolated from human AD and PA cases as well as from PS2APP mice in order to investigate plaque-dependent differences in Aβ composition and discuss the impact on neurodegeneration. Through the use of a modified MS protocol, we intended to get more detailed knowledge about disease relevant Aβ peptides.

Human AD patients and PS2APP mice show differences in the occurrence of plaque types which are correlated to specific differences in comprising Aβ variants. This suggests that amyloid plaque deposition proceeds elsewise in human AD patients and in PS2APP mice, which likely impacts differentially on concomitant neurodegeneration.

The approach enables the isolation and accumulation of microscopic structures like plaques or single cells. In combination with MALDI-TOF MS and Western blotting even the breakdown of oxidized and reduced Aβ species is possible. The accuracy and sensitivity of the method therefore harbors future potential for the investigation of various processes in Alzheimer's disease and other neurodegenerative disorders.

EXPERIMENTAL PROCEDURES

Human tissues and transgenic mice

Human brains from AD patients were obtained from the Sun Health Research Institute through Dr. Thomas G. Beach (Sun City, AZ, USA). The brain tissue was collected approximately two hours after death and was immediately frozen at -80°C. Brains were neuropathologically staged according to Braak (Braak and Braak, 1991). Plaques were isolated from the temporal, frontal and occipital association gyrus and hippocampus of 5 different AD patients (89, 84, 80, 78 and 77 years old) with Braak stages IV (n=1), V (n=2) and VI (n=2). Vascular amyloid was isolated from the superior parietal gyrus of an 84 year old patient with high incidence of CAA. Patients with Braak stage V and VI show heavy, with Braak stage IV moderate plaque load.

In addition, plaques were isolated from the temporal cortex of two PA individuals (87 and 88 years old) obtained from Dr. C. Wischik (Cambridge, UK).

The PS2APP transgenic mice develop an age-related cognitive decline associated with severe cerebral amyloidosis and reactive gliosis as described previously (Richards et al., 2003). Three twenty-month old mice were used. Mice were killed by decapitation after anesthesia with fluothane. The skull pan was opened with scissors and the brain was removed and divided into hemispheres before freezing in dry-ice and preparing sagittal sections.

Preparation of brain slices

Frozen brain tissue was used and sections of 10 μm thickness were cut with a cryostat microtome (Leica Microsystems, CM3050 S). The slices were directly mounted onto glass cover slip coated with a 1.35 μm thin polyethylene foil (PALM Robot Microbeam, LPC-MOMeNT-Object slides, 8150) and stored until staining at -20°C.

Staining of brain thin sections

Brain tissue slices were rehydrated for 5 min with phosphate buffered saline (PBS, Gibco, 14200-067) containing protease inhibitors (Roche Diagnostics GmbH, 1836145, 1 tablet per 50 ml) and fixed on the polyethylene foil covered glass slide by applying 70% acetone (0°C) for approximately 1 min. Sections were washed twice for 2 min with 1 ml PBS and thioflavine S was applied as a 1% aqueous solution for 3–5 min followed by a differentiation step with 70% ethanol for 3–5 min. By incubation of the sections with 500 μl PBS containing 1% bovine serum albumin (BSA, fraction V, Roche Applied Science) and 1% Ovalbumin (Sigma, St. Louis, MO, USA) for 15 min, unspecific binding sites were blocked. The slices were then incubated for 1 h at room temperature with 200 μl of 10 μg/ml of BAP-2 (mouse anti-Aβ antibody, amino-terminal specific; kindly provided by Dr. M. Brockhaus, F. Hoffmann-La Roche) or AT8 (mouse anti-PHF tau antibody; Pierce Biotechnology Inc, Rockford, IL, USA). Subsequently, the samples were washed three times for 5 min with 500 μl of PBS containing 1% BSA. Detection was performed using an Alexa Fluor 555- or 488-conjugated secondary antibody (goat anti-mouse antibody diluted 1:200 in PBS containing 1% BSA; Invitrogen AG, Molecular Probes, Basel, Switzerland) applied for 1 h at room temperature. The preparations were then washed once for 5 min with 1 ml PBS and once for 2 min with distilled H_2O before being air-dried and stored until submitted to laser dissection at -20°C.

Immuno-electron microscopy

Perfusion-fixation of 8 month old PS2APP mouse brains and subsequent immersion of brain tissue was done with 4% formaldehyde and 0.05% glutaraldehyde in PBS for two hours before cutting into approximately 100 μm thick sections using a vibratome and cryoprotected by immersion in increasing concentrations of glycerol (10 – 20 – 30% v/v) in 10 mM phosphate buffer, pH 7.4 for 30 min each concentration. Vibratome sections were carefully picked up by forceps and plunged into liquid ethane cooled by liquid nitrogen. Frozen tissue slices were stored in liquid nitrogen before being transferred to the pre-cooled chamber (-90°C) of an automated freeze-substitution apparatus (AFS, Reichert, Austria). The tissue was immersed overnight in anhydrous methanol at -90°C, containing 0.5% (w/v) uranyl acetate. The temperature was allowed to rise to -45°C, at a rate of 6.7˚C/h. Samples were washed three times with anhydrous methanol for 30 min each to remove residual water and excess uranyl acetate before infiltration with Lowicryl HM20 resin (Chemische Werke Lowi, Waldkraiburg, Germany). Infiltration with resin was done in mixtures of HM20 and methanol at volumes 1:1 and 2:1, each for 2 h, and pure HM20 for 2 h, 16 h and 20 h. Samples were processed in the flow through system of the Reichert

AFS apparatus and polymerized by indirect UV irradiation (360 nm) for 24 h at -45°C, followed by UV-irradiation for 1 day at room temperature to achieve complete resin polymerization.
Ultrathin sections were prepared on a Reichert Ultracut S using a diamond knife (Diatome) and collected onto formvar / carbon - coated 200-mesh nickel grids. The sections were floated on 0.05 mol/L glycine in PBS for 15 minutes to inactivate free aldehyde groups and then on 2.5% (w/v) hen egg white albumin (Fluka) with 2.5% (w/v) bovine serum albumin (Roche Applied Science) in PBS for 15 minutes to block nonspecific binding sites. Sections were incubated with 10 µg/ml mAb BAP-2 in 2% BSA/PBS for 1 hour. After 6 washes in BSA/PBS, the sections were incubated with a secondary goat anti-mouse IgG (Amersham, Arlington Heights, IL, USA), conjugated to 10 nm gold at 1:20 dilution in 2% BSA with 0.1% Tween 20 in PBS for 1 hour, and washed in BSA/PBS. For controls, we used sections treated with normal mouse serum, which resulted in a negligible background of not more than 10 gold particles in an area of 10 μm^2. The sections were postfixed in 2% glutaraldehyde in PBS for 5 minutes, washed, and stained with 4% aqueous uranyl acetate for 10 min, followed by lead citrate for 90 seconds. Electron micrographs were taken with a JEOL 1210 at 100 kV.

Laser dissection and sample preparation

Laser dissection microscopy was performed as previously reported (Schutze and Lahr, 1998). An inverse fluorescence microscope (Axiovert 135, Carl Zeiss AG, Oberkochen, Germany) attached to a pulsed nitrogen laser (PALM Robot MicroBeam, 337 nm, P.A.L.M. Microlaser Technologies GmbH, Bernried, Germany) with beam splitters, to allow for immunofluroescence inspection during laser dissection, was used. Laser dissection was performed in a two-step process comprising cold ablation, an excision process based on a restricted photodecomposition process without heating (Srinivasan, 1986), and laser pressure catapulting for contamination-free harvesting. The laser microbeam was focused through a 10x or 20x objective lens. Settings for laser focus and energy were re-optimized for each slide.

Immunostained mouse or human brain sections were first air-dried for 30 min before individual amyloid plaques were excised by laser ablation. A single laser pulse of increased energy with its focal plane slightly below the sample provoked the transport of the excised material directly into the cap of a 500 µl Eppendorf tube placed above the focused laser beam. By repeating this procedure several times, the excised material was accumulated in a single cap filled with 50 µl of distilled water for better adhesion of the material. After collection, the liquid was spun down at 15'500 x g into the tube. The cap containing the plaques was then additionally rinsed twice with 58.5 µl of concentrated formic acid, spun down, and all fractions were pooled. After a dissolution period of 18 h, the samples were subjected to sonication
(3 x 3 min in a water-bath at room temperature with intermediate vortex mixing) and were dried in an evacuated centrifuge to dryness for further processing of the amyloid peptides.

Amyloid peptides, quality control and quantification

The ^{15}N-labeled Aβ 1-42 ox (methionine at position 35 oxidized to methionine sulfoxide) peptide was produced by recombinant DNA technology using E. coli fed with ^{15}N–ammonium chloride (Dobeli et al., 1995, Riek et al., 2001). ^{15}N-labeled Aβ 1-40 red was obtained from rPeptide (rPeptide, Athens, Georgia, USA). Synthetic Aβ 1-42, Aβ 1-40, Aβ 1-38, and N3pE-42 (glutamate at position 3 converted to pyroglutamic acid) peptides were purchased from Bachem (Bachem Holding AG, Bubendorf, Switzerland) or Nova Biochem (Nova Biochem, Läufelfingen, Switzerland). The integrity of each Aβ species was checked by electrospray mass spectrometry and the exact concentration of the Aβ peptide stock solutions used for spiking was determined by amino acid analysis (Dr. P. Hunziker, Protein Analysis Unit, University of Zürich, Switzerland).

Synthesis of the ionization modifier

Conversion of 6-guanidohexanoic acid into its HBF_4 salt: 6-guanidohexanoic acid has a poor solubility in organic solvents, but when converted into its HBF_4 salt, it is soluble in methanol. A 346 mg quantity of 6-guanidohexanoic acid (2 mmol) was dissolved in 8 ml H_2O and then neutralized with ca 250 µl 8 M tetrafluoroboric acid. After lyophilization, 514 mg of a white powder was obtained; theoretical yield: 526 mg. Synthesis of the 6-guanidohexanoic acid N-hydroxy-succinimide adduct: 250 µl volume of a 200 mM solution of 6-guanidohexanoic acid HBF_4 salt (50 µmol) in methanol and 250 µl of a 200 mM solution of N-hydroxysuccinimide (50 µmol) dissolved in dimethylformamide were added to 77 mg N-cyclohexylcarbodiimide N'-methyl polystyrene beads (ca. 100 µmol reactive immobilized groups). The slurry was gently agitated on a rotary shaker at 20 °C and the reaction was monitored by electron spray mass spectrometry (positive ion mode, m/z = 271). After approximately 8 hours the reaction was completed and the 6-guanidohexanoic acid–N-hydroxysuccinimide (6-GuHe, Fig. 4A) reagent could then be introduced into the desired assay for up to 48 hours.

Endoproteinase Lys-C digestion, modification, desalting by ZipTip, mass spectrometry

As previously described (Rufenacht et al., 2005), the dried samples were digested with 10 µl of 10 mM $NaHCO_3$ solution, containing 15 ng of endoproteinase Lys-C (Wako Chemicals GmbH, 125-05061, Reuss, Germany) for 2 h at room temperature. For detection of the C-terminal part, the peptides were modified by adding 5 µl of 6-guanidohexanoic acid–N-hydroxysuccinimide reagent (ca. 500 nmoles, reaction conditions: 1 h at 20 °C). Prior to mass spectrometry, the samples were desalted using ZipTip pipette tips (Millipore, Billerica, MA, USA). Adsorption of the peptides was performed according to the suppliers recommendations using 0.6 µl RP-18 matrix ZipTip pipette tips, for desalting a 5% (v/v) methanol-water containing 0.1% (v/v) trifluoroacetic acid solution was used. In order to increase the sensitivity, the eluted peptides were divided into three pools using acetonitrile concentrations of 30%, 60% and 90% (v/v). The elution volume contained 2 x ca. 2.5 µl.

The eluate was mixed with an equal volume of a α-cyano-4-hydroxycinnamic acid solution (Sigma-Aldrich Chemie GmbH, C2020; 5 mg/ml in 50% (v/v) acetonitrile-water). One µl thereof was spotted onto a

standard stainless-steel Bruker MALDI 384-target plate (Bruker Daltonics GmbH, Bremen, Germany). The measurements were performed on a Bruker UltraFlex time of flight mass spectrometer in reflector mode using standard operating parameters. Spectra were acquired manually at 4 different shot locations and a total of 400 shots were added per spectrum.

Determination of the proportion of Aβ x-16, Aβ 17-28 and Aβ 29-40/42

In mass spectrometry profiles without ionization modifier, peak height ratios were determined by measuring the relative peak heights in a given peak pattern as described previously (Rufenacht et al., 2005). For comparison with Aβ isolated from plaques, we analyzed synthetic Aβ peptides and detected a ratio of Aβ 1-16 (m/z 1954.8) to Aβ 17-28 (m/z 1325.4) of ~3:2.

Spectra with ionization modifier show a more complex peak pattern. Aβ 1-16 and Aβ 17-28 may yield three peak signals: one representing the unmodified peptide, one with one 6-GuHe and one with two 6-GuHe attached. All Aβ-related peaks were measured and N-terminal, middle fragment and C-terminal related peaks were put into relation to the sum of all Aβ-related peaks heights. Since some of our plaque samples revealed mass spectra which were close to the detection limit, we performed control experiments to verify that the changed ratio of the Aβ fragments was not caused by dilution. Synthetic or biosynthetic Aβ 1-40 or Aβ 1-42 was titrated towards the detection limit. The proportions of Aβ 17-28 to Aβ 29-40/42 remained unchanged (A. Güntert, unpublished observations).

Quantification of the Aβ content was performed as described previously (Rufenacht et al., 2005) using ^{15}N labeled biosynthetic Aβ 1-42 ox or synthetic Aβ 1-40 red (rPeptide). By spiking the plaque samples with ^{15}N labelled Aβ, overall losses, both for ^{14}N and ^{15}N Aβ, induced by the sample preparation procedure could be controlled. Since endogenous and ^{15}N-Aβ peptides do not differ chemically from each other, except for the presence of the ^{15}N heavy isotope in the standard, all experimental losses can be assumed to be equally reflected on both Aβ species, thus allowing absolute quantification by comparing peak ratios. However, the carboxy-terminus is heterogeneous first due to the different endings (40 and 42) and second by the varying proportion of reduced or oxidized methionine at position 35. This leads to an overlap of the peak patterns, e.g. of the ^{14}N-Aβ 1-40 ox with ^{15}N-Aβ 1-40 red. In order to keep the option to detect all potential Aβ carboxy-terminal fragments we did not spike routinely.

SDS-PAGE / Western blot

For the separation of Aβ peptides, we applied the urea version of the N,N'-bis-(2-hydroxyethyl)-glycine / bis - Tris/Tris/ sulfate SDS-PAGE (Wiltfang et al., 1991). Due to urea-induced differential shifts in conformation, Aβ peptides that differ in only one amino acid can be separated (Klafki et al., 1996, Wiltfang et al., 1997). The composition of the separation gel initially applied for the analysis of Aβ peptides was modified from 15%T/5%C/8 M urea to 12%T/5%C/8 M urea (%T = percentage (w/v) of total acrylamide monomer; %C = percentage (w/w) of bisacrylamide / total acrylamide monomer), and gel thickness was reduced to 0.5 mm. Gels were run at room temperature for 2.15 h at a constant current of 12 mA/gel, using the MiniProtean II

electrophoresis unit (Bio-Rad Laboratories, Hercules, CA, USA). In an experiment, a known number of laser dissected plaques were compared to 100 pg synthetic Aβ 1-38 / 40 / 42 in 10 µl sample buffer.

Western blotting and immunostaining were performed as previously described (Wiltfang et al., 1997). Aβ peptides were transferred for 30 min at 1 mA/cm^2 and room temperature under semi-dry conditions onto Immobilon-P PVDF membranes (Millipore, IPVH08100, Billerica, MA, USA). For immunostaining, PVDF membranes were washed for 30 seconds in distilled H_2O and boiled for 3 min in PBS using a microwave oven (Ida et al., 1996, Wiltfang et al., 1997). Blocking was performed for 1 hour at room temperature in the presence of 5% nonfat dry milk in PBS-T (PBS containing 0.5% Tween-20). Incubation with the primary mouse antibody WO-2 (The Genetics Company, Zuerich, Switzerland) recognizing the N-terminal amino acids 4-10 of the Aβ peptide at a concentration of 2 µg/ml was done overnight at 4°C. Membranes were then washed for 30 min, 15 min, and 2 × 10 min in PBS-T. After the washing steps, the membranes were incubated with a horseradish peroxidase linked anti-mouse antibody (Amersham Biosciences, Piscataway, NJ, USA) for 1 h. After a wash for 3 × 10 min at room temperature, the membranes were developed for 5 min at room temperature with ECLPlus™ (Amersham) solution according to the protocol of the manufacturer. Visualization was done with conventional X-Ray films (Amersham).

The migration properties of the peptides were analyzed using the following synthetic amyloid peptide standards: 1-38, 1-40, 1-42 (M35M red, all with a reduced methionine at position 35) as well as with 1-40 and 1-42 (M35M ox, both with a sulfoxide at position 35).

RESULTS

Selection of plaque types

Using a doublestaining procedure with thioflavine S and BAP-2 antibody against Aβ, we could discern three morphologically different plaque types and vascular amyloid in human and PS2APP brains (Fig. 1). The discrimination of different plaque types essentially followed a morphological classification used to characterize the amyloid pathology in AD (Thal et al., 2006). Accordingly, we distinguished between thioflavine S positive and thioflavine S negative amyloid depositions. Thioflavine S negative plaques are commonly known as diffuse plaques. Thioflavine S positive depositions, which contain densely packed Aβ fibrils were further differentiated into cored and compact plaques. Compact plaques were positive for thioflavine S and BAP-2 antibody, while diffuse plaques were stained only by BAP-2 antibody (Fig. 1A, B, E, F). In cored plaques only the central core was stained by thioflavine S, while the peripheral Aβ was stained solely by BAP-2, comparable to the morphology of diffuse deposits (Fig. 1C, G). Vascular deposits were visible by both thioflavine S and immunostaining (Fig. 1D, H). Staining properties allowed to differentiate unambiguously cored, compact and diffuse plaques, enabling the specific isolation by subsequent laser dissection microscopy.

Although compact plaques occur in human as well as in PS2APP mice, their occurrences in the two species are different. In 20 month old PS2APP mice (Fig. 1A, E) compact plaques of different sizes represent the majority, whereas in the cortex and the hippocampus of AD patients (Fig. 1B, F) this plaque type occurs at only ~10%. Cored plaques predominate (~90%) in the AD patients investigated (Fig. 1C, G). Diffuse plaques (arrow

heads in Fig. 1 A, B, E, F) are detectable at high frequency in AD and PA, but occurred less often in PS2APP mice.

In PA individuals, primarily diffuse amyloid deposits were detected but only sporadically some cored plaques could be found, especially in the transition to the white matter. Compact plaques were not identified in these brains. A tau-specific staining with AT8 showed that neuritic plaques and tau pathology occured only occasionally as rare events in PA, whereas in AD brains a substantially higher number of neuritic plaques and very pronounced tau pathology was detectable as expected (A. Güntert, unpublished observations).

Ultrastructural morphology of amyloid-β plaques

Immuno-electron microscopy was carried out on low temperature-embedded brain tissue. The method combines the advantage of superior preservation of ultrastructure and antigenicity for efficient immunocytochemical staining.

Immunogold labeling, using a monoclonal antibody against the N-terminal portion of the Aβ peptide (BAP-2), revealed Aβ deposits which occur as fibrillar structures in diffuse plaques of PS2APP mice and human AD patients (Fig. 2). Remarkably, the Aβ fibrils of mouse diffuse plaques are intermingled as single or few fibrils in the extracellular space in the neuropil and thus can contact directly the cell membrane of neurites (Fig. 2A). In contrast, human diffuse plaques contain few Aβ fibrils that are surrounded by a considerable amorphous extracellular matrix (Fig. 2B). It was demonstrated by immuno-histochemistry, that human amyloid plaques are associated with a number of proteoglycans like decorin and laminin (van Horssen et al., 2002, Mok et al., 2006).

Compact mouse plaques contain a very high number of homogenously and densely packed Aβ fibrils (Supplementary data, Fig. 1A). Dystrophic neurites were found at the periphery of mouse plaques, especially mature compact plaques. Also, microglia cells were frequently observed in close contact with fibrillar plaques, forming an interdigitating complex of fibrils and the microglial cytoplasm.

Cored human plaques which resemble a more mature plaque stage are built up by numerous clusters of Aβ fibrils, which can occur as densely packed large bundles (Supplementary data, Fig. 1B). Immunogold labelling confirms that almost all detectable Aβ is present in its polymerized fibrillar state, although the local density of Aβ fibrils can vary considerably and domains of extracellular matrix are also visible. The fibrillar bundles are often in spatial contact to the surrounding neuropil, although the subcellular details are less evident, because of the used sample preparation that cannot avoid influences of the post-mortem time on ultrastructural preservation.

Vascular human amyloid is characterized by a type of dense packing of Aβ fibrils comparable to Aβ fibrils in compact plaques from PS2APP mice (Supplementary data, Fig. 2).

MALDI - TOF MS

The cleavage of the Aβ peptide by the restriction protease Lys-C generates three fragments. The amino-terminal and the middle fragments were detected with high sensitivity (Tab. 1) and could be used to quantify the amyloid content in the excised plaques. However, the C-terminal part could not be observed. A possible explanation would be the hydrophobicity of this Aβ fragment which interferes with adequate ionization, necessary for MS analysis. In order to overcome this limitation, we developed an ionization modifier (Fig. 4A) which allowed us

to detect for the first time the carboxy-terminal fragments as well, specifically Aβ 29-40 and Aβ 29-42. We are the first group to analyze, from minute amounts of plaque Aβ isolated by laser dissection microscopy, the C-terminal Aβ fragments. Notably, this method allowed the discrimination between the oxidized and the reduced form of Met-35.

We observed almost exclusively Aβ fragments when we used endoproteinase Lys-C for fragmentation, although very many more proteins have been reported to be present in plaques. Apparently, the Aβ 1-16 and Aβ 17-28 or the 6-GuHe derivatized Aβ 17-28 and Aβ 29-40/42 fragments dominate during the ionization procedure. As the number of plaques required to reach the detection limit of our mass spectrometric procedure was different depending on the plaque type and specimen, we typically collected and pooled 30 compact plaques from PS2APP mouse specimen, 50 cored plaques, 200 diffuse deposits and 70 compact plaques or 15 human vessels with CAA from human AD brain per sample. Mouse plaques contain a ~1.5 fold higher amount of detectable Aβ than human plaques, according to Rufenacht et al., 2005. Thioflavine S positive compact plaques represent a rare species in humans and thus needed to be gathered from five consecutive brain sections, whereas the abundant cored in human AD and the mouse compact plaques could be collected from one single brain section.

Detection of the amino-terminal Aβ peptides and Aβ fragment 17-28

Cored plaques were isolated from 5 different patients and 4 different brain regions thereof; diffuse plaques were dissected from hippocampal and temporal brain regions. In a previous study with one AD case, we found Aβ 1-16, 2-16, 3-16, pyroglutamate 3-16, 4-16 and 5-16 (Rufenacht et al., 2005). Findings are confirmed in the current study and extended by the analysis of five AD cases at different disease stages (Fig. 3 and Tab. 2). Arg-5 is likely most prone for ionization and truncations beyond that position are probably not detected due to poor ionization. Additionally, Aβ 11-16 or pyroglutamate 11-16 are likely to escape the detection range in our mass spectrometry procedure, due to their low mass.

To evaluate the ionization and Lys-C digestion properties of N-terminal truncated Aβ variants, commercially available synthetic pyroglutamate 3-42 was compared to biosynthetic ^{15}N-labelled Aβ 1-42. Defined amounts of Aβ 1-42 and pyroglutamate 3-42 were mixed in the ratios 3/7, 1/1, and 7/3, subsequently Lys-C digested and analyzed by MALDI-TOF-MS. The obtained standard curve revealed a linear relationship between the different ratios of Aβ peptides and showed comparable ionization properties of full length Aβ 1-16 and pyroglutamate 3-16 (Supplementary data, Fig. 3). Other N-terminally truncated Aβ peptides were not available and could therefore not be compared to full length Aβ. However, they can be assumed to have comparable ionization properties since only N-terminal truncations beyond Arg-5 are likely to exhibit different ionization properties in the MALDI-TOF MS.

The detected amounts and ratios of the various Aβ species did not vary markedly between investigated brain regions (Tab. 2)., Beside Aβ 1-16, which was found as the predominant type in all samples, pyroglutamate 3-16 represented the major detectable N-terminal truncated Aβ fragment and, according to peak heights, accounted for ~20-25% of total Aβ found in the analyzed samples. With increasing Braak stage a decreasing amount of Aβ 1-16 was found, while N-terminal truncations increase gradually with disease progression. This

was evident for cored plaques, showing an increase of approximately 20% from Braak stage IV, V to VI. The largest proportion of Aβ 1-16 could consistently be detected in diffuse plaques from AD cases at all Braak stages and in PA cases. Diffuse plaques from both PA cases did not show any differences to diffuse plaques isolated from AD patients' brains, regarding the pattern and relative peak heights of N-terminal truncated Aβ forms.

To exclude artifacts from the preparation procedure, we included every time samples with synthetic Aβ 1-40 / 42. Furthermore, to ensure that the pyroglutamate detected in amyloid isolated from senile plaques was not induced artificially, five synthetic peptides starting with a glutamate or glutamine were treated with concentrated formic acid and analyzed by mass spectrometry. Only minor amounts of glutamine were converted to pyroglutamate, whereas the glutamate-starting peptides did not show cyclisation (A. Güntert, unpublished observations).

Detection of the carboxy-terminal Aβ peptide and Aβ fragment 17-28

We used the 6-GuHe (Fig. 4A) to derivatize the peptides generated by the Lys-C digestion. The addition of the guanido group changes the detection limits of the three expected peptides in favour of the carboxy-terminus and at the expense of the amino-terminal peptide (Tab. 1). Derivatization with 6-GuHe leads to a poor detection of the amino-terminal peptides, probably because multiple guanido groups are deleterious. Since the middle fragment Aβ 17-28 is detected with both protocols, there is the possibility to compare the relative proportions of all three peptides.

The total data set was derived from spectra of 10 PS2APP mouse compact plaque samples , 2 human compact, 9 human cored and 3 human diffuse plaque samples (2 from a PA case, 1 from an AD case) as well as from 7 samples of human vascular amyloid and from 8 synthetic Aβ 1-40 and 15 Aβ 1-42 samples. Individual plaques or vessels were excised, pooled and analyzed by MALDI-TOF MS after chemical modification with ionization modifier 6-GuHe. To increase sensitivity, a pre-wash with 30% ACN was introduced and cleaner eluates with 60% ACN were obtained for analysis (Fig. 4). A third step with 90% ACN was performed to check for complete elution. For comparison of the relative quantities, we used only the 60% fraction.

Using this procedure, we were able to determine the relative proportions of the C-terminal Aβ fragments 29-40 and 29-42 in cored and diffuse plaques, as well as in vascular amyloid from human AD and in compact plaques from PS2APP mice. Carboxy-terminal fragments ending at residues other than Val-40 or Ala-42 were not detected.

Fig. 4B and C show spectra derived from the analysis of 50 human cored plaques, spiked with 0.6 pmol ^{15}N-Aβ 1-42 ox. The spectra show that the method allows discrimination between the reduced (m/z 1425.1) and the oxidized (m/z 1441.1) form of the methionine at position 35 of the Aβ fragment 29-42.

In all samples, the ratio of oxidized and reduced forms of Aβ 29-40 was comparable to the ratio of oxidized and reduced forms of Aβ 29-42. In the data set of Fig. 5, the amount of oxidized species increased in the following order: human vascular amyloid (47 ± 21%), human compact plaques (49 ± 20%), human cored (64 ± 14%), PS2APP compact plaques (72 ± 16%) and human diffuse plaques from from AD (91%) and PA (92 ± 2%). Since we did not work under an N_2 atmosphere during the plaque collection and sample preparation procedure, artificial oxidation cannot be excluded. Therefore, conclusions from the observed proportions between the oxidized and the reduced forms should be taken with caution.

Aβ fragments 17-28 and Aβ 29-40/42 are clearly detectable when synthetic Aβ is analyzed after 6-GuHe modification. In contrast, Aβ derived from human cored and diffuse plaques were consistently different from those of the synthetic or biosynthetic Aβ peptides with significantly decreased levels of Aβ 17-28. Compact plaques from PS2APP mice show intermediate proportions.

We found that in human plaques the Lys-C fragment Aβ 17-28 is detectable in a substantial excess over the full-length amino-terminal part without 6-GuHe modification (Fig. 5A). After the modification with 6-GuHe, the carboxy-terminus is detectable in human plaques in a twofold excess over Aβ 17-28 (example in Fig. 4C). This means that the relative proportions are Aβ 29-40/42 > Aβ 17-28 ≥ Aβ x-16. This relationship found in human brain specimen could be explained with the presence of inter-chain cross-links between Aβ peptides and N-terminal truncations thereof (Kuo et al., 2001, Sergeant et al., 2003). In comparison, human vascular amyloid and especially PS2APP mouse compact plaques show different peak proportions with higher detectable amounts of Aβ 17-28. This hints to less extensive cross-linking in PS2APP mouse compact plaques and vascular amyloid compared to human senile plaques.

Fig. 5B shows the peak ratios between the carboxy-terminal peptides Aβ 29-40 and Aβ 29-42 in the analyzed types of Aβ deposits. Vascular amyloid and compact plaques showed an excess of Aβ 29-40, whereas human cored plaques and diffuse plaques contained predominantly Aβ 29-42. As samples from different brains or Braak stages reveal identical spectra, all data were analyzed collectively. The findings fit well with the analysis by Western blotting as outlined below.

Western blot analysis

In order to study the major full length Aβ types that occur in vascular amyloid as well as in compact and cored plaques, they were isolated by laser dissection and analyzed by urea-based Western blots (Fig. 6A). Complementary to the results obtained by mass spectrometry we found mainly Aβ 1-40 in human compact plaques and vascular amyloid. In contrast, mainly Aβ 1-42 was detected in human cored plaques. The high sensitivity of the Western blot assay enabled us to study the composition of diffuse plaques from human and from PS2APP mice. Fig. 6B shows that diffuse plaques from PA as well as from AD cases and PS2APP mice contain, like human cored plaques, predominantly Aβ 1-42.

In addition to that, the employed laser dissection microscopy with subsequent Western blot analysis allowed the discrimination between oxidized and reduced Aβ species. To our knowledge, we are the first group able to show the oxidation state of Aβ peptides isolated from senile plaques by Western blotting. To compare migration distances, synthetic or biosynthetic Aβ 1-40/42 ox and red were used as reference peptides. Incidentally, Aβ 1-42 ox and Aβ 1-38 red migrate to almost identical positions, but because we did not detect any Aβ 1-38 in plaques by MALDI-TOF MS and because of a slight shift of the migration distance, we considered the appearing bands to be indicative for Aβ 1-42 ox. Again we observed differences in the proportions of oxidized to reduced Met-35 Aβ forms between different samples, these differences were more pronounced in the Western blot analysis as in the 6-GuHe MALDI-TOF MS analysis. The larger heterogeneity with respect to the oxidation state of Aβ detected by Western blotting can likely be explained by the smaller number of sampled plaques. However, Fig. 6 shows representative results.

By using an N-terminal specific Aβ antibody, extensive N-terminal truncated Aβ forms are less efficiently detected by Western blotting. Antibodies specific for N-terminal truncated Aβ species allow the detection of these peptides. With an Aβ N3pE-42 specific antibody we detected substantial amounts of pyroglutamate 3-42 in human cored plaques (Fig. 6C). Immunohistochemistry with this antibody was positive for all cored plaques (A. Güntert, unpublished observations). These findings confirm the data obtained by mass spectrometry.

DISCUSSION

The present study provides a detailed analysis of the Aβ composition in different amyloid plaque types from AD patients, PA individuals and PS2APP mice. Our method allowed to dissect morphologically different plaque types and to analyse them by three independent methods: 1) Western blotting, 2) mass-spectrometry using endoproteinase Lys-C and 3) mass-spectrometry using endoproteinase Lys-C in combination with the newly developed ionization modifier 6-GuHe for detection of the C-terminal Aβ fragments. Endoproteinase Lys-C generates Aβ fragments, which are detected by MALDI-TOF MS with a much higher sensitivity as would be the case for full-length Aβ. The addition of the ionization modifier 6-GuHe allows detection of the hydrophobic C-terminal Aβ fragment. The modification of α- and ε-amino groups with a guanido-group containing tag renders the C-terminal fragments accessible to mass spectrometric analysis. Without 6-GuHe modification, the carboxy-terminus of Aβ cannot be detected, while with 6-GuHe modification, the carboxy-terminus becomes detectable although at the expense of the amino-terminus. Likely, the amino-terminus after 6-GuHe modification could not be detected because of too many ionisable groups. In summary, both methods are complementary and enable the investigation of the entire Aβ peptide.

The used methodology has shown to be suitable for the analysis of minute amounts of Aβ obtained from distinct plaque types. This allowed to investigate Aβ deposits from well-defined regions. Aβ-related effects, especially with regard to down-stream neurodegeneration can be addressed at a cellular level. We have analysed the Aβ composition in diffuse, compact and cored plaques and also of vascular amyloid from different human AD brains at Braak stages IV, V and VI. Additionally, diffuse amyloid depositions were isolated and analyzed from cognitively normal, aged PA cases. In PS2APP mice we examined diffuse and compact plaques; cored plaques and vascular amyloid were only occasionally visible in the 20 month old mice.

Analysis by Western blotting and MALDI-TOF MS of vascular amyloid and compact plaques revealed mainly Aβ 1-40 and only minor amounts of Aβ 1-42. This is consistent with data from earlier studies using end-specific antibodies (Joachim et al., 1988, Suzuki et al., 1994). In contrast, the most abundant human plaque types, i.e., diffuse and cored plaques from cortical and hippocampal brain regions, revealed primarily Aβ 1-42, so did the analysis of diffuse plaques from PS2APP mice. This is in agreement with immunocytochemical studies which reported that diffuse plaques found in different anatomical brain regions of AD patients are Aβ 1-42 positive, but Aβ 1-40 negative (Iwatsubo et al., 1994). Accordingly, the data confirm the concept that the initially deposited Aβ variant in AD is Aβ 1-42 and that Aβ 1-40 is deposited at a later stage of plaque maturation (Selkoe, 2001). Therefore, it can be assumed that there is a similar process of initial plaque

deposition, both in human AD and PS2APP mice. Concerning the time course of plaque maturation, our data suggest that compact plaques with their high quantity of Aβ 40 cannot be precursors of cored plaques which contain mainly Aβ 42. More likely, plaque maturation starting with diffuse plaques can proceed towards typical cored plaques, resembling neuritic plaques with associated dystrophic neurites and reactive gliosis or towards compact plaques with a dense packing of Aβ fibrils (Fig. 7). Additional factor(s) like a plaque associated protein, kinetics of Aβ deposition / clearance or different ratio of Aβ variants present in brains of human AD patients compared to PS2APP mice, might lead to a divergent process resulting in mainly cored plaques in human and predominantly compact plaques in PS2APP mice. Ultrastructural differences were revealed, especially for diffuse plaques by immuno-electron microscopy. Diffuse plaques of AD patients develop with considerable involvement of extracellular matrix proteins even at an early stage of fibril formation indicative for compensatory processes to inactivate the extracellular deposits.

We aimed to get more information on factors that might impact directly or indirectly on synaptic plasticity and finally on neurodegeneration. Candidates could be an Aβ variant leading to increased cytotoxicity and/or a less degradable Aβ species that accumulates and serves as template for increased Aβ aggregation. It was reported, that oxidation of Met-35 reduces toxic effects of Aβ in vitro (Clementi et al., 2004). It was additionally demonstrated, that oxidation reduces fibril assembly and prevents the formation of protofibrils (Hou et al., 2002). We were able to discriminate between oxidized and reduced Aβ variants with MALDI-TOF MS, as well as with Western blot analysis. The encountered substantial heterogeneity of samples analyzed by Western blotting can be explained by the biological heterogeneity in sporadic AD and smaller sample sizes compared to MS analysis. However, we consistently detected only low levels of reduced and high levels of oxidized Aβ 42 by MS and by Western blotting in diffuse plaques from PA cases. Extensive oxidation of Aβ might be regarded as beneficial to attenuate toxic amyloid deposits; the absence of tau pathology and clinical symptoms in PA supports this view.

Another putative factor likely having impact on neurodegeneration in AD patients, which is less frequent or absent in transgenic animals is N3pE-40/42. This pyroglutamate variant is a major component of human plaques and less accessible to Aβ degrading enzymes (Saido et al., 1995, Tekirian et al., 1999, Harigaya et al., 2000). The occurence of N-terminally truncated Aβ species was demonstrated to be decreased in APP23 and PS2APP mice compared to human plaques (Kuo et al., 2001, Rufenacht et al., 2005). Other reports showed, that amino-truncated Aβ species represent more than 60% of all Aβ species in AD brains (Miller et al., 1993, Sergeant et al., 2003). However, the amyloid analyzed in these reports derived from brain homogenates averaging the senile plaque load. Laser dissection microscopy allowed the isolation of specific plaque types at microscopical precision. Small numbers of dissected plaques were then accessible for a detailed analysis. We could show that N-terminal truncation is minor in diffuse but substantial in cored plaques. Although considerable amounts of N-terminal truncated Aβ forms were found in cored human plaques, a substantial amount of full length Aβ 1-40/42 was also detectable. This fact is important regarding Aβ immunotherapies, where often amino-terminal specific antibodies are used. The fact that both, full length and N-terminal truncated, Aβ species are found in amyloid plaques indicates that the full-length species are sufficient to trigger a potential plaque clearance mechanism involving microglia, which finally removes all kinds of Aβ species.

The high level of amino-terminal truncations of Aβ, especially N3pE-40/42, in mature human plaques observed in this and other reports (Saido et al., 1996, Harigaya et al., 2005, Rufenacht et al., 2005) is likely

related to proteolytic processes taking place over prolonged time by a number of proteases (Iwata et al., 2005). The results given in Tab. 2 are in agreement with this explanation. The percentage of degraded amino-terminus in cored plaques increases at the expense of full length Aβ 1-16 and is directly correlated with AD progression. A recent report indicates, that full length Aβ is a minor component in cotton wool and diffuse plaques from an FAD patient (Miravalle et al., 2005). Laser dissection of 10'000 plaques and analysis by MALDI-TOF detected extensive N-terminal truncation, indicating a role in early-onset FAD. Our approach only requiring a small number of diffuse plaques detected high levels of full length Aβ in AD and PA. This adds further support to the concept that diffuse plaques resemble early amyloid assemblies and cored plaques mature depositions.

In AD mice, the abundance and extent of N-terminal truncated Aβ forms were reported, although at lower levels (Kuo et al., 2001, Rufenacht et al., 2005).

Since the extent of N-terminal truncation is likely to influence aggregation properties and also increase cell toxicity of Aβ (Pike et al., 1995, Saido, 2000), an accession of N-terminally truncated Aβ variants with certain FAD mutations or with disease progression in sporadic AD as we determined in cored plaques, might induce excessive neurodegeneration in advanced AD.

Beyond N-terminal truncated Aβ variants, the influence of other factors should be considered. Differences in the concentration of soluble Aβ 1-40 and Aβ 1-42 and the presence or absence of associated proteins that are known to impact on fibril and plaque formation, like apolipoprotein E and serum amyloid P (SAP) (Pepys et al., 1994, Thal et al., 2005), may account for species differences. Also, the dynamics of amyloidosis is accelerated in many AD models, but the extent of neuron loss variable and often less pronounced. Therefore AD models are limited for equivalent prediction of time course and degree of neurodegeneration encountered in human AD patients.

Additional differences between human plaques and PS2APP mice plaques compared to synthetic Aβ are found in the proportions between endoproteolytic Lys-C fragments. In human plaques, we observed that the amount of Aβ 29-40/42 exceeds the amount of Aβ 17-28. On the other hand, the proportions in PS2APP mouse plaques were comparable to synthetic Aβ, where Aβ 17-28 was the major detectable fragment. Previously, we demonstrated that the level of Aβ 17-28 exceeds the level of Aβ x-16 (Rufenacht et al., 2005), which could be explained by the existence of additional N-terminal truncated Aβ forms, that are not detected by the employed mass spectrometry procedure. More important, solubility experiments were performed with laser dissected plaques and we identified species dependent and solvent dependent differences for Aβ extraction. Formic acid was shown by us and others to be most efficient for Aβ solubilization. A considerable larger Aβ signal on Western blots could be detected from human plaques when incubated with formic acid than with SDS containing 8M urea. Contrary, no differences in Aβ amounts for PS2APP mouse plaques when extracted with SDS containing 8M urea compared to 70% formic acid were identified (A. Güntert, unpublished observations). Previous reports from APP23 and Tg2576 transgenic mice are consistent with these experiments (Kuo et al., 2001, Kalback et al., 2002).

Some of the above mentioned differences could be explained with different degrees of cross-linking of Aβ fibrils (Kuo et al., 2001). Interchain cross-linking between Gln-15 and Lys-16 could account for the observed decrease in detectable Aβ 17-28, since Lys-16, when engaged in a ε-side chain amide bond, is no longer a substrate for endoproteinase Lys-C. Additionally, cross-linking may have a substantial influence on the solubility

of Aβ fibrils. However, these cross-linked Aβ fragments most probably would escape detection in our mass spectrometry procedure. Attempts using other restriction proteases to prove the existence of such cross-links were not yet successful.

Aβ deposits can also be found in brains of PA individuals without clinical symptoms like cognitive deficits (Price et al., 1991, Arriagada et al., 1992, Thal et al., 2004). These depositions are almost exclusively of diffuse nature. Comparison of Aβ composition in diffuse plaques isolated from PA cases with AD cases did not show clear differences. In both cases they contain predominantly Aβ 1-42 and show low levels of N-terminal truncation. It was shown by neuropathological analysis that differences are found in the anatomical distribution (Thal et al., 2006). This suggests that the PA phenotype constitutes the onset of AD although in the absence of clinical symptoms.

Soluble brain Aβ was found to contain less N3pE-42 in PA compared to AD brains (Piccini et al., 2005). This makes sense, when the amyloid plaque load of PA brains is taken into consideration, where we demonstrated low levels of N-terminal truncated Aβ variants in plaques. However, the diffuse deposits found in PA brains are predominantly not neuritic and only an evanescent number of NFT's and neuropil threads could be detected. Since morphologically and biochemically comparable diffuse plaques can be found in AD patients as well as in PA individuals, our data are supportive for a view that diffuse deposits represent early and pre-symptomatic features of AD. Considering the generally low concentration of amyloid fibrils in diffuse plaques, it is likely that no substantial neurodegeneration occurred and the human brain can deal with this amount and type of Aβ. This is supported by the findings that many diffuse plaques in AD and almost all in PA are not neuritic. In addition, our ultrastructural findings might indicate a specific interaction with extracellular matrix components, also observed in wound healing. Single amyloid fibrils found in diffuse plaques are surrounded by amorphous extracellular matrix, thereby protecting the surrounding tissue from contact with the putative toxic amyloid aggregates. Continuous aggregation of additional Aβ might overstrain the compensatory mechanism and might finally induce onset of neurodegeneration.

It has been described before, that accumulation of Aβ leads to stimulation of the innate immune response, including activation of microglia and astrocytes, release of cytokines such as TNF-α and IL-β, complement activation and free-radical formation (Weiner and Selkoe, 2002). This innate immune activation may contribute to neurotoxicity. Brains of PA individuals do not display an extensive gliosis nor tau pathology and therefore precede a later stage in the events described in the amyloid hypotheses with extensive neurodegeneration.

The approach has future potential to measure subtle differences of Aβ composition, investigate the process of plaque formation in more detail and study the effect of specific Aβ species in relation to neurodegeneration in AD and models of AD. Aβ oligomers are first detected intraneuronally (Gouras et al., 2005) and may represent an intermediate step in plaque formation and neurodegeneration. As the methodology provides a high analytical sensitivity, the isolation and subsequent analysis of neurons containing intracellular Aβ will be possible and may be an important step to the understanding of Aβ deposition in brains of AD patients. As mentioned, glial activation in response to neuritic plaques induce proinflammatory stimuli and subsequent neurodegeneration. The specific analysis of neuritic plaques with this approach is likely to reveal important insight in pathophysiological processes occurring in the brain of AD patients. Currently, LC-MS/MS

studies are pursued for further investigation of plaque associated proteins apart from Aβ. The methodology of these ongoing studies holds promise to identify new disease-related proteins.

REFERENCES

Arriagada, P. V., Marzloff, K. and Hyman, B. T., 1992. Distribution of Alzheimer-type pathologic changes in nondemented elderly individuals matches the pattern in Alzheimer's disease. Neurology. 42, 1681-1688.

Braak, H. and Braak, E., 1991. Neuropathological stageing of Alzheimer-related changes. Acta Neuropathol (Berl). 82, 239-259.

Clementi, M. E., Martorana, G. E., Pezzotti, M., Giardina, B. and Misiti, F., 2004. Methionine 35 oxidation reduces toxic effects of the amyloid beta-protein fragment (31-35) on human red blood cell. Int J Biochem Cell Biol. 36, 2066-2076.

Dobeli, H., Draeger, N., Huber, G., Jakob, P., Schmidt, D., Seilheimer, B., Stuber, D., Wipf, B. and Zulauf, M., 1995. A biotechnological method provides access to aggregation competent monomeric Alzheimer's 1-42 residue amyloid peptide. Biotechnology (N Y). 13, 988-993.

Glenner, G. G., Wong, C. W., Quaranta, V. and Eanes, E. D., 1984. The amyloid deposits in Alzheimer's disease: their nature and pathogenesis. Appl Pathol. 2, 357-369.

Gouras, G. K., Almeida, C. G. and Takahashi, R. H., 2005. Intraneuronal Abeta accumulation and origin of plaques in Alzheimer's disease. Neurobiol Aging. 26, 1235-1244.

Haass, C., 2004. Take five-BACE and the gamma-secretase quartet conduct Alzheimer's amyloid beta-peptide generation. Embo J. 23, 483-488.

Hardy, J. A. and Higgins, G. A., 1992. Alzheimer's disease: the amyloid cascade hypothesis. Science. 256, 184-185.

Harigaya, Y., Saido, T. C., Eckman, C. B., Prada, C. M., Shoji, M. and Younkin, S. G., 2000. Amyloid beta protein starting pyroglutamate at position 3 is a major component of the amyloid deposits in the Alzheimer's disease brain. Biochem Biophys Res Commun. 276, 422-427.

Harigaya, Y., Tomidokoro, Y., Ikeda, M., Sasaki, A., Kawarabayashi, T., Matsubara, E., Kanai, M., Saido, T. C., Younkin, S. G. and Shoji, M., 2005. Type-specific evolution of amyloid plaque and angiopathy in APPsw mice. Neurosci Lett.

Hou, L., Kang, I., Marchant, R. E. and Zagorski, M. G., 2002. Methionine 35 oxidation reduces fibril assembly of the amyloid abeta-(1-42) peptide of Alzheimer's disease. J Biol Chem. 277, 40173-40176.

Hu, L., Wong, T. P., Cote, S. L., Bell, K. F. and Cuello, A. C., 2003. The impact of Abeta-plaques on cortical cholinergic and non-cholinergic presynaptic boutons in alzheimer's disease-like transgenic mice. Neuroscience. 121, 421-432.

Ida, N., Hartmann, T., Pantel, J., Schroder, J., Zerfass, R., Forstl, H., Sandbrink, R., Masters, C. L. and Beyreuther, K., 1996. Analysis of heterogeneous A4 peptides in human cerebrospinal fluid and blood by a newly developed sensitive Western blot assay. J Biol Chem. 271, 22908-22914.

Iwata, N., Higuchi, M. and Saido, T. C., 2005. Metabolism of amyloid-beta peptide and Alzheimer's disease. Pharmacol Ther. 108, 129-148.

Iwatsubo, T., Mann, D. M., Odaka, A., Suzuki, N. and Ihara, Y., 1995. Amyloid beta protein (A beta) deposition: A beta 42(43) precedes A beta 40 in Down syndrome. Ann Neurol. 37, 294-299.

Iwatsubo, T., Odaka, A., Suzuki, N., Mizusawa, H., Nukina, N. and Ihara, Y., 1994. Visualization of A beta 42(43) and A beta 40 in senile plaques with end-specific A beta monoclonals: evidence that an initially deposited species is A beta 42(43). Neuron. 13, 45-53.

Jarrett, J. T., Berger, E. P. and Lansbury, P. T., Jr., 1993. The carboxy terminus of the beta amyloid protein is critical for the seeding of amyloid formation: implications for the pathogenesis of Alzheimer's disease. Biochemistry. 32, 4693-4697.

Joachim, C. L., Duffy, L. K., Morris, J. H. and Selkoe, D. J., 1988. Protein chemical and immunocytochemical studies of meningovascular beta-amyloid protein in Alzheimer's disease and normal aging. Brain Res. 474, 100-111.

Kalback, W., Watson, M. D., Kokjohn, T. A., Kuo, Y. M., Weiss, N., Luehrs, D. C., Lopez, J., Brune, D., Sisodia, S. S., Staufenbiel, M., Emmerling, M. and Roher, A. E., 2002. APP transgenic mice Tg2576 accumulate Abeta peptides that are distinct from the chemically modified and insoluble peptides deposited in Alzheimer's disease senile plaques. Biochemistry. 41, 922-928.

Kang, J., Lemaire, H. G., Unterbeck, A., Salbaum, J. M., Masters, C. L., Grzeschik, K. H., Multhaup, G., Beyreuther, K. and Muller-Hill, B., 1987. The precursor of Alzheimer's disease amyloid A4 protein resembles a cell-surface receptor. Nature. 325, 733-736.

King, D. L. and Arendash, G. W., 2002. Maintained synaptophysin immunoreactivity in Tg2576 transgenic mice during aging: correlations with cognitive impairment. Brain Res. 926, 58-68.

Klafki, H. W., Wiltfang, J. and Staufenbiel, M., 1996. Electrophoretic separation of betaA4 peptides (1-40) and (1-42). Anal Biochem. 237, 24-29.

Kuo, Y. M., Kokjohn, T. A., Beach, T. G., Sue, L. I., Brune, D., Lopez, J. C., Kalback, W. M., Abramowski, D., Sturchler-Pierrat, C., Staufenbiel, M. and Roher, A. E., 2001. Comparative analysis of amyloid-beta chemical structure and amyloid plaque morphology of transgenic mouse and Alzheimer's disease brains. J Biol Chem. 276, 12991-12998.

Masliah, E., Sisk, A., Mallory, M., Mucke, L., Schenk, D. and Games, D., 1996. Comparison of neurodegenerative pathology in transgenic mice overexpressing V717F beta-amyloid precursor protein and Alzheimer's disease. J Neurosci. 16, 5795-5811.

McGowan, E., Eriksen, J. and Hutton, M., 2006. A decade of modeling Alzheimer's disease in transgenic mice. Trends Genet.

Miller, D. L., Papayannopoulos, I. A., Styles, J., Bobin, S. A., Lin, Y. Y., Biemann, K. and Iqbal, K., 1993. Peptide compositions of the cerebrovascular and senile plaque core amyloid deposits of Alzheimer's disease. Arch Biochem Biophys. 301, 41-52.

Miravalle, L., Calero, M., Takao, M., Roher, A. E., Ghetti, B. and Vidal, R., 2005. Amino-terminally truncated Abeta peptide species are the main component of cotton wool plaques. Biochemistry. 44, 10810-10821.

Mok, S. S., Losic, D., Barrow, C. J., Turner, B. J., Masters, C. L., Martin, L. L. and Small, D. H., 2006. The beta-amyloid peptide of Alzheimer's disease decreases adhesion of vascular smooth muscle cells to the basement membrane. J Neurochem. 96, 53-64.

Mori, H., Takio, K., Ogawara, M. and Selkoe, D. J., 1992. Mass spectrometry of purified amyloid beta protein in Alzheimer's disease. J Biol Chem. 267, 17082-17086.

Nunan, J. and Small, D. H., 2002. Proteolytic processing of the amyloid-beta protein precursor of Alzheimer's disease. Essays Biochem. 38, 37-49.

Oddo, S., Caccamo, A., Shepherd, J. D., Murphy, M. P., Golde, T. E., Kayed, R., Metherate, R., Mattson, M. P., Akbari, Y. and LaFerla, F. M., 2003. Triple-transgenic model of Alzheimer's disease with plaques and tangles: intracellular Abeta and synaptic dysfunction. Neuron. 39, 409-421.

Pepys, M. B., Rademacher, T. W., Amatayakul-Chantler, S., Williams, P., Noble, G. E., Hutchinson, W. L., Hawkins, P. N., Nelson, S. R., Gallimore, J. R., Herbert, J. and et al., 1994. Human serum amyloid P component is an invariant constituent of amyloid deposits and has a uniquely homogeneous glycostructure. Proc Natl Acad Sci U S A. 91, 5602-5606.

Piccini, A., Russo, C., Gliozzi, A., Relini, A., Vitali, A., Borghi, R., Giliberto, L., Armirotti, A., D'Arrigo, C., Bachi, A., Cattaneo, A., Canale, C., Torrassa, S., Saido, T. C., Markesbery, W., Gambetti, P. and Tabaton, M., 2005. beta-amyloid is different in normal aging and in Alzheimer disease. J Biol Chem. 280, 34186-34192.

Pike, C. J., Overman, M. J. and Cotman, C. W., 1995. Amino-terminal deletions enhance aggregation of beta-amyloid peptides in vitro. J Biol Chem. 270, 23895-23898.

Price, J. L., Davis, P. B., Morris, J. C. and White, D. L., 1991. The distribution of tangles, plaques and related immunohistochemical markers in healthy aging and Alzheimer's disease. Neurobiol Aging. 12, 295-312.

Richards, J. G., Higgins, G. A., Ouagazzal, A. M., Ozmen, L., Kew, J. N., Bohrmann, B., Malherbe, P., Brockhaus, M., Loetscher, H., Czech, C., Huber, G., Bluethmann, H., Jacobsen, H. and Kemp, J. A., 2003. PS2APP transgenic mice, coexpressing hPS2mut and hAPPswe, show age-related cognitive deficits associated with discrete brain amyloid deposition and inflammation. J Neurosci. 23, 8989-9003.

Riek, R., Guntert, P., Dobeli, H., Wipf, B. and Wuthrich, K., 2001. NMR studies in aqueous solution fail to identify significant conformational differences between the monomeric forms of two Alzheimer peptides with widely different plaque-competence, A beta(1-40)(ox) and A beta(1-42)(ox). Eur J Biochem. 268, 5930-5936.

Rufenacht, P., Guntert, A., Bohrmann, B., Ducret, A. and Dobeli, H., 2005. Quantification of the A beta peptide in Alzheimer's plaques by laser dissection microscopy combined with mass spectrometry. J Mass Spectrom. 40, 193-201.

Saido, T. C., 2000. Involvement of polyglutamine endolysis followed by pyroglutamate formation in the pathogenesis of triplet repeat/polyglutamine-expansion diseases. Med Hypotheses. 54, 427-429.

Saido, T. C., Iwatsubo, T., Mann, D. M., Shimada, H., Ihara, Y. and Kawashima, S., 1995. Dominant and differential deposition of distinct beta-amyloid peptide species, A beta N3(pE), in senile plaques. Neuron. 14, 457-466.

Saido, T. C., Yamao-Harigaya, W., Iwatsubo, T. and Kawashima, S., 1996. Amino- and carboxyl-terminal heterogeneity of beta-amyloid peptides deposited in human brain. Neurosci Lett. 215, 173-176.

Schutze, K. and Lahr, G., 1998. Identification of expressed genes by laser-mediated manipulation of single cells. Nat Biotechnol. 16, 737-742.

Selkoe, D. J., 1991. The molecular pathology of Alzheimer's disease. Neuron. 6, 487-498.

Selkoe, D. J., 2001. Alzheimer's disease: genes, proteins, and therapy. Physiol Rev. 81, 741-766.

Sergeant, N., Bombois, S., Ghestem, A., Drobecq, H., Kostanjevecki, V., Missiaen, C., Wattez, A., David, J. P., Vanmechelen, E., Sergheraert, C. and Delacourte, A., 2003. Truncated beta-amyloid peptide species in pre-clinical Alzheimer's disease as new targets for the vaccination approach. J Neurochem. 85, 1581-1591.

Srinivasan, R., 1986. Ablation of polymers and biological tissue by ultraviolet lasers. Science. 234, 559-565.

Suzuki, N., Iwatsubo, T., Odaka, A., Ishibashi, Y., Kitada, C. and Ihara, Y., 1994. High tissue content of soluble beta 1-40 is linked to cerebral amyloid angiopathy. Am J Pathol. 145, 452-460.

Tanzi, R. E., Gusella, J. F., Watkins, P. C., Bruns, G. A., St George-Hyslop, P., Van Keuren, M. L., Patterson, D., Pagan, S., Kurnit, D. M. and Neve, R. L., 1987. Amyloid beta protein gene: cDNA, mRNA distribution, and genetic linkage near the Alzheimer locus. Science. 235, 880-884.

Tekirian, T. L., Yang, A. Y., Glabe, C. and Geddes, J. W., 1999. Toxicity of pyroglutaminated amyloid beta-peptides 3(pE)-40 and -42 is similar to that of A beta1-40 and -42. J Neurochem. 73, 1584-1589.

Thal, D. R., Capetillo-Zarate, E., Del Tredici, K. and Braak, H., 2006. The development of amyloid beta protein deposits in the aged brain. Sci Aging Knowledge Environ. 2006, re1.

Thal, D. R., Capetillo-Zarate, E., Schultz, C., Rub, U., Saido, T. C., Yamaguchi, H., Haass, C., Griffin, W. S., Del Tredici, K., Braak, H. and Ghebremedhin, E., 2005. Apolipoprotein E co-localizes with newly formed amyloid beta-protein (Abeta) deposits lacking immunoreactivity against N-terminal epitopes of Abeta in a genotype-dependent manner. Acta Neuropathol (Berl). 110, 459-471.

Thal, D. R., Del Tredici, K. and Braak, H., 2004. Neurodegeneration in normal brain aging and disease. Sci Aging Knowledge Environ. 2004, pe26.

van Horssen, J., Kleinnijenhuis, J., Maass, C. N., Rensink, A. A., Otte-Holler, I., David, G., van den Heuvel, L. P., Wesseling, P., de Waal, R. M. and Verbeek, M. M., 2002. Accumulation of heparan sulfate proteoglycans in cerebellar senile plaques. Neurobiol Aging. 23, 537-545.

Weiner, H. L. and Selkoe, D. J., 2002. Inflammation and therapeutic vaccination in CNS diseases. Nature. 420, 879-884.

Wiltfang, J., Arold, N. and Neuhoff, V., 1991. A new multiphasic buffer system for sodium dodecyl sulfate-polyacrylamide gel electrophoresis of proteins and peptides with molecular masses 100,000-1000, and their detection with picomolar sensitivity. Electrophoresis. 12, 352-366.

Wiltfang, J., Smirnov, A., Schnierstein, B., Kelemen, G., Matthies, U., Klafki, H. W., Staufenbiel, M., Huther, G., Ruther, E. and Kornhuber, J., 1997. Improved electrophoretic separation and immunoblotting of beta-amyloid (A beta) peptides 1-40, 1-42, and 1-43. Electrophoresis. 18, 527-532.

ACKNOWLEDGEMENTS

We thank Francoise Gerber and Jürg Messer for preparing brain slices for histology, Christian Czech for establishing the contact to Professor Jens Wiltfang in Erlangen, Jens Wiltfang and his group for providing the opportunity to learn the handling of the urea-based Western blot assay. Furthermore, we thank Nicole Soder for mass spectrometry sample preparation and general assistance, Daniel Roeder, Arno Friedlein and Eirini Tsirogianni for assistance with MS measurements. Finally, we thank Professor Theodor Güntert for critical review of the manuscript.

Abbreviations: AD, Alzheimer's disease; PA, pathological aging; Aβ, amyloid beta peptide; APP, amyloid precursor protein; CAA, cerebral amyloid angiopathy; FAD, familial Alzheimer's disease; 6-GuHe, N-hydroxysuccinimido 6-guanidohexanoic acid; MALDI-TOF MS, matrix assisted laser desorption ionization-time of flight mass spectrometry; N3pE-42, pyroglutamate 3-42; Lys-C, lysyl endopeptidase; ox, M35M oxidized; red, M35M reduced; LC-MS/MS, liquid chromatography-tandem mass spectroscopy; pl., plaque(s)

Method	WB	MS	MS	MS
Peptide	no Lys-C no 6-GuHe	no Lys-C no 6-GuHe	Lys-C digestion no 6-GuHe	Lys-C digestion 6-GuHe modified
Aβ 1-40 / 42	0.002 pmol	10 pmol	-	-
Aβ 1-16	-	-	0.2 pmol	1.3 pmol
Aβ 17-28	-	-	0.2 pmol	0.3 pmol
Aβ 29-40 / 42	-	-	-	0.3 pmol

Tab. 1. Comparison of the sensitivities of the Western blot assay and different MS protocols.

The values given in the table represent the amount of Aβ present in a collection of excised plaques to obtain a signal with the indicated method. WB, Western blotting; MS, mass spectrometry

		cored plaques					diffuse plaques*
Human Brain	**Aβ species**	**occipital cortex**	**temporal cortex**	**frontal cortex**	**hippocampus**	**average**	**hippocampus**
PA n=2	Aβ 1-16	-	-	-	-	-	**61**
	Aβ 2-16						12
	Aβ 3-16						0
	Aβ N3pE-16						15
	Aβ 4-16						12
	Aβ 5-16						0
	total % fragmentation						**39**
AD Braak IV n=1	Aβ 1-16	n.e.	65	67	49	**62**	**64**
	Aβ 2-16		7	7	8	7	10
	Aβ 3-16		6	0	6	4	0
	Aβ N3pE-16		16	16	19	16	14
	Aβ 4-16		8	6	7	7	7
	Aβ 5-16		0	3	11	4	5
	total % fragmentation					**38**	**36**
AD Braak V n=2	Aβ 1-16	52	42	47	62	**51**	**63**
	Aβ 2-16	10	11	10	11	10	9
	Aβ 3-16	4	11	12	0	7	10
	Aβ N3pE-16	18	16	17	14	16	10
	Aβ 4-16	10	10	9	7	9	8
	Aβ 5-16	6	8	4	6	6	0
	total % fragmentation					**49**	**37**
AD Braak VI n=2	Aβ 1-16	39	42	40	44	**41**	**61**
	Aβ 2-16	18	12	12	11	13	11
	Aβ 3-16	4	3	0	4	3	3
	Aβ N3pE-16	21	27	26	22	24	15
	Aβ 4-16	9	8	10	15	10	8
	Aβ 5-16	11	7	12	4	9	2
	total % fragmentation					**59**	**39**

*** diffuse plaques from PA cases isolated from temporal cortex**

Tab. 2. Relative ratios of N-terminal truncated Aβ variants isolated from human plaques.

The peak height magnitude of the peaks corresponding to Aβ 1-16, 2-16, 3-16, N3pE-16, 4-16 and 5-16 were added and the relative portion of the respective peaks determined. The relative ionization properties of Aβ 2-16, 3-16, 4-16 and 5-16 are not known, but because Aβ N3pE-16 has almost identical ionization properties to Aβ 1-16, they were assumed to be comparable. n.e., not evaluable, represents MS-profiles of the type given in Fig. 4B, (bottom: elution 90% ACN); PA, pathological aging

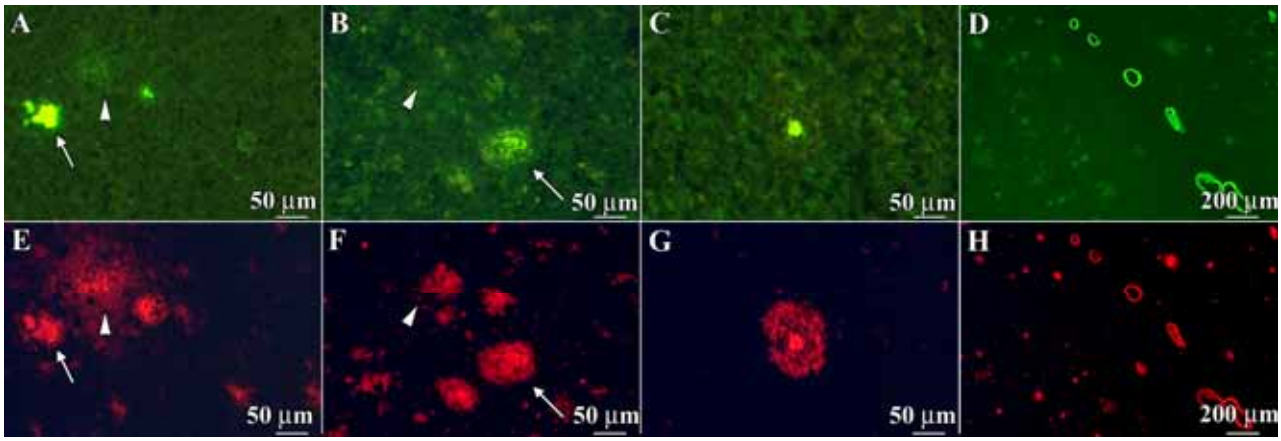

Fig. 1. Histology of human and PS2APP transgenic mouse brain sections.

Brain sections from PS2APP mice (A, E) and from human AD (B-D, F-H) specimen were doublestained with thioflavine S and an antibody specific for the amino terminal amino acids 2-8 (BAP-2) in order to differentiate between the three plaque types and to guide the dissection procedure. Arrowheads indicate diffuse plaques (thioflavine S negative and BAP-2 positive), arrows indicate compact plaques (thioflavine S positive and BAP-2 positive). A typical example of a cored plaque is given in C and G (core: thioflavine S positive and BAP-2 positive; corona: thioflavine S negative and BAP-2 positive). Diffuse plaques were found occasionally in transgenic mice and more frequently in human brain. Compact plaques were rare in humans, but predominate in PS2APP mice. Human vessels with CAA were visualized by both methods (D, H).

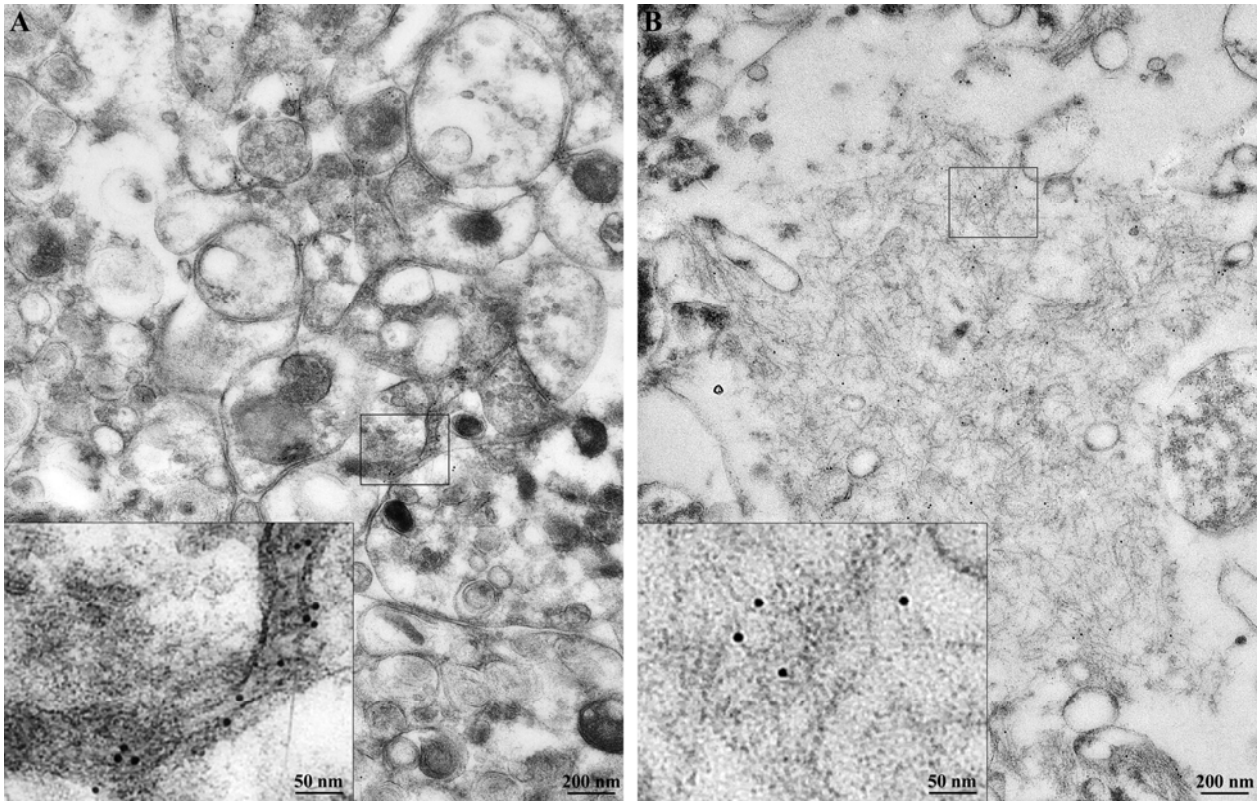

Fig. 2. Ultrastructural differences between diffuse plaques in PS2APP mice and human Alzheimer's disease brains.

Sections of PS2APP (A) and human AD (B) brain were labeled using BAP-2 antibody. Visualization was achieved using a goat anti-mouse secondary antibody conjugated to 10 nm colloidal gold spheres, each seen as a black dot. Diffuse plaques from PS2APP mice show single or few Aβ fibrils deposited in the extracellular space, which can directly contact the cell membrane of neurites. In contrast, Aβ fibrils of human diffuse plaques are colocalized within confined clusters of extracellular matrix proteins.

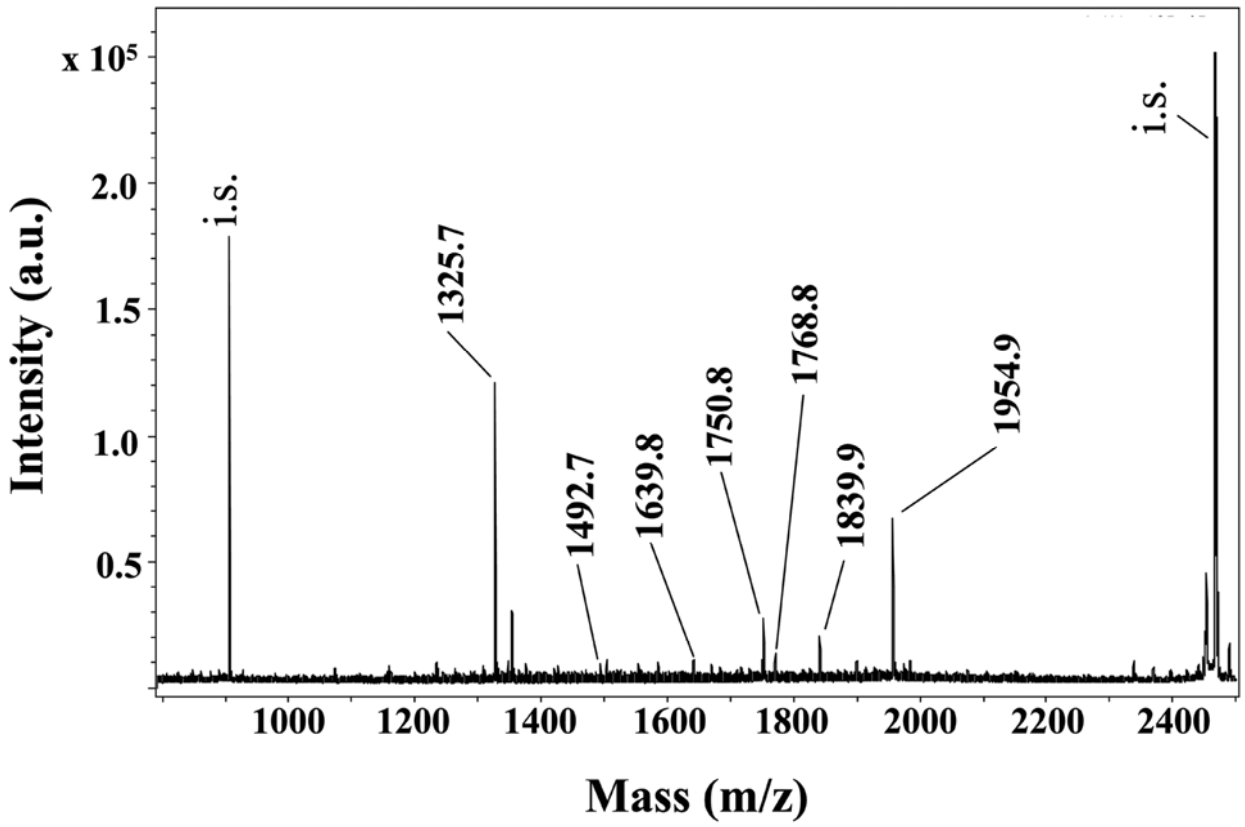

Fig. 3. Detection of the amino-termini of Aβ by mass spectrometry.

Mass spectrometric profile derived from 30 human cored plaques from the occipital association cortex of a patient with severe AD (Braak VI). Typically, N-terminal Aβ peaks corresponding to Aβ 1-16 (1954.9), 2-16 (1839.9), 3-16 (1768.8), N3pE-16 (1750.8), 4-16 (1639.8) and 5-16 (1492.7) can be observed. None of the carboxy-terminal peptides were detected due to poor ionization properties. i.s., internal standard.

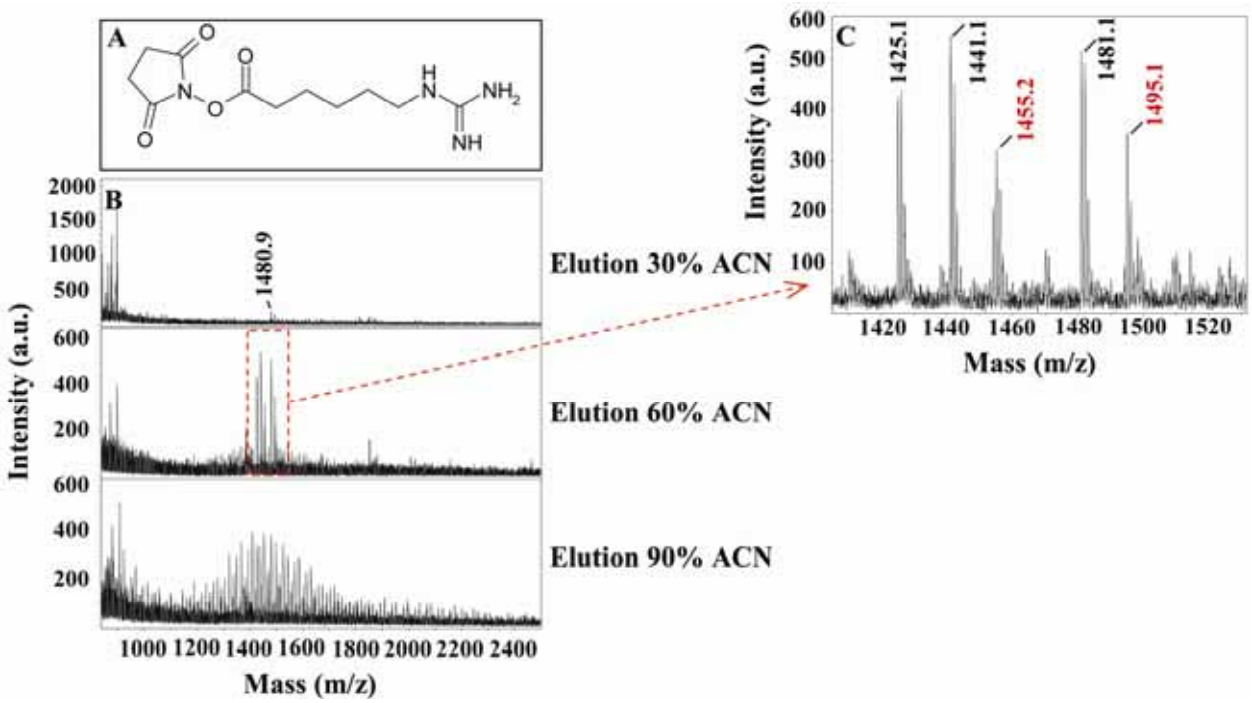

Fig. 4. Detection of the carboxy-termini of Aβ by mass spectrometry.

(A) In order to improve the ionization, the peptides were modified by derivatization with 6-guanidohexanoic acid - N-hydroxysuccinimide (6-GuHe). (B) Mass spectrometric profiles derived from 50 human cored plaques from the occipital association cortex of a patient with severe AD (Braak VI). The sample was spiked with 0.6 pmol ^{15}N-Aβ 1-42 ox for quantification. Desalting prior to MS was performed with ZipTip using step gradients of 30%, 60% and 90% acetonitrile. This additional procedure results in a better signal to noise ratios in the 60% eluate. (C) Peak pattern at higher resolution. The method allows to discriminate between oxidized and reduced Met-35. m/z values are: Aβ 29-42 ox: 1441.1, Aβ 29-42 red: 1425.1, Aβ 17-28: 1481.1, ^{15}N-Aβ 29-42 ox: 1455.2 and ^{15}N-Aβ 17-28: 1495.1.

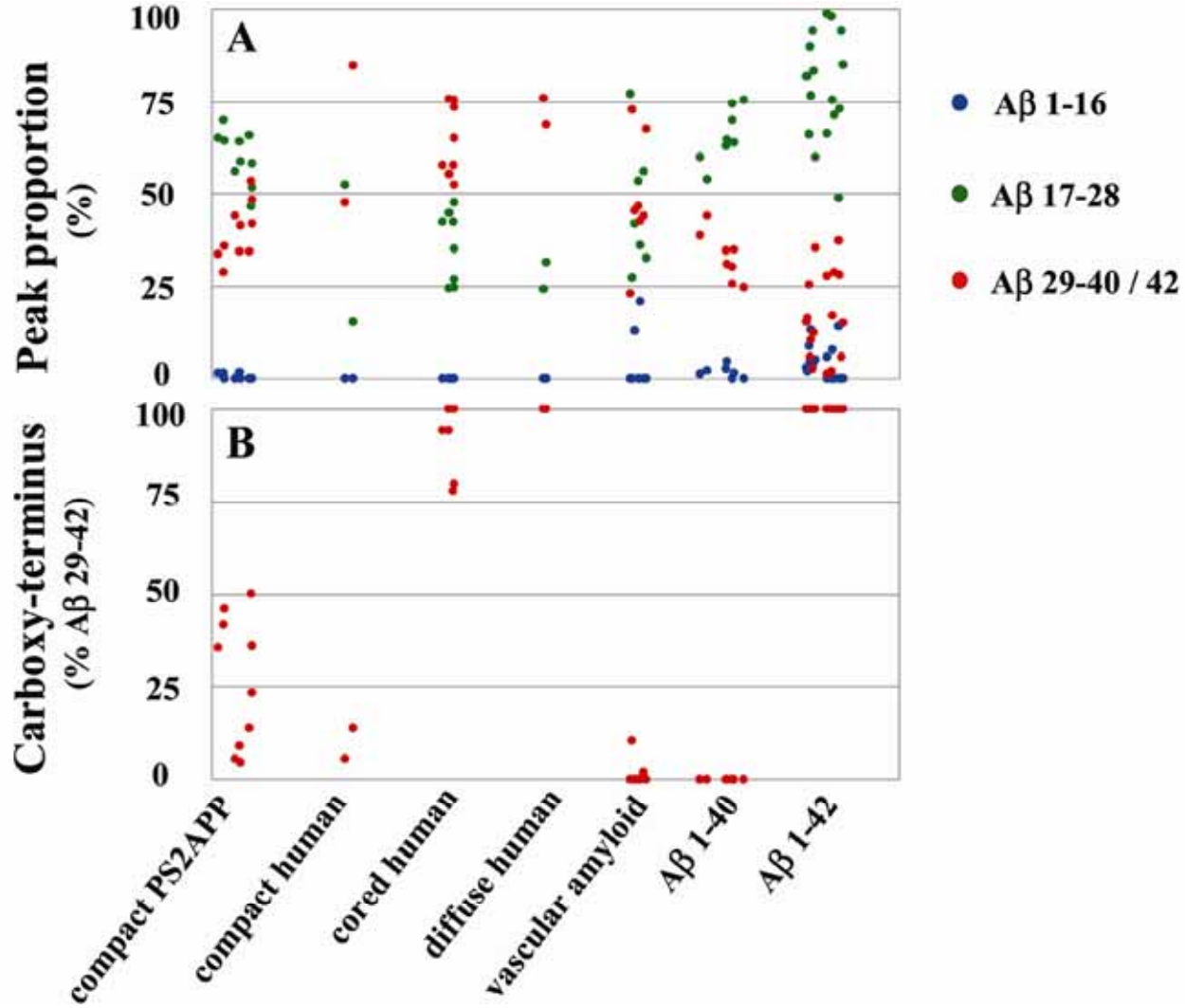

Fig. 5. Peak proportions after 6-GuHe modification.

Determination of the proportion of Aβ 1-16, Aβ 17-28 and Aβ 29-40/42 was performed as described in the method section. (A) The proportion of Aβ 17-28 to Aβ 29-40/42 is in favor of Aβ 17-28 when synthetic Aβ or plaques from PS2APP mice were analyzed. In human plaques we found the inverse proportion (example given in Fig. 4C). 6-GuHe modification leads to an almost complete quenching of Aβ x-16. (B) Comparison of C-terminal proportions Aβ 29-40 and Aβ 29-42. Human cored and diffuse plaques both contain high amounts of Aβ 42.

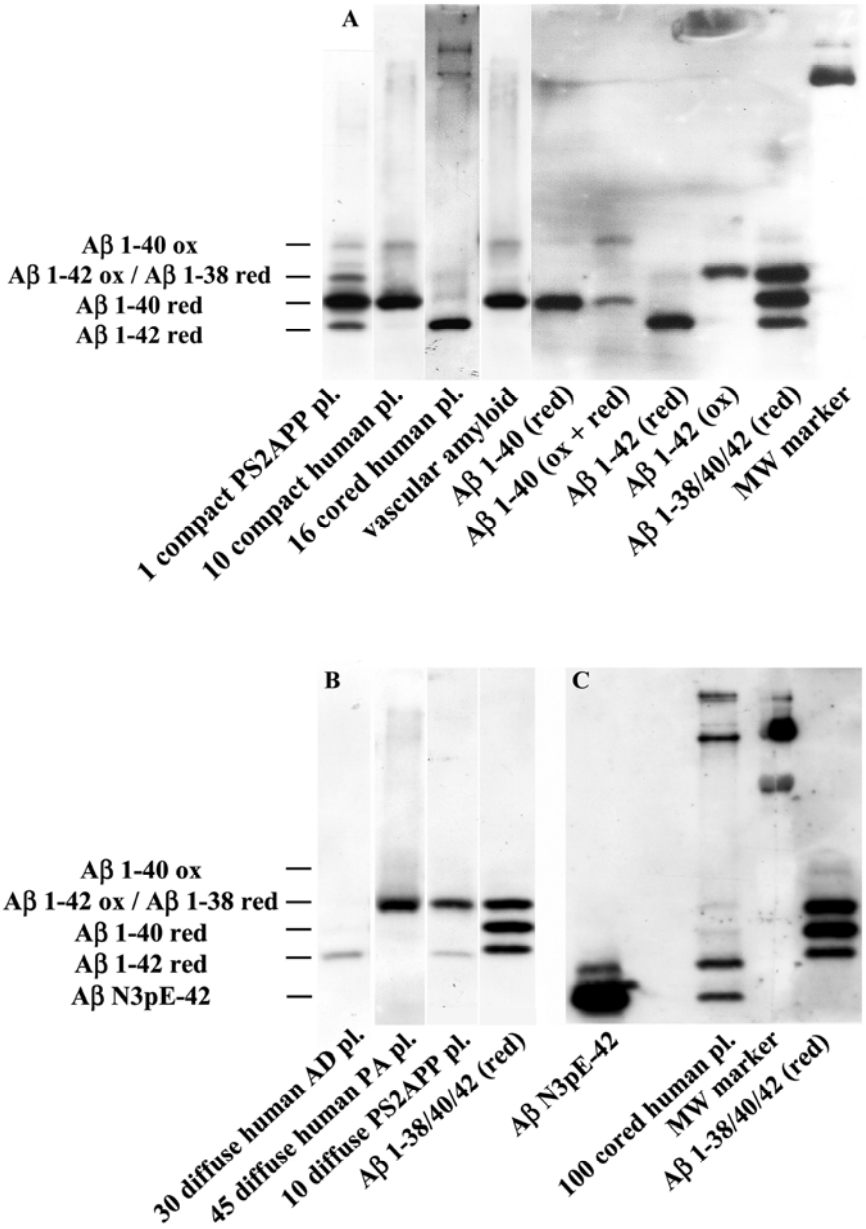

Fig. 6. Western blot analysis of amyloid deposits.

(A) Analysis of thioflavine S positive amyloid deposits from human and PS2APP transgenic mice. Note that Aβ 1-42 ox and Aβ 1-38 red migrate to almost identical positions. (B) Analysis of diffuse plaques from human and from transgenic mice. They contain predominantly Aβ 1-42, in the present example the plaques from the human AD specimen contain reduced, from the human PA case oxidized and the plaques from mouse a mixture of reduced and oxidized Aβ 1–42. (C) Western blot analysis of human cored plaques with an N3pE-specific antibody. Pyroglutamate 3-42 could be detected as suggested by MALDI-TOF MS analysis. Two blots with an N3pE-specific antibody (left) and WO-2 antibody (right) are shown.

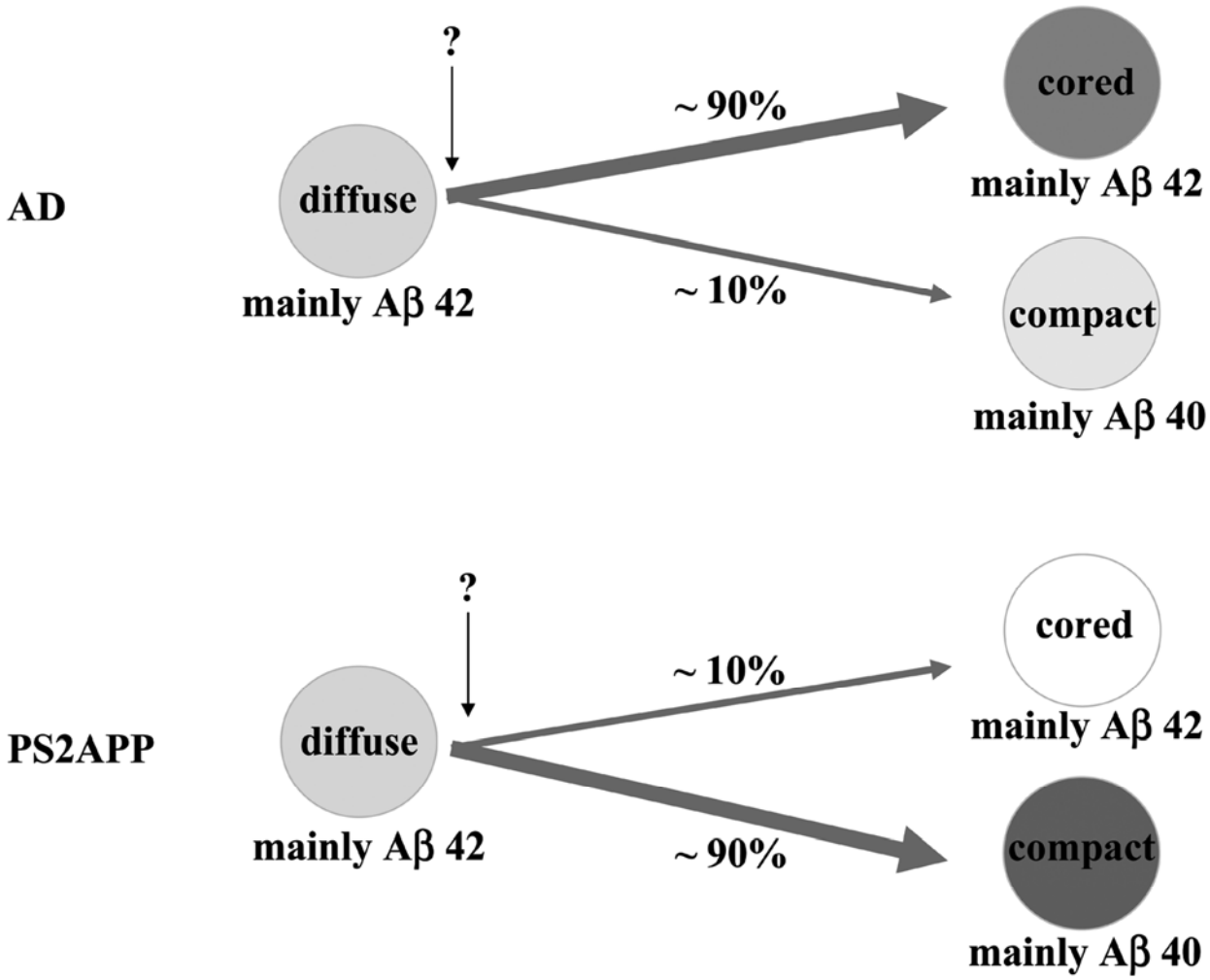

Fig. 7. Hypothetical model of stages in the plaque deposition process.

Diffuse plaques are found in human AD brain and in PS2APP mice and are considered to be the initial plaque type. Although in both cases diffuse plaques contain mainly Aβ 1-42, electron microscopy revealed ultrastructural differences already in this early state of plaque formation. The maturation into cored plaques cannot proceed over compact plaques, due to their Aβ 40 to Aβ 42 contents. Therefore, we postulate disparate deposition of amyloid in plaques in human AD and in PS2APP mice, respectively.

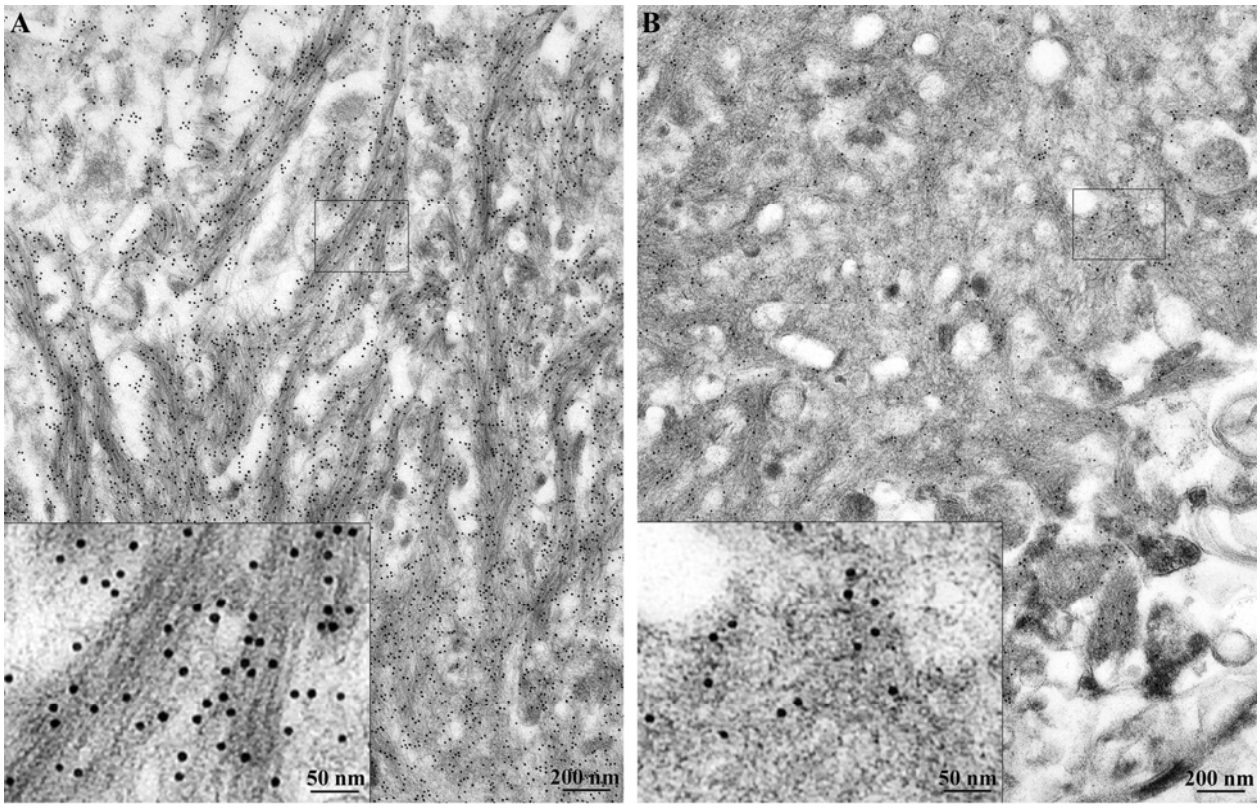

Supplementary data, Fig. 1. Ultrastructure of PS2APP compact plaques and cored plaques from human Alzheimer's disease brain.

Sections of PS2APP (A) and human AD (B) brain were labeled using an anti-Aβ monoclonal antibody (BAP-2). Visualization was achieved using a goat anti-mouse secondary antibody conjugated to 10 nm colloidal gold spheres. Aβ fibrils in compact mouse plaques are very densely packed with dystrophic neurites and reactive microglia at the periphery. Cored human plaques consist of numerous clusters of densely packed large bundles of Aβ fibrils. The fibrillar bundles are often in contact with the surrounding neuropil.

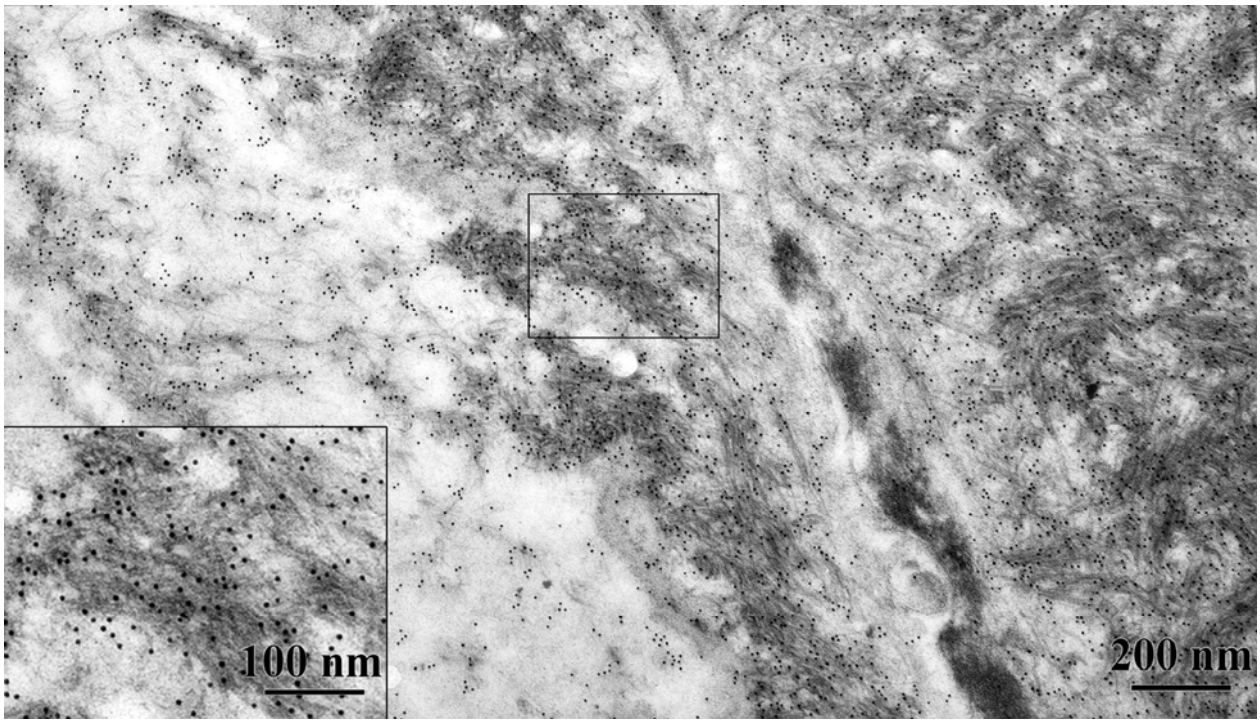

Supplementary data, Fig. 2. Ultrastructure of vascular amyloid from human Alzheimer's disease brain. Sections of human AD brain were labeled using an anti-Aβ monoclonal antibody (BAP-2). Visualization was achieved using a goat anti-mouse secondary antibody conjugated to 10 nm colloidal gold spheres. Characteristic for human vascular amyloid is the dense packing of Aβ fibrils at the basement membrane.

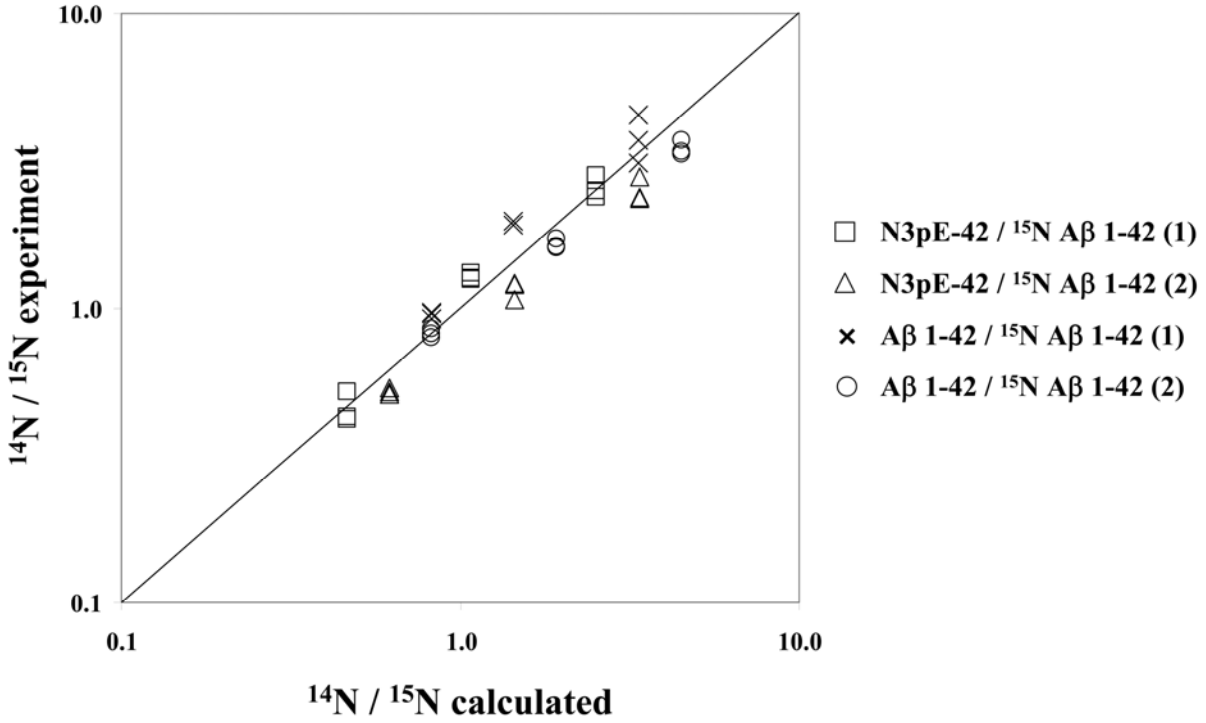

Supplementary data, Fig. 3 Ionization properties of the N-terminal fragment of Aβ 1-42 and N3pE-42. Different ratios (3/7, 1/1 and 7/3) of synthetic Aβ N3pE-42 and Aβ 1-42 were mixed with ^{15}N labelled Aβ 1-42 to compare ionization and Lys-C digestion properties in the MALDI-TOF MS. As can be seen, the calculated ^{14}N / ^{15}N ratios correlate linearly with the experimentally measured peak ratios. This clearly indicates comparable ionization and Lys-C digestion properties for Aβ 1-16 and Aβ N3pE-16. Three measured points were obtained per sample, since three dilutions (1:1, 1:4 and 1:12) were performed for each preparation. Numbers in brackets of the indicated standards indicate the first and second of two independent experiments.

APPENDIX III

Studying the Role of Pyroglutamate in Alzheimer's Disease

by

Andreas Güntert, Céline Adessi, Heinz Döbeli and Bernd Bohrmann

prepared for Submission

Studying the Role of Pyroglutamate in Alzheimer's Disease

Andreas Güntert[a], Céline Adessi[a], Heinz Döbeli[a] and Bernd Bohrmann[a]

[a]Pharma Research Basel, F. Hoffmann-La Roche Ltd, Grenzacherstrasse 124, CH-4070 Basel, Switzerland

Key words: pyroglutamate, mass spectrometry, laser dissection microscopy, Alzheimer's disease, amyloid, aggregation

We have investigated the N-terminal modification of amyloid-β (Aβ) protein in Alzheimer's disease (AD) brains. Laser dissection microscopy of human cored plaques from AD brains with Braak stage IV, V and VI and subsequent mass spectrometric analysis revealed an increase of N-terminally truncated Aβ variants, especially pyroglutamate 3-40 / 42, of ~20% correlating with disease progression. Pyroglutamate 3-40 / 42 was consistently detected as the major N-terminal truncated Aβ species in human cored plaques. We aimed to determine, whether pyroglutamate was artificially induced by the sample preparation procedure or indeed is an *in vivo* generated major component of amyloid plaques in human and may be responsible for the high level of neurodegeneration observed AD brains. We used immunohistochemistry, Western blot analysis of laser dissected cored plaques, mass spectrometric analysis of synthetic oligopeptides starting with either glutamine or glutamate and *in vitro* aggregation and toxicity studies with synthetic pyroglutamate 3-42 (N3pE-42) to get more insight into the role of pyroglutamate in AD. Our findings show that pyroglutamate is a major constituent of all amyloid plaques in AD and PS2APP transgenic mice. Synthetic N3pE-42 seems to be less toxic and exhibits a significantly lower rate of aggregation than Aβ 1-42. It must therefore be considered much more as an abundant metabolite and not as a particular harmful seed for Aβ oligomerization. However, due to its abundance it is worth to follow pyroglutamate 3-40 / 42 in CSF or blood and test its usefulness as suitable biomarker for AD.

Manuscript [III],
prepared for Submission

INTRODUCTION

Alzheimer's disease is a progressive dementing disorder characterized by the occurrence of two pathological hallmarks: intraneuronal neurofibrillary tangles consisting of hyperphosphorylated protein tau and senile plaques, which form upon extracellular deposition of Aβ. The cognitive decline that characterizes AD is well correlated to the cortical spreading of tau pathology (Delacourte et al., 1999). However, a strong correlation of the amyloid pathology and the dynamic progression of tau pathology was shown, suggesting an inductive role for amyloid deposition in the spreading of tau pathology (Delacourte et al., 2002, Oddo et al., 2004).

Aβ peptides are the main protein component of plaques (Glenner et al., 1984). They are deposited as full length Aβ 1-40 and 1-42 as determined by the use of C-terminal specific antibodies several years ago (Jarrett et al., 1993, Iwatsubo et al., 1994). Upon deposition, Aβ peptides undergo extensive N-terminal truncation and several groups characterized the occurrence of various N-terminal truncated Aβ species by immunohistochemistry (Iwatsubo et al., 1996, Saido et al., 1996), the analysis of brain homogenates (Mori et al., 1992, Miller et al., 1993, Hosoda et al., 1998, Sergeant et al., 2003) or the laser dissection of thousands of plaques (Miravalle et al., 2005). A quantification and determination of the extent of N-terminal truncated Aβ forms from small numbers of laser dissected plaques of PS2APP transgenic mice and human AD brains was performed by our group (Rufenacht et al., 2005). Furthermore, we were able to correlate disease progression with an increase of N-terminally truncated Aβ variants in laser dissected cored human plaques (Güntert et al., 2006, submitted to *Neuroscience*). We detected pyroglutamate 3-40 / 42 as the major N-terminal truncated Aβ variant, with an incidence of 15-25% depending on the Braak stage of the investigated brains. Consistently, N3pE-40 / 42 was described previously to be a major component of amyloid plaques in AD brains (Mori et al., 1992, Saido et al., 1995, Harigaya et al., 2000).

N3pE-40 / 42 is an Aβ species beginning with glutamic acid 3, but blocked by conversion to pyroglutamate through intramolecular dehydration. This modification is of particular interest because it may contribute to the deposition of Aβ by inhibiting the proteolytic degradation of Aβ by aminopeptidases (Hosoda et al., 1998, Harigaya et al., 2000). In addition, it was proposed that
N3pE-40 / 42 Aβ variants could be more prone to aggregation and deposition through its enhanced hydrophobicity due to the loss of one positive and two negative charges (Saido et al., 1995, Saido, 2000). Other reports showed a general increase in aggregation properties for N-terminal truncated Aβ peptides (Pike et al., 1995) or a similar toxicity in cell based assays (Tekirian et al., 1999).

To prove that Aβ N3pE-40 / 42 is not artificially induced by the sample preparation procedure, we incubated several synthetic oligopeptides starting with either a glutamine or a glutamate with hexa-fluoro-isopropanol (HFIP, 1,1,1,3,3,3-hexafluoro-2-propanol), 70% formic acid (FA) or trifluoroacetic acid (TFA) and determined the amount of pyroglutamine / pyroglutamate formed. Furthermore, we identified N3pE-40 / 42 as a constituent of amyloid plaques in human by immunohistochemistry and Western blotting and performed *in vitro* aggregation and toxicity experiments with synthetic N3pE-42.

MATERIALS AND METHODS

Human tissues and transgenic mice

Human brains from AD patients were obtained from the Sun Health Research Institute through Dr. Thomas G. Beach (Sun City, AZ, USA). The brain tissue was collected approximately two hours after death and was immediately frozen at -80°C. Brains were neuropathologically staged according to Braak (Braak and Braak, 1991). Laser dissection and immunohistochemistry were performed on a superior parietal gyrus from an 84-year-old patient with Braak stage V, showing heavy plaque load. 16 month old PS2APP mice were used for immunostaining (Richards et al., 2003).

Synthetic oligopeptides

Synthetic oligopeptides starting either with glutamine or glutamate were purchased from Bachem (Bachem Holding AG, Bubendorf, Switzerland). We used peptide 810 (H-2586-0001), Apelin-13 (H4566.0001) and anxiety peptide (H-1770.0001) starting with glutamine and neuropeptide el (H-2396.0001) and fibrinogen β-chain (H-3034.0001) with a glutamate at position 1. The sequence and molecular weight of the oligopeptides can be seen in Tab. 1.

Laser dissection microscopy and mass spectrometry of plaques

Laser dissection microscopy and mass spectrometry of laser dissected plaques was performed as previously described (Rufenacht et al., 2005) with minor modifications. For dissolution, the cap containing the plaques was rinsed twice with 58.5 µl of HFIP instead of 70% FA, to omit sample preparation artifacts that may result from FA treatment.

Sample preparation and mass spectrometry of oligopeptides

The oligopeptides were dissolved in 1 ml of HFP to obtain a concentration of 1 mg / ml.
50 nmoles of the respective peptides were incubated with 100 µl of either HFIP, 70% FA or concentrated TFA. After an incubation period of 6h, 18 h, 48h and 96h, the samples were sonicated (3 x 3 min in a water-bath at room temperature with intermediate vortex mixing) and were dried in an evacuated centrifuge for further processing of the peptides. The pellet was dissolved in 10 µl of 10 mM $NaHCO_3$ solution. One µl thereof was mixed with an equal volume of a α-cyano-4-hydroxycinnamic acid solution (Sigma-Aldrich Chemie GmbH, C2020; 5 mg/ml in 50% (v/v) acetonitrile-water) and spotted onto a standard stainless-steel Bruker MALDI 384-target plate (Bruker Daltonics GmbH, Bremen, Germany). The measurements were performed on a Bruker UltraFlex time of flight mass spectrometer in reflector mode using standard operating parameters. Spectra were acquired manually at 4 different shot locations and a total of 400 shots were added per spectrum.

Immunohistochemistry

Immunohistochemistry was performed as previously described (Güntert et al., 2006, submitted to *Neuroscience)*. As primary antibody, anti-N3pE (Assay designs, Ann Arbor, MI, USA), specific for pyroglutaminated Aβ forms, was used at a concentration of 1 μg / ml.

Urea- based Western blot assay and dot blots

Western blotting was performed as previously described (Güntert et al., 2006, submitted to *Neuroscience)*. As primary antibody, anti-N3pE (Assay designs) was used at a dilution of 1:1000 in PBS-T.

For dot blots, synthetic Aβ 1-40 / 42 and N3pE-42 was diluted and applied at 5μl drops to PVDF membranes (50 ng – 0.005 ng), which were previously activated for 10 sec in methanol and rinsed in H_2O. The membranes were air-dried and unspecific binding sites were blocked using 5% skim milk in PBS-T for 1 hr at room temperature. Following primary antibodies were compared: 8E1 (anti-N3pE, Assay designs), WO-2 (The Genetics Company, Zürich, Switzerland) and 6E10 (Sigma-Aldrich Chemie GmbH). Primary antibodies were used at 0.1, 0.5 and 1μg/ml concentrations and applied for 2 hrs at room temperature. After the incubation period, washing steps with PBS-T were performed for 30 min, 15 min and 2 x 10 min. The membranes were then incubated with a horseradish peroxidase linked anti-mouse secondary antibody for 1 hr at room temperature, before three more washing steps with PBS-T for 3 x 10 min were performed. Detection was achieved with conventional X-ray films (Amersham Biosciences, Piscataway, NJ, USA) after a 5 min development period with ECLPlus™ (Amersham Biosciences) according to the manufacturer's protocol.

Aggregation studies

Synthetic Aβ 1-42 and N3pE-42 peptides were solubilized according to a previously described method (Stine et al., 2003). Aβ was solubilized in HFIP to 0.22 mM, sonicated for 10 min and incubated overnight at room temperature. The solutions were aliquoted in Eppendorf tubes, evaporated at room temperature under a fume hood, dried completely in an evacuated centrifuge and stored at -80°C. Aliquots were analyzed for amino acid composition to determine the precise amount of peptide in each vial and the purity was checked by MALDI-TOF mass spectrometry analysis. The amyloid fibril formation was analyzed by the thioflavin-T fluorometric assay. Thioflavin-T, by specifically binding to amyloid fibrils, induces a shift in its emission spectrum and a allows to measure a fluorescent signal proportional to the amount of amyloid fibrils formed (LeVine, 1993, Golabek et al., 1996). HFIP pretreated Aβ 1-42 and N3pE-42 were solubilized to a final concentration of 10 μM and 50 μM in PBS. The solutions were submitted to gentle swirling (450 rpm) for 2.5 days at 0 and 37°C in an Eppendorf-Thermomixer. Incubated samples were transferred to a black 96-well plate (Costar, Basel, Switzerland) and assay buffer [50 mM glycine, pH 9, 60 μM Thioflavin-T (Sigma, Switzerland)] was added. Fluorescence was measured at an excitation of 435 nm and an emission of 480 nm in a spectrophotometer (Polarstar Galaxy, BMG Labtechnologies, Offenburg, Germany) and the signal was compared between Aβ 1-42 and N3pE-42 at 0°C and 37°C respectively.

Toxicity assay on PC-12 cells

Aβ was incubated as described above (thioflavine T assay). Aβ 1-42 and N3pE-42 were added to PC12 cells cultured in 96-well flat-bottom plates, in Ham's F12 medium with 10% horse serum and 5% fetal calf serum. Final concentrations of Aβ N3pE-42 in 96-well format were 0.1, 0.5, 1, 2 and 5 μM per well, whereas concentrations for Aβ 1-42 were 1 μm at 0°C and 0.25 μm at 37°C. After 20 hrs of incubation the cellular viability was compared between Aβ N3pE-42 and 1-42 using the MTT assay [3-(4.5-dimethylthiazol-2-yl)-2,5-diphenyl tetrasodium] according to the protocol of the manufacturer (F. Hoffmann-La Roche Ltd., Basel, Switzerland). Values of cell viability were calculated by dividing the absorbance of the sample by the absorbance of the vehicle multiplied by one hundred.

RESULTS AND DISCUSSION

Dot blots

To determine whether the pyroglutamate antibody cross-reacts with full length Aβ 1-40 and 1-42, we performed dot blot assays. The pyroglutamate antibody detects N3pE-42 at least 100 times more specifically than full length Aβ 1-40 / 42. On the other hand, an N-terminal Aβ antibody specific for full length Aβ, is about a factor of 100 more sensitive for Aβ 1-40 / 42.

Immunohistochemistry

Staining of human AD brain sections with N3pE-antibody showed that most amyloid plaques are labeled with the pyroglutamate specific antibody (Fig. 1A). This suggests that N3pE-40 / 42 is a constituent of these plaques. Cored as well as diffuse plaques were stained and detected, although with a different fluorescent signal intensity. Interestingly, vascular amyloid was also labeled and seems to contain considerable amounts of pyroglutaminated Aβ.

Plaques from PS2APP mice were also stained with the N3pE-specific antibody (Fig. 1B), this confirms the occurrence of pyroglutamate in PS2APP mouse plaques as detected with MADLI-TOF MS and described in an earlier report of our group (Rufenacht et al., 2005). As the staining protocol differs completely from the MALDI-TOF MS sample preparation protocol, pyroglutamate is very unlikely to be induced artificially. Taken together, immunohistochemistry supports the view that pyroglutamate Aβ N3pE-40 / 42 is present in large quantities in human and PS2APP amyloid plaques and is present in vascular amyloid.

Solvent effects on oligopeptides and plaque-derived Aβ

Five different peptides starting with either glutamine or glutamate (Tab. 1) were incubated for 96 hrs at room temperature with HFIP, 70% FA and concentrated TFA. The amount of artificially induced pyroglutamate was then determined in the respective incubation assays. Pyroglutamate formation can be detected in MALDI-

TOF MS with the loss of a H_2O molecule (-17 m/z). Furthermore, formylation events (+28 m/z) in the 70% FA assay and sodium adducts (+22 m/z) in general were observed (Fig. 2).

For evaluation, peak heights related to pyroglutamate were measured, added and put in relation to the sum of peak heights for all peaks related to the respective peptide. Like this, mean values for pyroglutamate induction could be calculated. For HFIP incubation, we determined a pyroglutamate ratio of 7 ± 2% for glutamate starting peptides (like Aβ) and of 25 ± 20% for glutamine starting peptides. For 70% FA, these values were 6 ± 2% and 80 ± 2% respectively, whereas for TFA incubation we found pyroglutamate of 10 ± 7% and 60 ± 5%. Our results indicate that glutamine is far more susceptible to artificial induction of pyroglutamate than is glutamate with either of the solvents. They also show that HFIP incubation induces artificial pyroglutamate formation only to a small extent. Consequently, to further exclude sample preparation artifacts by FA, the dissolution of plaque amyloid with HFIP was performed. Even though the dissolution of plaque amyloid with HFIP was not as efficient as with FA, we were able to detect pyroglutamate in 50 cored plaques by mass spectrometry (Fig. 3). HFIP instead of 70% FA revealed three peaks corresponding to Aβ fragments: 1955.7 (Aβ 1-16), 1326.0 (Aβ 17-28) and 1751.5 (Aβ N3pE-16).This supports the idea that the detected N3pE-40 / 42 is not induced artificially through FA treatment, but indeed resembles an *in vivo* constituent of human and also PS2APP mouse plaques.

Western blotting

Laser dissection of 100 human cored plaques and subsequent analysis by urea-based Western blotting revealed the occurrence of pyroglutamate (Fig. 4). By comparing migration distances of synthetic N3pE-42 with Aβ isolated from cored plaques, we were able to detect a considerable amount of pyroglutamate 3-42 and could thereby confirm the data obtained by mass spectrometry.

Aggregation and Toxicity

To determine the *in vitro* rate of aggregation and toxicity properties we compared synthetic Aβ N3pE-42 with Aβ 1-42. Oligomers stable at 0°C were used as reference and compared to Aβ peptides incubated at 37°C. When incubated for 2.5 days at 37°C, the fluorescent signal of thioflavine T is four times higher for Aβ 1-42 than for Aβ N3pE-42. This suggests that Aβ N3pE-42 has a significantly lower rate of fibril association than Aβ 1-42 (Fig. 5A). The toxicity properties of Aβ are likely dependent on the aggregation state. Consistently, a markedly reduced cellular toxicity of N3pE-42 was observed when compared to Aβ 1-42 *in vitro* (Fig. 5B). To obtain a comparable cellular toxicity to 0.25 μM Aβ 1-42, a concentration of 5 μM N3pE-42 was necessary, which corresponds to a 20 fold increase. Our observations are supported by experiments performed on murine hippocampal neurons. These experiments, showed a decreased cellular toxicity of synthetic Aβ N3pE-42 after five days compared to full length Aβ (personal communications Prof. Y.-A. Barde, Biocenter, University Basel, Switzerland).

Taking our *in vitro* data into account, it can be suggested that pyroglutamate 3-40 / 42 alone is an unlikely seed for plaque deposition in brains of Alzheimer's patients. However, it is possible that pyroglutamate together with

Aβ 1-40 / 42 as present *in vivo* may speed up the aggregation process of full length Aβ peptides. Further experiments will be necessary to determine the rate of aggregation of N3pE-42 in combination with full length Aβ 1-40 / 42.

Other groups reported a higher rate of oligomerization (Harigaya et al., 2000, Saido, 2000) and suggested an early involvement of pyroglutamate in the plaque development process (Saido et al., 1995). Furthermore, it was described that pyroglutamate and N-terminally truncated Aβ forms in general, show comparable or even enhanced toxicity compared to Aβ 1-42 (Pike et al., 1995, Tekirian et al., 1999, Russo et al., 2002). A likely explanation for this discrepancy comes from the used sample preparations. A detailed physicochemical characterization of the assembly state of the starting material is necessary to directly compare the results.

Concluding Remarks

This investigation aimed to prove that pyroglutamate is an *in vivo* constituent of amyloid plaques. We detected 15 – 25% N3pE-40 / 42 in human plaques by mass spectrometry in an earlier report (Rufenacht et al. 2005, Güntert et al., 2006, submitted to *Neuroscience*) and confirmed the presence of this posttranslationally modified Aβ peptide by Western blotting and immunohistochemistry in this study. Further, we show that pyroglutamate is not artificially induced by the sample preparation procedure, but is present in all types of plaques and vascular amyloid in human and PS2APP transgenic mice. Our *in vitro* results with synthetic Aβ peptides suggest, that Aβ N3pE-40 / 42 alone is an unlikely starting point for plaque deposition, due to its aggregation properties. Also, toxic effects of Aβ N3pE-42 are less pronounced compared to full length Aβ 1-42. However, pyroglutamate may contribute to the amyloid plaque load in the brain through its enhanced resistance to most aminopeptidases. Therefore, the abundance of N3pE-40 / 42 reflects decreased clearance and its amount in the brain mirrors the progress of the pathologic process in AD. This is supported by the detection of increasing amounts of pyroglutamate from Braak stage IV – VI in a MALDI-TOF analysis by our group (Güntert et al., 2006, submitted to *Neuroscience*).

Considering the abundance of pyroglutamate in AD brains and its solubility, it would be of great interest if N3pE-40 / 42 can also be detected in CSF or even in blood samples and might finally serve as a biomarker for diagnosis and progression of the disease.

REFERENCES

Braak, H. and Braak, E., 1991. Neuropathological stageing of Alzheimer-related changes. Acta Neuropathol (Berl). 82, 239-259.

Delacourte, A., David, J. P., Sergeant, N., Buee, L., Wattez, A., Vermersch, P., Ghozali, F., Fallet-Bianco, C., Pasquier, F., Lebert, F., Petit, H. and Di Menza, C., 1999. The biochemical pathway of neurofibrillary degeneration in aging and Alzheimer's disease. Neurology. 52, 1158-1165.

Delacourte, A., Sergeant, N., Champain, D., Wattez, A., Maurage, C. A., Lebert, F., Pasquier, F. and David, J. P., 2002. Nonoverlapping but synergetic tau and APP pathologies in sporadic Alzheimer's disease. Neurology. 59, 398-407.

Glenner, G. G., Wong, C. W., Quaranta, V. and Eanes, E. D., 1984. The amyloid deposits in Alzheimer's disease: their nature and pathogenesis. Appl Pathol. 2, 357-369.

Golabek, A. A., Soto, C., Vogel, T. and Wisniewski, T., 1996. The interaction between apolipoprotein E and Alzheimer's amyloid beta-peptide is dependent on beta-peptide conformation. J Biol Chem. 271, 10602-10606.

Harigaya, Y., Saido, T. C., Eckman, C. B., Prada, C. M., Shoji, M. and Younkin, S. G., 2000. Amyloid beta protein starting pyroglutamate at position 3 is a major component of the amyloid deposits in the Alzheimer's disease brain. Biochem Biophys Res Commun. 276, 422-427.

Hosoda, R., Saido, T. C., Otvos, L., Jr., Arai, T., Mann, D. M., Lee, V. M., Trojanowski, J. Q. and Iwatsubo, T., 1998. Quantification of modified amyloid beta peptides in Alzheimer disease and Down syndrome brains. J Neuropathol Exp Neurol. 57, 1089-1095.

Iwatsubo, T., Odaka, A., Suzuki, N., Mizusawa, H., Nukina, N. and Ihara, Y., 1994. Visualization of A beta 42(43) and A beta 40 in senile plaques with end-specific A beta monoclonals: evidence that an initially deposited species is A beta 42(43). Neuron. 13, 45-53.

Iwatsubo, T., Saido, T. C., Mann, D. M., Lee, V. M. and Trojanowski, J. Q., 1996. Full-length amyloid-beta (1-42(43)) and amino-terminally modified and truncated amyloid-beta 42(43) deposit in diffuse plaques. Am J Pathol. 149, 1823-1830.

Jarrett, J. T., Berger, E. P. and Lansbury, P. T., Jr., 1993. The carboxy terminus of the beta amyloid protein is critical for the seeding of amyloid formation: implications for the pathogenesis of Alzheimer's disease. Biochemistry. 32, 4693-4697.

LeVine, H., 3rd, 1993. Thioflavine T interaction with synthetic Alzheimer's disease beta-amyloid peptides: detection of amyloid aggregation in solution. Protein Sci. 2, 404-410.

Miller, D. L., Papayannopoulos, I. A., Styles, J., Bobin, S. A., Lin, Y. Y., Biemann, K. and Iqbal, K., 1993. Peptide compositions of the cerebrovascular and senile plaque core amyloid deposits of Alzheimer's disease. Arch Biochem Biophys. 301, 41-52.

Miravalle, L., Calero, M., Takao, M., Roher, A. E., Ghetti, B. and Vidal, R., 2005. Amino-terminally truncated Abeta peptide species are the main component of cotton wool plaques. Biochemistry. 44, 10810-10821.

Mori, H., Takio, K., Ogawara, M. and Selkoe, D. J., 1992. Mass spectrometry of purified amyloid beta protein in Alzheimer's disease. J Biol Chem. 267, 17082-17086.

Oddo, S., Billings, L., Kesslak, J. P., Cribbs, D. H. and LaFerla, F. M., 2004. Abeta immunotherapy leads to clearance of early, but not late, hyperphosphorylated tau aggregates via the proteasome. Neuron. 43, 321-332.

Pike, C. J., Overman, M. J. and Cotman, C. W., 1995. Amino-terminal deletions enhance aggregation of beta-amyloid peptides in vitro. J Biol Chem. 270, 23895-23898.

Richards, J. G., Higgins, G. A., Ouagazzal, A. M., Ozmen, L., Kew, J. N., Bohrmann, B., Malherbe, P., Brockhaus, M., Loetscher, H., Czech, C., Huber, G., Bluethmann, H., Jacobsen, H. and Kemp, J. A.,

2003. PS2APP transgenic mice, coexpressing hPS2mut and hAPPswe, show age-related cognitive deficits associated with discrete brain amyloid deposition and inflammation. J Neurosci. 23, 8989-9003.

Rufenacht, P., Guntert, A., Bohrmann, B., Ducret, A. and Dobeli, H., 2005. Quantification of the A beta peptide in Alzheimer's plaques by laser dissection microscopy combined with mass spectrometry. J Mass Spectrom. 40, 193-201.

Russo, C., Violani, E., Salis, S., Venezia, V., Dolcini, V., Damonte, G., Benatti, U., D'Arrigo, C., Patrone, E., Carlo, P. and Schettini, G., 2002. Pyroglutamate-modified amyloid beta-peptides--AbetaN3(pE)--strongly affect cultured neuron and astrocyte survival. J Neurochem. 82, 1480-1489.

Saido, T. C., 2000. Involvement of polyglutamine endolysis followed by pyroglutamate formation in the pathogenesis of triplet repeat/polyglutamine-expansion diseases. Med Hypotheses. 54, 427-429.

Saido, T. C., Iwatsubo, T., Mann, D. M., Shimada, H., Ihara, Y. and Kawashima, S., 1995. Dominant and differential deposition of distinct beta-amyloid peptide species, A beta N3(pE), in senile plaques. Neuron. 14, 457-466.

Saido, T. C., Yamao-Harigaya, W., Iwatsubo, T. and Kawashima, S., 1996. Amino- and carboxyl-terminal heterogeneity of beta-amyloid peptides deposited in human brain. Neurosci Lett. 215, 173-176.

Sergeant, N., Bombois, S., Ghestem, A., Drobecq, H., Kostanjevecki, V., Missiaen, C., Wattez, A., David, J. P., Vanmechelen, E., Sergheraert, C. and Delacourte, A., 2003. Truncated beta-amyloid peptide species in pre-clinical Alzheimer's disease as new targets for the vaccination approach. J Neurochem. 85, 1581-1591.

Stine, W. B., Jr., Dahlgren, K. N., Krafft, G. A. and LaDu, M. J., 2003. In vitro characterization of conditions for amyloid-beta peptide oligomerization and fibrillogenesis. J Biol Chem. 278, 11612-11622.

Tekirian, T. L., Yang, A. Y., Glabe, C. and Geddes, J. W., 1999. Toxicity of pyroglutaminated amyloid beta-peptides 3(pE)-40 and -42 is similar to that of A beta1-40 and -42. J Neurochem. 73, 1584-1589.

ACKNOWLEDGEMENTS

We thank Francoise Gerber and Anita Amhof for the help with the immunohistochemistry, Viviane Anquez for sample preparation in the toxicity and aggregation studies. Furthermore, we thank Prof. Yves-Alain Barde and Rita Andraus for performing toxicity studies with synthetic N3pE-42 on murine hippocampal cell cultures.

Peptide	Sequence	Molecular weight
Peptide 810	H-**Gln-Asp**-Leu-Thr-Met-Lys-Tyr-Gln-Ile-Phe-OH	**1286.52**
Neuropeptide El	H-**Glu-Ile**-Gly-Asp-Glu-Glu-Asn-Ser-Ala-Lys-Phe-Pro-Ile-NH2	**1447.57**
Apelin-13	H-**Gln-Arg**-Pro-Arg-Leu-Ser-His-Lys-Gly-Pro-Met-Pro-Phe-OH	**1550.85**
Anxiety Peptide	H-**Gln-Ala**-Thr-Val-Gly-Asp-Val-Asn-Thr-Asp-Arg-Pro-Gly-Leu-Leu-Asp-Leu-Lys-OH	**1912.13**
Fibrinogen β-Chain	H-**Glu-Glu**-Ala-Pro-Ser-Leu-Arg-Pro-Ala-Pro-Pro-Pro-Ile-Ser-Gly-Gly-Gly-Tyr-Arg-OH	**1951.17**

Tab. 1. Amino acid sequence of synthetic oligopeptides.

Three peptides, namely peptide 810, anxiety peptide and apelin-13, start with a glutamine, whereas neuropeptide el and fibrinogen β-chain contain a glutamate as first amino acid. Amyloid-β peptide contains a glutamate at position three, followed by a phenylalanine. Accordingly, artificial pyroglutamate formation in neuropeptide el, which contains a glutamate followed by an isoleucine, can best be compared to the situation in Aβ.

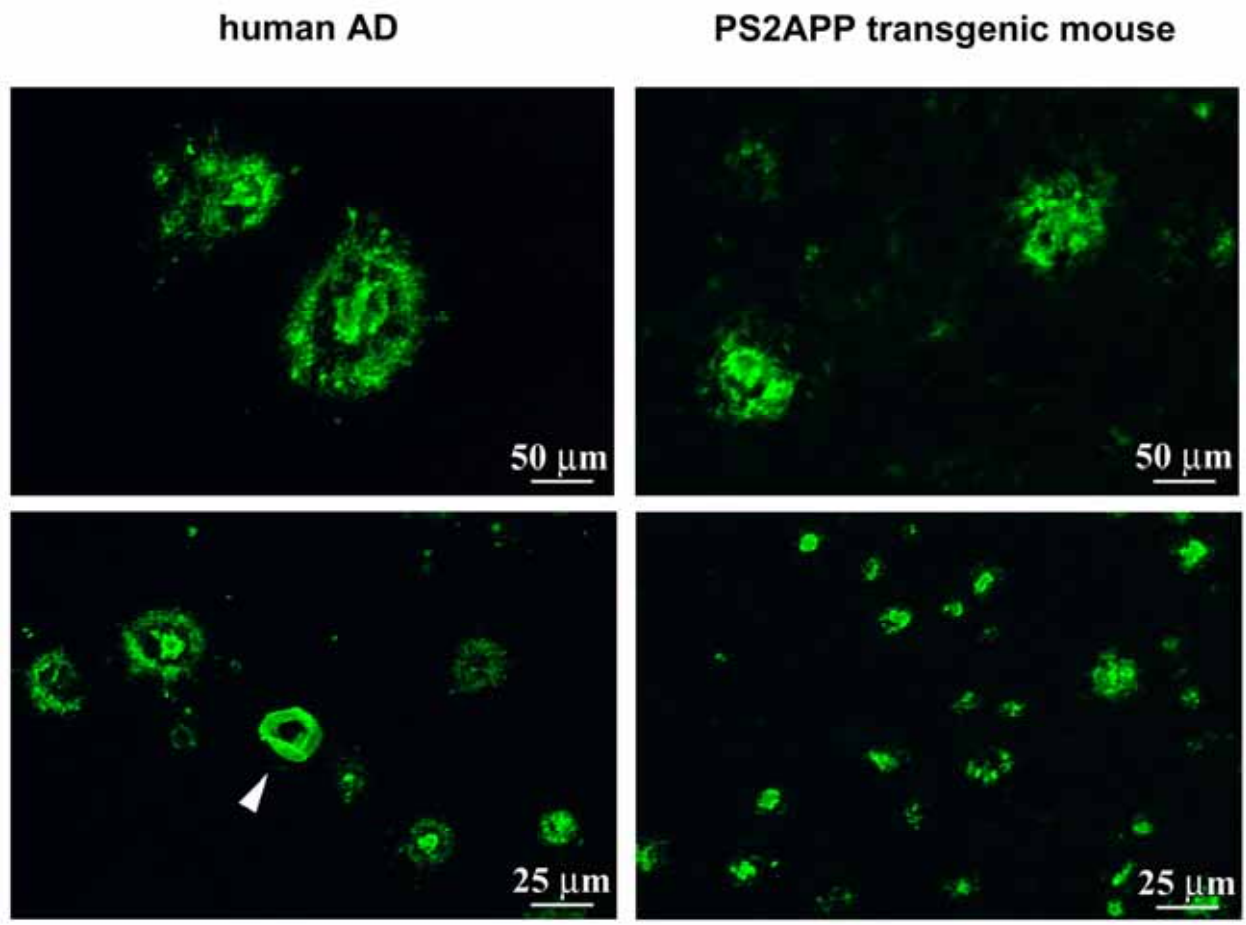

Fig. 1. Immunohistochemistry with a pyroglutamate specific antibody.

Substantial amounts of pyroglutamate 3-40 / 42 were detected in human and PS2APP mouse plaques, as well as in human vascular amyloid. Virtually all and all types of plaques were labeled and suggest that N3pE-40 /42 is a constituent of these plaques. Arrowhead indicates vascular amyloid.

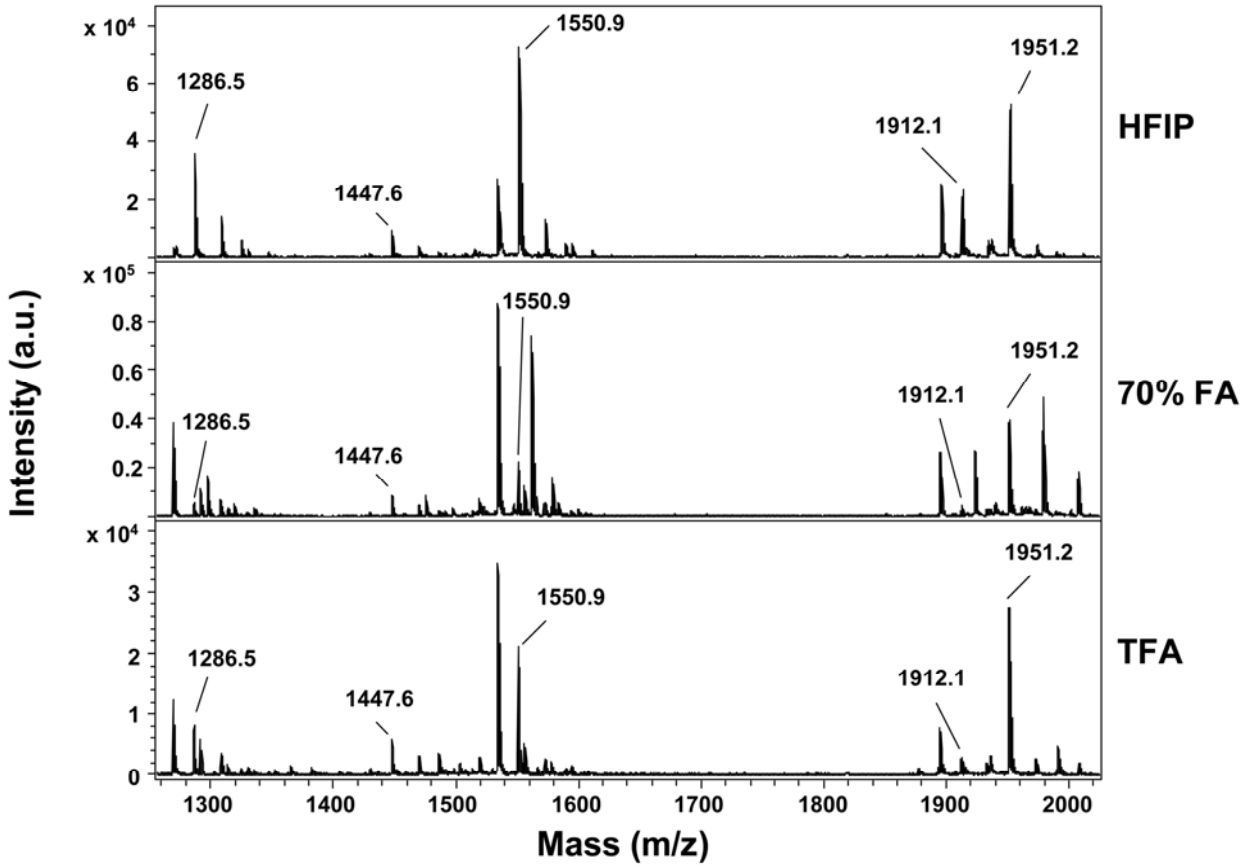

Fig. 2. Mass spectrometric analysis of synthetic oligopeptides.

Synthetic oligopeptides were incubated with either HFIP, 70% FA or concentrated TFA for 96 hrs and the proportion of induced pyroglutamate was determined. The specific masses are listed in Tab.1. According to these data, glutamine is far more susceptible to pyroglutamate formation than glutamate, where less than 10% of the original peptides were converted to pyroglutamate. HFIP, 1,1,1,3,3,3-hexafluoro-2-propanol; FA, formic acid; TFA, trifluoroacetic acid

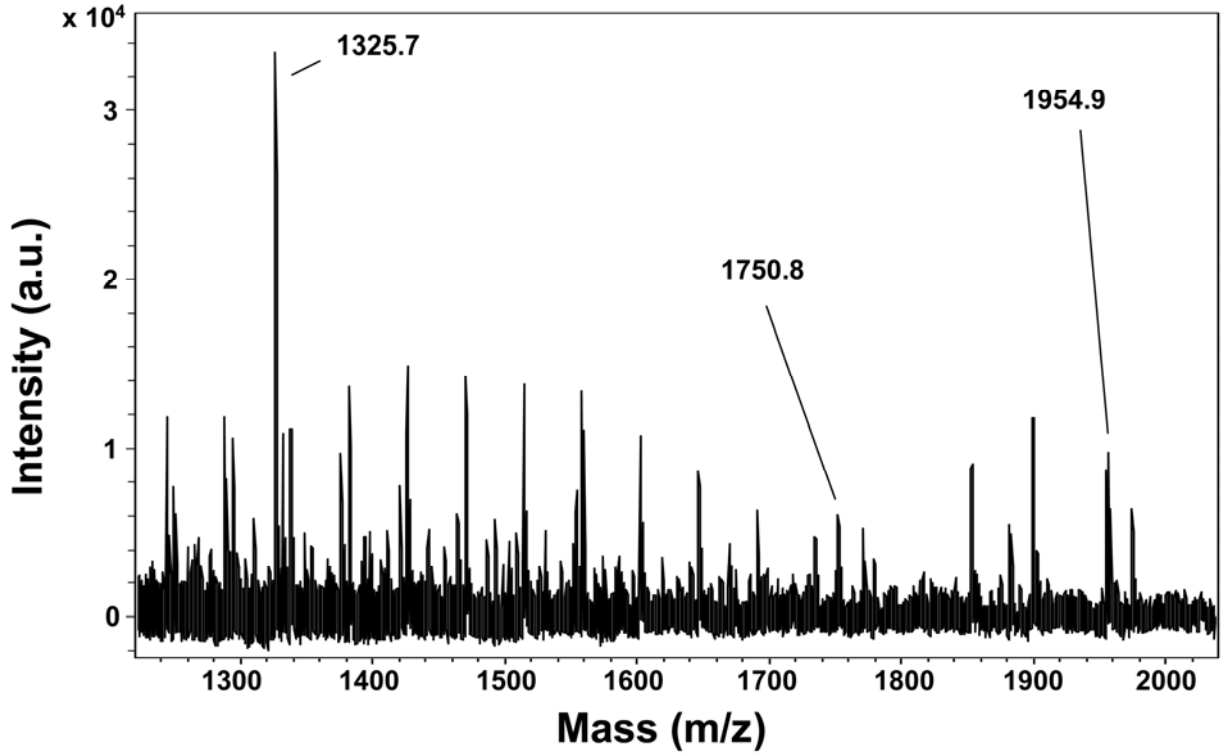

Fig. 3. Mass spectrometric analysis of human cored plaques after HFIP dissolution.

Fifty laser dissected cored plaques were incubated with HFIP and subsequently analyzed by mass spectrometry. By omitting the formic acid treatment in the sample preparation procedure, the exclusion of artificial pyroglutamate induction was aimed. The dissolution of plaque amyloid was not as efficient as with 70% formic acid and a considerable background was obtained. However, three peaks related to Aβ were still detected. Beside Aβ 1-16 (m/z 1954.9) and Aβ 17-28 (m/z 1325.7), also pyroglutamate 3-16 (1750.8) could be identified after HFIP treatment.

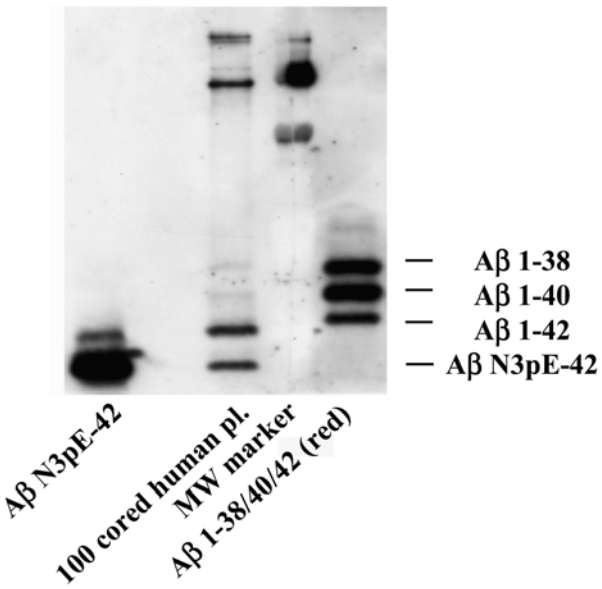

Fig. 4. Western blot analysis of human cored plaques.

Laser dissection of 100 cored plaques and subsequent analysis by Western blotting using an N3pE-specific antibody revealed the existence of pyroglutamate 3-42. pl, plaques; MW marker, molecular weight marker

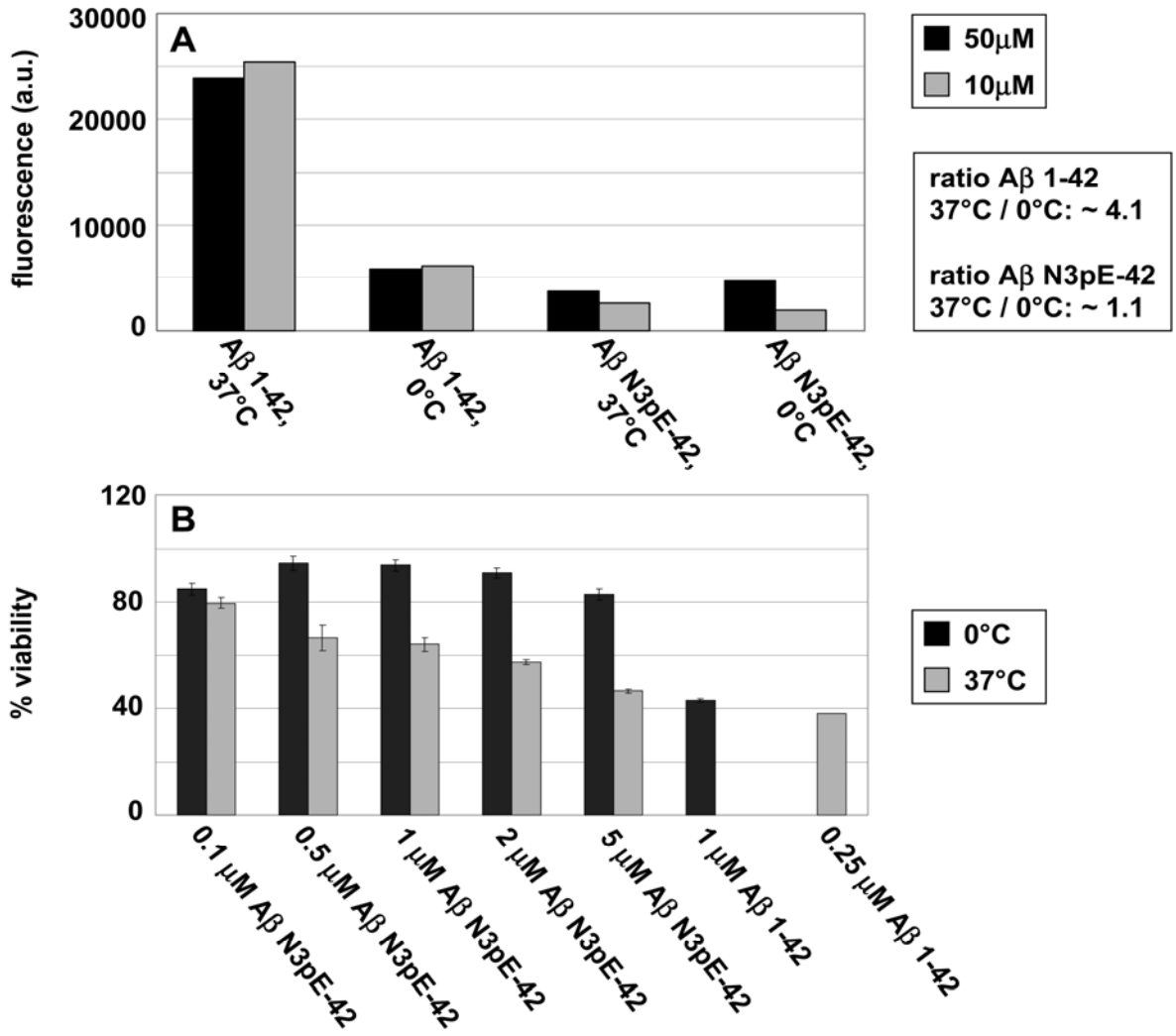

Fig. 5. ***In vitro*** **aggregation and cytotoxicity assay with synthetic Aβ N3pE-42.**

(A) 10mM and 50mM were incubated at either 0°C or 37°C and the fibril formation was evaluated with thioflavin T assay. The rate of fibril formation was markedly decreased for synthetic Aβ N3pE-42 compared to Aβ 1-42. (B) Different amounts of Aβ N3pE-42 and Aβ 1-42 were added to PC12 cells cultured in 96-well plates. After 20 h of incubation,the viability of cells was measured using an MTT assay. The toxicity of Aβ N3pE-42 was markedly reduced compared to Aβ 1-42. To obtain a comparable cellular toxicity at 37°C, a 20 fold higher amount of Aβ N3pE-42 than Aβ 1-42 was necessary.

APPENDIX IV

Altered Protein Levels in Alzheimer's Disease: A Proteomic Characterization

by

Andreas Güntert, Bernd Müller, Christian Miess, Nikos Berntenis, Françoise Gerber, Jürg Messer, Kristina, Oroszlan and Bernd Bohrmann

submitted to *Neurobiology of Disease*

Altered Potein Levels in Alzheimer's Disease: A Proteomic Characterization

Andreas Güntert, Bernd Müller[a], Christian Miess, Nikos Berntenis, Françoise Gerber, Jürg Messer, Krisztina Oroszlan and Bernd Bohrmann[*]

Pharma Research Basel, F. Hoffmann - La Roche Ltd, Grenzacherstrasse 124, CH-4070 Basel, Switzerland
[a]Department of Biology I, Ludwig-Maximilians-University, Menzingerstrasse 67, D-80638 Munich, Germany

[*]corresponding author. Tel: +41-61-688-8369; Fax: +41-61-688-1720
E-mail address: bernd.bohrmann@roche.com

Key words: Alzheimer's disease, liquid chromatography coupled with tandem mass spectrometry, proteomics, biomarker, occipital association cortex, protein level

Alzheimer's disease (AD) is the most common form of dementia in the elderly, but the molecular mechanisms leading to neurodegenerative and cognitive changes are not fully elucidated. We analyzed the soluble proteome from grey matter in the occipital cortex by liquid chromatography coupled with tandem mass spectrometry to compare protein levels in human AD and control tissue. In addition to proteins generally accepted to be related to AD like Aβ, tau, GFAP and apolipoprotein E, we found 18 new proteins from different functional classes, e.g. cell adhesion and synaptic molecules, with significantly altered levels in AD not described previously. Selected proteins were further investigated by immunohistochemistry and Western blotting. Specifically, we detected increased levels of synaptogyrin-1 and decreased reticulon-1 and syntaxin-1A levels in severe AD. Overall, this study provides new information that might be useful for the development of biomarkers in AD.

Manuscript [IV],
submitted to *Neurobiology of Disease*

INTRODUCTION

Alzheimer's disease (AD) is a complex neurodegenerative dementing illness. It is histopathologically characterized by the deposition of extracellular amyloid plaques mainly consisting of amyloid-β peptide (Aβ) and the intracellular accumulation of hyperphosphorylated tau into neurofibrillary tangles. At present, the amyloid cascade hypothesis (Selkoe, 2001, Hardy, 2006) and neurodegenerative tauopathies (Lee et al., 2005) provide a framework for studying AD pathogenesis. According to the former hypothesis, neurodegeneration in AD begins with the abnormal processing of the amyloid precursor protein (APP) and results in the production, aggregation and deposition of the Aβ peptide. However, current research indicates that soluble Aβ oligomers are the toxic amyloid species and not necessarily amyloid deposited in plaques (Watson et al., 2005). Many additional factors and pathways are described to be involved in neurodegeneration, like cytoskeletal alterations (Goldstein, 2003) leading to neurofibrillary tangles (NFTs) that impair intracellular transport processes to name only one. However, the molecular mechanisms leading from Aβ deposition to tau accumulation and neurodegeneration with cognitive deficits are still not entirely established.

In clinical practice, the diagnosis of AD is presently based on cognitive tests. The current diagnostic biomarkers in AD are derived from the cerebrospinal fluid (CSF) which is in direct contact with the extracellular space of the central nervous system allowing the measurement of solutes related to AD. A number of biological markers for AD are used, like tau (Andreasen et al., 1998) and phospho-tau levels (Parnetti et al., 2001), Aβ 1-42 levels (Ida et al., 1996, Andreasen and Blennow, 2002) or a combination of all three (Andreasen et al., 2003). Yet, a definitive diagnosis of AD relies on a postmortem assessment of brain neuropathology and there is clearly a need for a reliable, highly specific and sensitive biomarker for AD, preferentially, in peripheral fluids, i.e. plasma or serum.

A first step towards biomarker discovery for improved diagnostic assessment would be the detailed knowledge of which proteins and processes in brains of AD patients may be affected by the disease. Several proteins have been reported by immunohistochemistry to be colocalized with amyloid plaques or to have altered protein levels in AD, but biochemical verification of these candidates has been sparse. Previously, proteomic analysis was performed by comparing samples between AD cases and controls using 2D-gel electrophoresis and subsequent identification of the proteins by mass spectrometry (Schonberger et al., 2001, Tsuji et al., 2002). A complete proteomic approach is yet not straight forward with 2D-gel electrophoresis. A substantial technical advancement came up with mass spectrometry (MS) instrumentation over the last few years, in particular with the development of liquid chromatography combined with tandem mass spectrometry (LC/MS/MS). This allows the analysis of thousands of proteins from a complex protein mixture even with concentrations in the femto- or sub-femtomolar range. LC/MS/MS technique was demonstrated to be suitable for proteomic characterization in various fields, like cancer research (Baker et al., 2005, Gagne et al., 2005) or glycoproteomic analysis (Hashii et al., 2005, Wuhrer et al., 2005). The analysis of amyloid plaque associated proteins by use of laser capture microdissection and LC/MS/MS (Liao et al., 2004) revealed various proteins with increased levels in amyloid plaques compared to non-plaque control samples. Laser dissection microscopy was also used in our group to establish a high sensitivity analysis of Aβ peptides in different plaque types by MALDI-TOF MS (Rufenacht et al., 2005).

Here we investigated the entire grey matter tissue of postmortem occipital association cortex of two severe AD patients, which were compared to age-matched control samples by the use of LC/MS/MS. The occipital lobe is known to be the visual processing center in human and to exhibit an extensive amyloidosis in AD. Analysis of grey matter enabled the investigation of changes in protein levels in a region, where synaptic changes and other disease-related processes occur. The used methodology confirmed known AD related proteins, like Aβ, tau, GFAP, apolipoprotein E, Ubiquitin, Hsp90 and others, which are known to be more abundant in AD. More importantly, we report significantly altered levels of various other proteins in AD brain samples which have not been described previously. We confirmed the findings obtained by LC/MS/MS for selected proteins by immunohistochemistry and Western blotting.

Altogether, this proteomic study provides important new information in the elucidation of biochemical pathways involved in AD and presents potential new biomarker candidates required for an improved diagnosis of the disease.

MATERIALS AND METHODS

Human tissues

Human brains from AD patients were obtained from the Sun Health Research Institute through Dr. Thomas G. Beach (Sun City, Arizona, USA). The brain tissue was collected approximately two hours after death and was immediately frozen at -80°C. Brains were neuropathologically staged according to Braak and Braak (Braak and Braak, 1991). Brain tissue was isolated from the occipital association gyrus of 2 different AD patients (80 and 78 years old) with Braak stage VI and one control case (88 years old) with Braak stage II. For Western blotting, an additional control patient (85 years) with Braak stage II was employed. The individuals with Braak stage II showed no plaque pathology, while the patients with Braak stage VI showed heavy plaque load.

Preparation of brain slices

Frozen brain tissue was used and sections of 30 µm thickness were cut with a cryostat microtome (Leica Microsystems, CM3050 S). The slices were directly mounted onto glass cover slip coated with a 1.35 µm thin polyethylene foil (PALM Robot Microbeam, LPC-MOMeNT-Object slides, 8150) and stored at -20°C. Brain tissue sections for immunohistochemistry were cut at a thickness of 10 µm and mounted onto glass cover slips (SuperFrost Plus, Menzel GmbH & Co KG, Braunschweig, Germany).

Immunohistochemistry

Brain tissue slices were rehydrated for 5 min with phosphate buffered saline (PBS, Gibco, 14200-067) and fixed onto the glass slide by applying 70% acetone (0°C) for approximately 1 min. Sections were washed twice for 2 min with 1 ml PBS and incubated with 500 µl PBS containing 1% bovine serum albumin (BSA, fraction V, Roche Applied Science) and 1% Ovalbumin (Sigma-Aldrich Chemie GmbH, 05440) for 20 min to block unspecific binding sites. The slices were then incubated for 1 hr at room temperature with 200 µl of primary antibody.

The following primary antibodies were applied: anti-synaptogyrin-1 (clone 80.1, 10 µg / ml, Synaptic Systems GmbH, Goettingen, Germany), anti-reticulon-1 (clone Mon-160, 10 µg / ml, Santa Cruz Biotechnologies, Santa Cruz, CA, USA), anti-syntaxin-1A (clone MAB336, 10 µg / ml, Chemicon International, Temecula, CA, USA), anti-Aβ (clone BAP-2a, 5 µg / ml, kindly provided by Dr. M. Brockhaus), anti-SAP (clone5.4A, 10 µg / ml, Monosan, Uden, Netherlands), anti-apolipoprotein E (clone M212166, 10µg / ml, Fitzgerald Industries International, Inc, Concord, MA, USA) and anti-GFAP (clone EA-53, 1:400, BioMakor, Israel).

The samples were then washed three times for 5 min with 500 µl of PBS containing 1% BSA. Detection was performed using either an Alexa Fluor 488- or 555-conjugated secondary antibody (1:200 in PBS containing 1% BSA; Invitrogen AG, Molecular Probes, Basel, Switzerland) applied for 1 hr at room temperature. The preparations were then washed once for 5 min with 1 ml PBS and once for 2 min with distilled H_2O before being air-dried and stored until submitted to confocal laser scanning microscopy.

SDS-PAGE / Western blot

Frozen grey matter tissue from the corresponding brain areas were isolated after preparing 200 µm thick slices with a cryostat microtome using a surgical blade. The tissue was balanced and 4 µl of 2% SDS-buffer was added per mg brain. The brain tissue was homogenized using ceramic bead-containing tubes (MagNa Lyser Green Beads, 3 358 941, Roche Diagnostics GmbH, Mannheim, Germany) using a shaker (Precellys 24, Bertin Technologies, Montigny-le-Bretonneux, France) for 20 seconds. The supernatant was isolated and frozen at -20°C until analysis by Western blot. One µl of brain homogenate was separated on a 4–12% SDS gel (1 mm thick) using 2-(N-Morpholino)ethanesulfonic Acid (MES) running buffer for 1 hr 15 min at 150 Volt. Western blotting and immunostaining was performed as described by Wiltfang and colleagues (Wiltfang et al., 1997). Proteins were transferred for 60 min at 1 mA/cm^2 and room temperature under semi-dry conditions onto Hybond membranes (GE Healthcare, Piscataway, NJ, USA). For immunostaining, membranes were air-dried for 15 min and boiled for 5 min in PBS at 500 W using a microwave oven (Ida et al., 1996, Wiltfang et al., 1997). Blocking was performed for 1 hr at room temperature in the presence of 5% nonfat dry milk in PBS-T (PBS + 0.5% Tween-20) or Tris-Buffered Saline Tween-20 (TBS-T), respectively. Incubation with the primary antibodies was done overnight at 4°C.

The following primary antibodies were applied: anti-Aβ (clone WO-2, 2 µg / ml, The Genetics Company, Zuerich, Switzerland), anti-phosphotau pSer422 (1:1000, kindly provided by Dr. F. Grüninger), anti-

tau (clone HT7, 1:5000, Perbio Science, Lausanne, Switzerland) and anti-syntaxin-1A (clone MAB336, 1:1000, Chemicon International, Temecula, CA, USA).

Membranes were then washed for 2 x 15 min, in PBS-T (or TBS-T). After the washing steps, the membranes were incubated with horseradish peroxidase linked secondary antibodies (GE Healthcare) for 1 hr at room temperature. After 2 x 15 min washing in PBS-T (or TBS-T), the membranes were developed for 2 min at room temperature with ECL™ (GE Healthcare) solution according to the protocol of the manufacturer. Visualization was done with conventional X-Ray films (GE Healthcare) and band intensities were compared. For the image analysis, GeneTools software (Syngene, Cambridge, United Kingdom) was used.

Confocal microscopy

The immunofluorescence images were recorded on Leica TCS SP2 AOBS confocal laser scanning microscope (Leica Microsystems, Glattbrugg, Switzerland). For quantification of intensity difference in AD and control samples, the 10 μm sections were immunostained with either reticulon-1 or syntaxin-1A antibody at 10 μg / ml as described above. Three and five images from grey matter regions were taken from reticulon-1 and syntaxin-1A stained sections, respectively. Optical sections at an interval of 0.4 μm were recorded using a HCX-PL APO CS 40x 1.25 oil objective. Instrument settings for laser intensity, scan speed and averaging were adjusted to enable recording of the fluorescence signal in the effective dynamic range of the photomultiplier tube (PMT) and kept constant for a given staining to allow intensity comparison. Images were processed and analyzed using Imaris Software (Bitplane AG, Zuerich, Switzerland). The sum of intensities of the fluorescence emission signal was quantified from the layer with the highest intensity within a tissue section. The background from secondary antibodies was regarded as negligible by visual inspection.

High resolution confocal immunofluorescence images of double stained specimen for co-localization analysis were acquired by sequential scanning and with a resolution accordingly to satisfy the Nyquist criteria using a HCX PL APO CS 63x 1.3 glycerol immersion objective. The xy-projections were superimposed using Imaris Software (Bitplane). Images were sharpened with ImageAccess software (Imagic Bildverarbeitung AG, Glattbrugg, Switzerland).

Sample preparation for LC/MS/MS

The brain tissue was isolated using a sterile surgical blade and areas of 30 and 35 mm^2 (AD) and 32 and 36 mm^2 (control) were collected, which corresponds to less than one mg of brain tissue. Exclusively grey matter areas from the first apical layer to white matter were gathered. Brain tissue was solubilized by addition of 2 x 50 μl of 2 % SDS-buffer (2 % SDS, 66 mM Na_2CO_3, 2 % β-mercapto-ethanol, 10 % sucrose) with intermediate heating for 10 min at 70°C. Supernatants were combined and protein was precipitated according to Wessel and Flugge (Wessel and Flugge, 1984). Briefly, 400 μl methanol were added to the supernatant and mixed thoroughly. 200 μl of chloroform were added and after another mixing step and addition of 300 μl H_2O, the sample was incubated on ice for 5 min and centrifuged at 10000 rpm for 2 min until a clear phase separation was achieved. The denatured proteins resided in the interphase and were concentrated by carefully removing the hydrophilic phase. After addition of 300 μl methanol, mixing and a second incubation on ice for 5 min, the

proteins were sedimented by centrifugation for 5 min at 10000 rpm. The supernatant was removed and the protein pellet was dried at room temperature.

Proteins in each sample were separated on a 4–12% SDS gel (1 mm thick) using 3-(N-morpholino) propanesulphonic acid (MOPS) running buffer for 1.5 hrs at 120 volts. Subsequently, the gels were stained with Coomassie Blue G-250 overnight and destained for
6 hrs in H_2O.

The entire lane was cut into 14 pieces followed by in-gel trypsin digestion. Several washing steps with 2 x 1 ml H_2O, H_2O / acetonitrile (ACN) (50% / 50%) and destainer solution (0.1M NH_4HCO_3 / ACN, 50% / 30% v/v) for 5 min each and incubation with 1 ml ACN preceded a reduction step with 0.1M NH_4HCO_3 / 10mM dithioerythritol for 45 min at 56°C. After two incubation steps with 1 ml ACN, the samples were alkylated with 0.1M NH_4HCO_3 / 55 mM iodoacetamide in the dark at room temperature for 30 min. The gel pieces were digested after two additional washing steps with NH_4HCO_3 and ACN by incubation with 30 µl trypsin (0.02 µg / ml, Seq. Grade modified trypsin, Promega, Madison, WI, USA) overnight at room temperature. The peptides were eluted by addition of 250 µl 25mM NH_4HCO_3 and 5% formic acid for 15 min at 37°C. The eluates were combined and evaporated to dryness.

Analysis by LC/MS/MS

The resulting peptides from each gel piece were analyzed by liquid chromatography (LC) coupled to a LTQ ion trap mass spectrometer (Thermo Electronics, San Jose, CA USA) equipped with a nano-LC electrospray ionization source. Peptides were dissolved in buffer A (1% formic acid, 0.5% Acetic acid, 0.012% Heptafluorobutyric acid) and concentrated and desalted online on a C18 PepMap 100 micro precolumn (5 µm particle size, 300 µm x 1 mm; Dionex Corporation, Sunnyvale, CA, USA) that was coupled to a self packed (7 cm, 3µm; ProntoSil C18-ACE-EPS, Bischoff Chromatography, Atlanta, GA, USA) and pulled (P-2000 laser puller, Sutter Instrument, Novato, CA, USA) fused silica capillary (100 µm i.d. × 365 µm o.d.). The chromatographic separation was then performed by a 100 minute nonlinear gradient from 5 to 55% buffer B (80% ACN / 0.5% Acetic Acid / 0.012% HFBA) with a constant flow rate of 0.20 µl / min. The mass spectrometric data acquisition was performed with a survey scan followed by 7 data dependent MS / MS scans with a repeat count of 2. The collision energy was set to 35%.

Database searching for protein identification

SEQUEST (Bioworks, Thermo Electron Corporation, Waltham, MA, USA) was used to search the HumanGP database for peptide sequence and protein identification. HumanGP is a protein sequence database that is derived by assembling in sequences the results of Blast searches against the human chromosomes of a non-redundant protein set from Swissprot and Trembl (from human, mouse and other major organisms). Search parameters included differential mass modification to methionine due to possible oxidation and static mass modification to cysteine due to alkylation by iodoacetamide. Furthermore one missed cleavage of trypsin was accepted.

Protein quantification and normalization

Protein quantification was based on the comparison of peptide counts in samples derived from AD patients with samples from control tissue. Peptide counts reflect the number of peptides identified for a given protein. This number is indicative for the relative abundance of a protein in a sample. The comparison was performed with an in-house developed software (MSPresso).

As the brain tissue was isolated from tissue sections using a surgical blade, it was not possible to isolate exactly the same amount of brain tissue. To overcome this limitation, we normalized the peptide counts of the AD patients. Therefore, we used the averaged ratios of several abundant proteins that were assumed to be unchanged both in AD and control tissue, namely alpha-actinin 1, tubulin alpha-1 chain, tubulin alpha-8 chain, tubulin beta-2 chain, tubulin beta-4 chain and glyceraldehyde-3-phosphate dehydrogenase (GAPDH) for normalization of AD samples. Obtained normalization factors were 0.93 and 1.44 for AD cases 1 and 2, respectively.

Criteria for peptide and protein identification

For the comparisons of peptide counts, the single datasets from the analysis of the respective samples were combined to final sets. Peptides identified by SEQUEST may have three different charge states (+1, +2, or +3), each of which results in a unique spectrum for the same peptide. Except in rare instances, an accepted SEQUEST result had to have a delta cross-correlation (ΔCn) score of at least 0.1 (regardless of charge state). Peptides with a +1 charge state were accepted if they were fully tryptic or represented C-terminal fragments of a protein and had a cross correlation (Xcorr) of at least 1.8. Peptides with a +2 charge state were accepted if they were fully or partially tryptic with Xcorr ranges of at least 2.3 and higher. Finally, peptides with charge state +3 were accepted if they were fully or partially tryptic and had an Xcorr larger than 2.8. Only proteins identified with at least 2 different peptides with a peptide count (number of MS/MS events that lead to the identification of a certain peptide) larger than 7 were taken into account. In addition, only proteins identified in both of the two independent datasets of AD versus control were accepted.

RESULTS

Comparison of protein levels in AD brain and control

To compare protein levels from AD brains with control tissue, two comparable sized brain areas of grey matter of the occipital cortex of AD patients with Braak stage VI were isolated, the protein samples resolved on an SDS gel (Fig. 1 A), trypsin digested and finally submitted to LC/MS/MS. An overview of the preparative stages is illustrated in a flowchart (Fig. 1 B). The sample preparation procedure included a protein precipitation step where interfering lipids were removed, but which is suitable to isolate many of the membrane proteins. It is therefore assumed, that most of the soluble brain proteins, as well as part of the membrane proteins could be analyzed.

For acceptance of proteins, several filter criteria were applied. Only proteins, for which the measured peptide ratio in the respective pair of samples was in a range of ± 0.3 were accepted. For example, if a protein X was found in the first measurement with a ratio of 0.6 between AD and control and in the second series with a ratio of 0.8, the average of 0.7 was taken and the protein was accepted for the analysis and evaluation.

To evaluate the proteins with significantly altered protein levels in AD brain samples, we classified them into functional groups. As the number of proteins from less than 1 mg of brain tissue detected by this method reached more than 2000, we accepted only proteins with a peptide count of larger than 7. The peptide count is indicative for protein amount present in the brain. The approach is semi-quantitative, but the obtained results demonstrate applicability to reveal alterations in protein amount. A protein with an averaged ratio of $x > 1.3$ was considered to be increased. A protein with an averaged ratio of $0.7 \leq x \leq 1.3$ was regarded as comparable, whereas a ratio being $x < 0.7$ was accepted as being decreased. Ubiquitous proteins with comparable protein levels were not considered as important and are therefore not listed.

To overcome limitations concerning the amount of isolated brain tissue, we normalized the detected protein levels. The used cytoskeletal proteins and GAPDH levels were assumed not to be affected in the pathogenesis of AD. This approach appears to be adequate, since most proteins were comparable after the normalization. Substantial alterations of identified protein levels are more significant when the abundance of most of the observed proteins remains unchanged. Therefore, the proteins of the AD patients and control tissue were ordered by their observed abundance. The comparison of respective proteins in AD and control was assessed and a correspondence of over 90% was determined. This enabled us to extract a set of proteins with significantly altered protein levels revealed by LC/MS/MS.

A large number of previously identified proteins related to AD could be confirmed and demonstrate the feasibility of the approach. Among these proteins were few proteins like Aβ and complement C3 and C4 that are only detectable in AD tissue. Also, highly increased levels of tau, apolipoprotein E, ubiquitin, several heat shock proteins (e.g. Hsp 90) and the astroglial protein GFAP were revealed in grey matter tissue of the investigated AD cases. Other proteins known to be associated with AD (e.g. antichymotrypsin (ACT), serum amyloid P component (SAP) or C-reactive protein) were detected, but only with low peptide counts. This might result from their low abundance, restricted accessibility for solubilization or unfavorable ionization properties in the LC/MS/MS approach. Proteins most abundant are listed in Table 1. In the functional groups mentioned below, we describe the findings for elevated, decreased or comparable proteins after applying the filter criteria

described, what is known about their function, especially in relation to AD pathogenesis and also putative new AD related biomarkers.

Cell adhesion and neurite outgrowth

Molecules involved in cell adhesion are usually localized at the cell surface. They are predominantly glycoproteins that mediate cell-to-cell adhesion and their functions include the assembly and interconnection of cells, as well as maintenance of tissue integration, morphogenic movement and cellular migration. We detected various neural specific cell adhesion molecules, as well as ubiquitously expressed ones. Among these, Collagen α3 (VI), which acts as a cell-binding protein, was present only in AD, whereas various proteins previously reported to also play a role in neurite extension were either at comparable or decreased levels. For example, neural cell adhesion molecules (NCAMs) have been shown to be effective neurite outgrowth promoters. We detected tendentially decreased levels of NCAM 1. Previously, unchanged levels in AD and control in occipital association cortex were reported (Yew et al., 1999). In contrast, connexin-43 was found by LC/MS/MS to be tendentially increased in AD, consistent with elevated immunoreactivity at sites of amyloid plaques in AD (Nagy et al., 1996).

The oligodendrocyte specific protein claudin-11 plays an important role in minimizing the intercellular space through calcium-dependent cell adhesion activity. We detected decreased levels of claudin-11 in AD compared to control tissue. An implication of claudin-11 in AD was not reported previously.

The contactins mediate cell surface interactions during nervous system development. Contactin 1 participates in oligodendrocytes generation by acting as a ligand of notch 1, whereas contactin 2 may play a role in the initial growth and guidance of axons. We found slightly decreased levels of contactin 1 and more significantly decreased levels of contactin 2 and contactin associated protein 1 (Neurexin IV).

A different protein involved in axonal guidance and which we found decreased is dihydropyrimidinase related protein-5 (DRP-5). Another member of this family, DRP-2, was previously described to be disregulated in AD (Lubec et al., 1999).

We detected low Thy-1 membrane glycoprotein levels in AD. Thy-1 was implicated to promote neurite outgrowth and decreased levels in AD were reported earlier (Leifer and Kowall, 1992).

Notably, two other proteins which were not reported before in relation to AD and which show significantly decreased levels with our approach are the myelin oligodendrocyte glycoprotein (MOG) and the myelin-associated glycoprotein (MAG). These proteins are adhesion molecules important for maintaining the myelin sheet and for cell-cell communication. This is indicative for deteriorations of axonal integrity (Kalback et al., 2004).

Overall, most of the identified proteins involved in cell adhesion and important for the development and maintenance of the neuritic functions show consistently lower protein levels in AD than in the control samples, which is indicative for disease related deficits in the neuritic network.

Chaperones

In biology, chaperones are proteins whose function is to assist other proteins in achieving proper protein folding. Many chaperones are heat shock proteins expressed in response to elevated temperatures or other cellular stresses. Chaperones can also play an important role in signal transduction, in the maintenance of the proper organization of the cytoplasm and other intracellular compartments, in intracellular trafficking and other vital functions of the cells.

We found increased levels of heat shock protein 90 (Hsp 90) and Hsp 27. An upregulation and colocalization of Hsp 90 with Aβ plaques or reactive astrocytes in AD brain was previously reported (Renkawek et al., 1993, Kakimura et al., 2002, Liao et al., 2004). By using Hsp 90 inhibitors, a reduced ERK phosphorylation was detected, implicating a role for Hsp 90 in tau phosphorylation (Dou et al., 2005).

Interestingly, a significant increase of Hsp 75 was also observed, which was not described previously. Other heat shock proteins like Hsp 70.1 and glucose-regulated protein 78 (GRP 78) were found at comparable and Hsp 60 at decreased levels, which was previously shown by Yoo and colleagues (Yoo et al., 2001).

Cytoskeleton

The cytoskeleton is a dynamic structure that maintains cell shape, enables cell motion and plays important roles in both intracellular transport and cellular division. We identified the major cytoskeletal proteins, including actin and tubulin, with high peptide counts. As mentioned above, we normalized the peptide count of AD brain proteins against an average of the peptide counts of tubulin, actinin and GAPDH in the controls, because they were assumed as proteins at basically unchanged levels both in AD and age-matched controls.

As expected, we identified the microtubule-associated protein tau, the major constituent of NFTs, beeing substantially increased in AD brains.

Plectin 1 interlinks intermediate filaments with microtubules and microfilaments and anchors intermediate filaments to desmosomes or hemidesmosomes. Plectin 1 may be involved not only in the cross-linking and stabilization of cytoskeletal intermediate filaments network, but also in the regulation of their dynamics. Plectin 1 was found abundantly and detected at a tendentially elevated level in AD. No implications of plectin 1 in AD were described previously. Other cytoskeletal proteins like neurofilament or spectrin were identified at comparable levels. Interestingly, gelsolin was found to be decreased. Gelsolin plays a role in a familial form of AD and it was suggested, that gelsolin may inhibit Aβ-induced cytotoxicity (Qiao et al., 2005). A decrease in gelsolin during the progression of AD might therefore have serious effects on neuronal survival and apoptotis of nerve cells.

Another abundant structural protein is α-internexin which belongs to the intermediate filament family of cytoskeletal proteins. We found lower levels of α-internexin in AD samples than in control tissue. A role of α-internexin in AD was demonstrated recently by Dickson and colleagues (Dickson et al., 2005).

A decrease in other cytoskeletal proteins, like α-adducin or ankyrin 2, is likely to reflect also cytoskeletal impairment of neuronal cells in AD, which may result in a deficit in axonal transporting and neuritic dystrophy.

The most pronounced reduction was observed in the microtubule-associated proteins (MAP) 1B and MAP RP / EB, which show markedly decreased peptide counts in AD brain, indicative for a deficit and impairment of axonal transport.

Inflammation

Triggered by the deposition of amyloid plaques, an inflammatory response is known to occur in AD. Glial fibrillary acidic protein (GFAP) and vimentin, two members of the intermediate filament group, are expressed in reactive astrocytes and were both found at significantly increased levels in AD. This is consistent with the literature (Porchet et al., 2003). Remarkably, complement C3 and C4, both activators of the complement system, were only found in AD brains. The complement system stimulates inflammation, facilitates antigen phagocytosis, and lyses some cells directly upon activation by a pathogen. Significant changed levels of complement isoforms were recently detected and suggested as potential biomarkers in AD (Finehout et al., 2005, Selle et al., 2005).

Kinases, enzymes and metabolism

Different enzymes involved in diverse biochemical pathways were previously reported to play a role in AD. One of these enzymes is the Protein-arginine deiminase type II and Ishigami and co-workers showed the abnormal accumulation of citrullinated proteins catalyzed by peptidylarginine deiminase in hippocampal extracts from patients with Alzheimer's disease (Ishigami et al., 2005). Consistent with this data, we detected significantly increased levels of peptidylarginine deiminase in AD samples.

The hyperphosphorylation of tau is crucial for its assembly into NFTs and the control of phosphorylation versus dephosphorylation events is likely to be important in the progression of the disease. Accordingly, mitogen-activated protein kinase 3 (ERK 1) was found only in AD brains, while mitogen-activated protein kinase 1 (ERK 2) was found at comparable levels between AD and control. They were described previously to phosphorylate tau on serine / threonine residues (Goedert et al., 1992, Ledesma et al., 1992, Hyman et al., 1994, Pei et al., 2002). Further, we identified a significant decrease in the protein level of the serine / threonine phosphatase 2A, which dephosphorylates tau and it was reported earlier that a decrease in the activity promotes the abnormal hyperphosphorylation of tau (Drewes et al., 1993, Gong et al., 1994). Overall, a decrease in the phosphatase activity and increased phosphorylation of tau in AD is likely to result in the abnormal hyperphosphorylation and to an enhanced deposition of tau in NFTs.

Oxidative stress refers to a state in which oxidant production surpasses the endogenous antioxidant capability leading to oxidative molecular damage of the tissue. Such a state can result from increased production of oxidants and/or decreased concentration of antioxidants. Stepwise reduction of oxygen during normal metabolism produces reactive oxygen species (ROS), such as superoxide anion, hydrogen peroxide, and hydroxyl radicals. Oxidative stress-associated cell damage has also been described in Alzheimer's disease (Multhaup et al., 1997, Aksenova et al., 1999) and accordingly we could identify several enzymes involved in the disposing of ROS. Peroxiredoxin 1 level was unchanged in AD and control as previously described (Krapfenbauer et al., 2003), whereas Peroxiredoxin 5, Superoxide dismutase (SOD2) and microsomal

glutathione-S transferase 3 (MGST-3) levels were decreased, likely to indicate reduced elimination of ROS and enhanced susceptibility to oxidative damage.

It is well documented, that a decreased brain glucose turnover can have serious effects on the onset and/or progression of AD (Hoyer, 1991, Hoyer, 1996, Meier-Ruge and Bertoni-Freddari, 1997, Schubert, 2005). Several glycolytic key proteins, such as phosphofructokinase 1 (PFK), were described to have decreased activities in AD brains (Meier-Ruge et al., 1984), which might finally contribute to a disturbance of the glucose turnover and an insufficient amount of ATP to maintain the neuronal function and survival. The consequence is nerve cell atrophy. Numerous enzymes and proteins involved in various metabolic pathways were detected with our approach, among them we found a decrease in several enzymes involved in glucose turnover, like PFK-B, Isocitrate dehydrogenase, Malate dehydrogenase, Succinyl-CoA ligase and Succinate dehydrogenase, thereby indicating the aberrant energy metabolism in brains of AD patients.

Membrane trafficking and synaptic proteins

Membrane traffic occurs by vesicular transport between successive compartments of the secretory pathway. Dynein plays an important role in protein sorting and occurred at tendentially decreased levels in AD compared to control in our measurements. It was shown previously, that dynein is increased at sites of amyloid plaques (Liao et al., 2004).

Clathrin is the major protein of the polyhedral coat in coated pits, which form during endocytosis. We found, with high peptide counts, unchanged levels of clathrin in AD compared to control samples, whereas the clathrin coat assembly protein AP180, which is central for clathrin alignment, showed reduced levels in AD brains as suggested previously by immunohistochemistry (Yao et al., 1999).

Other synaptic proteins like presynaptic density protein 95 (PSD-95), syntaxin-1A and synaptotagmin-1 and -12 were also found to be significantly decreased. The loss of synaptic proteins in AD is expected and reflects the synapse loss that occurs in the disease. Contrary to that was the finding of marked elevated levels of synaptogyrin-1 and synaptogyrin-3, implications of synaptogyrins in AD are discussed below.

Synaptophysin was found at only slightly decreased levels in one AD patient and at comparable levels in the second patient, which is not subsidiary to earlier reports, which reported a decrease of synaptophysin up to 25% in AD brains (Zhan et al., 1993, Masliah et al., 1994). An explanation may be the enlargement of synaptic boutons surrounding the plaques and the accumulation of synaptophysin in dystrophic axons (Lassmann et al., 1993).

Interestingly, we found three members of the reticulon (rtn) family with altered protein levels in AD. Rtn-3 was tendentially decreased, whereas rtn-1 and rtn-4, the neurite outgrowth inhibitor protein Nogo, showed significantly lower levels in AD. This was not described previously.

Proteolysis

The ubiquitin proteasome system (UPS) is the major protein quality control system in eukaryotic cells. The last few years have seen increasing evidence for the involvement of the UPS in neurodegenerative disorders, including AD. The involvement of ubiquitin in AD has been extensively reviewed (Forloni et al., 2002, de Vrij et al., 2004, Song and Jung, 2004) and the colocalization of ubiquitin with senile plaques was reported almost 20 years ago (Perry et al., 1987). It was therefore not surprising to find ubiquitin with high peptide counts at markedly increased levels in AD brains compared to control tissue. Other proteins involved in proteolysis, like cystatin B and C, antitrypsin or cathepsin D, were detected, but due to their low abundance not listed. It was recently reported that these proteins colocalize with amyloid plaques (Liao et al., 2004). However, our analysis of entire grey matter areas did not show significant changes in protolytic enzymes, except for ubiquitin. The high abundance of ubiquitin in AD grey matter tissue supports a role in activation of protein degradation mechanisms and / or stress-induced processes.

Others

We detected the Aβ peptide only in AD and enhanced levels of apolipoprotein E. Also, ACT was detected only in the AD samples but with low peptide counts, whereas α-synuclein, a non-Aβ component of senile plaques, was identified at comparable levels in AD and control. SAP was detected in only one AD patient, whereas C-reactive protein appears to be increased. However, both pentraxins were detected only with very low peptide counts and are therefore not listed.

We detected decreased levels of the neuroprotective major prion protein in AD, which is consistent with a report showing decreased levels in AD brain in occipital association cortices (Rezaie et al., 2005). Contradictory to the literature, we found decreased levels of NDRG2 in AD, even though it was described to be associated with senile plaques and elevated in hippocampal pyramidal neurons (Mitchelmore et al., 2004). Moreover, we detected some proteins not described previously to be related to AD, like decreased neuronal protein 25 (NP 25, transgelin-3) and Matrin-3 whose functions are not known. Furthermore, we determined low levels of programmed cell death protein 8, which is a caspase-independent mitochondrial effector of apoptotic cell death. This finding might also present a compensatory mechanism to prevent redundant nerve cell death.

Correlation of LC/MS/MS with immunohistochemistry and Western blotting

To validate selected candidates identified at altered levels in AD by LC/MS/MS, immunohistochemistry and Western blots were performed.

Analysis of known AD related proteins with Western blotting of homogenates from the same brain regions analyzed by LC/MS/MS showed the expected increase in Aβ, tau and phospho-tau in AD compared to control samples (Fig. 2 A – C). Furthermore, syntaxin-1A antibody was used to compare with MS and immunostaining (Fig. 2 D). Densitometric analysis revealed a decrease for syntaxin-1A of ~ 15% (data not shown). Although the lower abundance of syntaxin-1A in AD brains could also be demonstrated by Western blot analysis, the decrease was more sensitively revealed by LC/MS/MC and immunohistochemistry as seen below.

For immunohistochemistry of brain tissue, we tested antibodies against Aβ, GFAP, SAP, apolipoprotein E, reticulon-1, synaptogyrin-1, and syntaxin-1A.

A double staining of Aβ with SAP (Fig. 3 A – C) and apolipoprotein E (Fig. 3 D – F) showed a clear co-localization of these proteins with amyloid plaques. As amyloid plaques are pathological hallmarks in AD patients, an increase of these proteins was expected and was shown for apolipoprotein E with the LC/MS/MS assay. SAP was detected in only very low amounts in one AD patient in the LC/MS/MS; an explanation for this can be the low rate of solubilization of SAP from the Aβ fibrils. The immunohistochemistry clearly shows the presence of SAP in plaques, which is consistent with a described association of SAP with amyloid deposits (Pepys et al., 1994).

Immunostaining analysis with synaptogyrin-1 antibody revealed a higher immunoreactivity in AD, thereby supporting the data obtained by mass spectrometry, where increased levels of synaptogyrin-1 in AD were detected. Confocal analysis of immunolabeled brain slices showed a co-localization of synaptogyrin-1 with GFAP positive cells (Fig. 3 G - I), suggesting that synaptogyrin-1 is expressed in reactive astrocytes. Since amyloid plaques in AD brains trigger an inflammatory response, which is absent or greatly reduced in control brains, a considerably higher number of reactive astrocytes can be found in diseased brains. This may explain the observed increase in synaptogyrin-1. However, the expression of synaptogyrin-1 in astrocytes is indicative for a local compensatory response to nerve cell atrophy, as synaptogyrin-1 was reported to play a role in synaptic plasticity (Janz et al., 1999).

Reticulon-1 and syntaxin-1A were found at decreased levels in AD patients by LC/MS/MS. Immunostaining for these proteins and quantification by confocal laser scanning microscopy revealed an intensity decrease in AD patients, demonstrating a clear correlation with the data from the mass spectrometry approach
(Fig. 4).

DISCUSSION

Methodological approach

We used a high sensitivity proteomic approach to analyze low amounts of brain tissue from two severe Alzheimer's patients and control tissue. The study provides insight into altered molecular components of various processes involved in the pathogenesis of AD. By semi-quantitative mass spectrometry, we were able to detect numerous proteins previously described in relation with AD and in addition to this, we identified 18 new proteins with significantly altered levels in AD, which were not described yet. The overall good consistency with available data demonstrates the validity of the methodological approach and confirmed altered protein levels reported in AD as obtained by different approaches from earlier studies. In addition, we employed immunohistochemistry and Western blotting as independent approaches to get a first validation of selected proteins detected with LC/MS/MS.

Proteins implicated in AD

AD related proteins like Aβ, apolipoprotein E and microtubule associated protein tau were found most prominently at increased levels in AD. Furthermore, the approach enabled the study of multiple pathogenic processes affected in the disease progression of AD and, consistent with the literature, we detected the activation of an inflammatory cascade indicated by increased levels of GFAP, vimentin and complement factors, the activation of the ubiquitin proteasome system, synaptic nerve cell loss reflected by a decrease of PSD-95, syntaxin-1A, synaptotagmin and AP-180, as well as an impaired glucose turnover, indicated by a decrease of enzymes involved in the citrate cycle.

One protein previously reported to occur at altered protein levels in AD is syntaxin-1A. This protein is a plasma membrane protein at presynaptic sites and was described to be decreased in AD (Minger et al., 2001). It was also shown, that dystrophic neurites of senile plaques are defective in proteins involved in exocytosis and neurotransmission, like syntaxin-1A or synapsin (Ferrer et al., 1998). The markedly reduced levels of syntaxin-1A in AD brains detected with our method support these findings and indicate impaired synaptic function. Relevant to these findings is the described binding of syntaxin-1A to the presenilin 1 complex (Smith et al., 2000). It is possible that presenilin 1 is involved in the control of calcium entering the cell (LaFerla, 2002), required for initiation of synaptic vesicle exocytosis. Mutations in presenilin 1 may interfere with this process by altering syntaxin-1A function, thus interfering with the docking and fusing of vesicles with the presynaptic membrane. Taken together, syntaxin-1A seems to play an important role in the maintenance of exocytosis and a significant decrease might therefore be detrimental for neurotransmission and contribute to cognitive impairment in AD.

Another protein family proposed to be involved in the pathogenesis of AD is the reticulon family (Selkoe et al., 1996, Lynch and Mobley, 2000). However, the protein level of rtns in AD was not reported earlier and we are the first group to show tendentially lower levels of rtn-3 and considerably decreased rtn-1 and -4 (Nogo) levels in AD. Rtns are a group of integral membrane proteins, consisting of four members, rtn-1 to rtn-4. Their precise cellular function remains to be established, although rtns have already been shown to regulate many different cellular processes such as neuroendocrine secretion or membrane trafficking and to interact with diverse cellular proteins such as BACE 1 (He et al., 2004) or SNARE proteins (Steiner et al., 2004). Rtn-4 has been intensively investigated and was shown to be a critical inhibitory molecule controlling axonal growth and regeneration (Strittmatter, 2002). Rtns are localized in the ER, Golgi and plasma membranes, which suggests an involvement of rtns in endo- and exocytosis along the secretory compartments. A disregulation of rtns in AD indicates abnormalities in endo- or exocytosis. Furthermore, BACE 1 was shown to interact with all four rtn proteins by co-immunoprecipitation and an increased expression of a single rtn member in HEK-293 cells expressing Swedish mutant APP was shown to reduce the levels of Aβ (He et al., 2004) . Lowered rtn levels may cause a dysfunction of the endoplasmic reticulum that could lead to altered processing of membrane proteins such as APP (Katayama et al., 2004). Reduced rtn levels in AD are also indicative for an accelerated Aβ production, which may further contribute to amyloid plaque formation typical for AD. On the other hand, Nogo was reported to inhibit neurite outgrowth (Prinjha et al., 2000) and a down regulation of Nogo might indicate a compensatory mechanism in response to nerve cell atrophy in AD (Strittmatter, 2002).

New potential AD related proteins

In addition to numerous proteins described to be implicated in AD, we determined altered levels of 18 proteins previously unknown in relation to AD. These are the synaptic proteins synaptogyrin-1 and -3, MAG, MOG, contactin-1, contactin-2, contactin associated protein 1 and claudin-11 involved in cell adhesion, the chaperone protein Hsp 75, plectin 1, ankyrin, α-adducin and microtubule-associated protein RP/EB family member 3 as structural cytoskeletal proteins, peroxiredxin 5 and microsomal glutathione S-transferase 3 for the protection against oxidative stress and programmed cell death protein 8, matrin-3 and transgelin-3 (NP 25), whose functions are not known.

We detected significantly increased levels of synaptogyrin-1 and -3 in AD. The synaptogyrin family consists of three members, two neuronal isoforms and a ubiquitous isoform (cellugyrin) and is distantly related to the synaptophysin family. It is known that synaptogyrins are associated with presynaptic vesicles in neuronal cells; the functions of synaptogyrins however have remained obscure despite considerable efforts (Stenius et al., 1995, Kedra et al., 1998, Zhao and Nonet, 2001, Belizaire et al., 2004, Verma et al., 2004). In studies using transgenic mice with a double knockout for synaptogyrin and synaptophysin, the mice were still viable and fertile, suggesting that these proteins can be substituted (Janz et al., 1999). However, major changes in synaptic plasticity were detected and an essential role in the regulation of neurotransmitter release was proposed. Conversely, another study reported that all synaptogyrins and the distantly related synaptophysin-1 severely inhibit exocytosis in transfected PC12 cells, suggesting a direct involvement in the exocytotic process (Sugita et al., 1999). We revealed by immunohistochemistry a localization of synaptogyrin-1 in reactive astrocytes, which likely explains the measured increase in synaptogyrin-1 levels in AD tissue. This increase may resemble a compensatory response of astrocytes in AD in response to the nerve cell loss and impaired synaptic activity.

Concluding remarks

Another aspect of the findings relate to the identification of potential new biomarkers. AD is a common disease, but a definite diagnosis can still only be made by a postmortem assessment of the brain and to follow progression of the disease is difficult. A specific biomarker, preferentially measurable in the periphery, is urgently needed for improved diagnosis and also for monitoring drug response in AD treatment. Identified biomarker candidates found at altered levels in AD brain tissue, like synaptogyrin and reticulons, are possibly reflected in the CSF and eventually in the periphery through increased or decreased levels of their metabolized protein fragments. The determination and confirmation of peripheral fragment levels in blood presents therefore a promising approach for biomarker development.

Taken together, the understanding of the molecular pathogenesis underlying AD is necessary for the establishment of surrogate markers. Newly identified proteins described in this report are candidates for such markers, but need further investigation and validation. It will require independent replication in a larger number of samples before biomarkers for clinical diagnosis of AD can be firmly established. However, the results obtained clearly indicate the potential of the approach in the development of biomarkers in AD and other diseases.

REFERENCES

Aksenova, M. V., Aksenov, M. Y., Payne, R. M., Trojanowski, J. Q., Schmidt, M. L., Carney, J. M., Butterfield, D. A. and Markesbery, W. R., 1999. Oxidation of cytosolic proteins and expression of creatine kinase BB in frontal lobe in different neurodegenerative disorders. Dement Geriatr Cogn Disord. 10, 158-165.

Andreasen, N. and Blennow, K., 2002. Beta-amyloid (Abeta) protein in cerebrospinal fluid as a biomarker for Alzheimer's disease. Peptides. 23, 1205-1214.

Andreasen, N., Sjogren, M. and Blennow, K., 2003. CSF markers for Alzheimer's disease: total tau, phospho-tau and Abeta42. World J Biol Psychiatry. 4, 147-155.

Andreasen, N., Vanmechelen, E., Van de Voorde, A., Davidsson, P., Hesse, C., Tarvonen, S., Raiha, I., Sourander, L., Winblad, B. and Blennow, K., 1998. Cerebrospinal fluid tau protein as a biochemical marker for Alzheimer's disease: a community based follow up study. J Neurol Neurosurg Psychiatry. 64, 298-305.

Baker, H., Patel, V., Molinolo, A. A., Shillitoe, E. J., Ensley, J. F., Yoo, G. H., Meneses-Garcia, A., Myers, J. N., El-Naggar, A. K., Gutkind, J. S. and Hancock, W. S., 2005. Proteome-wide analysis of head and neck squamous cell carcinomas using laser-capture microdissection and tandem mass spectrometry. Oral Oncol. 41, 183-199.

Belizaire, R., Komanduri, C., Wooten, K., Chen, M., Thaller, C. and Janz, R., 2004. Characterization of synaptogyrin 3 as a new synaptic vesicle protein. J Comp Neurol. 470, 266-281.

Braak, H. and Braak, E., 1991. Neuropathological stageing of Alzheimer-related changes. Acta Neuropathol (Berl). 82, 239-259.

de Vrij, F. M., Fischer, D. F., van Leeuwen, F. W. and Hol, E. M., 2004. Protein quality control in Alzheimer's disease by the ubiquitin proteasome system. Prog Neurobiol. 74, 249-270.

Dickson, T. C., Chuckowree, J. A., Chuah, M. I., West, A. K. and Vickers, J. C., 2005. alpha-Internexin immunoreactivity reflects variable neuronal vulnerability in Alzheimer's disease and supports the role of the beta-amyloid plaques in inducing neuronal injury. Neurobiol Dis. 18, 286-295.

Dou, F., Yuan, L. D. and Zhu, J. J., 2005. Heat shock protein 90 indirectly regulates ERK activity by affecting Raf protein metabolism. Acta Biochim Biophys Sin (Shanghai). 37, 501-505.

Drewes, G., Mandelkow, E. M., Baumann, K., Goris, J., Merlevede, W. and Mandelkow, E., 1993. Dephosphorylation of tau protein and Alzheimer paired helical filaments by calcineurin and phosphatase-2A. FEBS Lett. 336, 425-432.

Ferrer, I., Marti, E., Tortosa, A. and Blasi, J., 1998. Dystrophic neurites of senile plaques are defective in proteins involved in exocytosis and neurotransmission. J Neuropathol Exp Neurol. 57, 218-225.

Finehout, E. J., Franck, Z. and Lee, K. H., 2005. Complement protein isoforms in CSF as possible biomarkers for neurodegenerative disease. Dis Markers. 21, 93-101.

Forloni, G., Terreni, L., Bertani, I., Fogliarino, S., Invernizzi, R., Assini, A., Ribizzi, G., Negro, A., Calabrese, E., Volonte, M. A., Mariani, C., Franceschi, M., Tabaton, M. and Bertoli, A., 2002. Protein misfolding in Alzheimer's and Parkinson's disease: genetics and molecular mechanisms. Neurobiol Aging. 23, 957-976.

Gagne, J. P., Gagne, P., Hunter, J. M., Bonicalzi, M. E., Lemay, J. F., Kelly, I., Le Page, C., Provencher, D., Mes-Masson, A. M., Droit, A., Bourgais, D. and Poirier, G. G., 2005. Proteome profiling of human epithelial ovarian cancer cell line TOV-112D. Mol Cell Biochem. 275, 25-55.

Goedert, M., Cohen, E. S., Jakes, R. and Cohen, P., 1992. p42 MAP kinase phosphorylation sites in microtubule-associated protein tau are dephosphorylated by protein phosphatase 2A1. Implications for Alzheimer's disease [corrected]. FEBS Lett. 312, 95-99.

Goldstein, L. S., 2003. Do disorders of movement cause movement disorders and dementia? Neuron. 40, 415-425.

Gong, C. X., Grundke-Iqbal, I. and Iqbal, K., 1994. Dephosphorylation of Alzheimer's disease abnormally phosphorylated tau by protein phosphatase-2A. Neuroscience. 61, 765-772.

Hardy, J., 2006. Has the amyloid cascade hypothesis for Alzheimer's disease been proved? Curr Alzheimer Res. 3, 71-73.

Hashii, N., Kawasaki, N., Itoh, S., Hyuga, M., Kawanishi, T. and Hayakawa, T., 2005. Glycomic/glycoproteomic analysis by liquid chromatography/mass spectrometry: analysis of glycan structural alteration in cells. Proteomics. 5, 4665-4672.

He, W., Lu, Y., Qahwash, I., Hu, X. Y., Chang, A. and Yan, R., 2004. Reticulon family members modulate BACE1 activity and amyloid-beta peptide generation. Nat Med. 10, 959-965.

Hoyer, S., 1991. Abnormalities of glucose metabolism in Alzheimer's disease. Ann N Y Acad Sci. 640, 53-58.

Hoyer, S., 1996. Oxidative metabolism deficiencies in brains of patients with Alzheimer's disease. Acta Neurol Scand Suppl. 165, 18-24.

Hyman, B. T., Elvhage, T. E. and Reiter, J., 1994. Extracellular signal regulated kinases. Localization of protein and mRNA in the human hippocampal formation in Alzheimer's disease. Am J Pathol. 144, 565-572.

Ida, N., Hartmann, T., Pantel, J., Schroder, J., Zerfass, R., Forstl, H., Sandbrink, R., Masters, C. L. and Beyreuther, K., 1996. Analysis of heterogeneous A4 peptides in human cerebrospinal fluid and blood by a newly developed sensitive Western blot assay. J Biol Chem. 271, 22908-22914.

Ishigami, A., Ohsawa, T., Hiratsuka, M., Taguchi, H., Kobayashi, S., Saito, Y., Murayama, S., Asaga, H., Toda, T., Kimura, N. and Maruyama, N., 2005. Abnormal accumulation of citrullinated proteins catalyzed by peptidylarginine deiminase in hippocampal extracts from patients with Alzheimer's disease. J Neurosci Res. 80, 120-128.

Janz, R., Sudhof, T. C., Hammer, R. E., Unni, V., Siegelbaum, S. A. and Bolshakov, V. Y., 1999. Essential roles in synaptic plasticity for synaptogyrin I and synaptophysin I. Neuron. 24, 687-700.

Kakimura, J., Kitamura, Y., Takata, K., Umeki, M., Suzuki, S., Shibagaki, K., Taniguchi, T., Nomura, Y., Gebicke-Haerter, P. J., Smith, M. A., Perry, G. and Shimohama, S., 2002. Microglial activation and amyloid-beta clearance induced by exogenous heat-shock proteins. Faseb J. 16, 601-603.

Kalback, W., Esh, C., Castano, E. M., Rahman, A., Kokjohn, T., Luehrs, D. C., Sue, L., Cisneros, R., Gerber, F., Richardson, C., Bohrmann, B., Walker, D. G., Beach, T. G. and Roher, A. E., 2004. Atherosclerosis, vascular amyloidosis and brain hypoperfusion in the pathogenesis of sporadic Alzheimer's disease. Neurol Res. 26, 525-539.

Katayama, T., Imaizumi, K., Manabe, T., Hitomi, J., Kudo, T. and Tohyama, M., 2004. Induction of neuronal death by ER stress in Alzheimer's disease. J Chem Neuroanat. 28, 67-78.

Kedra, D., Pan, H. Q., Seroussi, E., Fransson, I., Guilbaud, C., Collins, J. E., Dunham, I., Blennow, E., Roe, B. A., Piehl, F. and Dumanski, J. P., 1998. Characterization of the human synaptogyrin gene family. Hum Genet. 103, 131-141.

Krapfenbauer, K., Engidawork, E., Cairns, N., Fountoulakis, M. and Lubec, G., 2003. Aberrant expression of peroxiredoxin subtypes in neurodegenerative disorders. Brain Res. 967, 152-160.

LaFerla, F. M., 2002. Calcium dyshomeostasis and intracellular signalling in Alzheimer's disease. Nat Rev Neurosci. 3, 862-872.

Lassmann, H., Fischer, P. and Jellinger, K., 1993. Synaptic pathology of Alzheimer's disease. Ann N Y Acad Sci. 695, 59-64.

Ledesma, M. D., Correas, I., Avila, J. and Diaz-Nido, J., 1992. Implication of brain cdc2 and MAP2 kinases in the phosphorylation of tau protein in Alzheimer's disease. FEBS Lett. 308, 218-224.

Lee, V. M., Kenyon, T. K. and Trojanowski, J. Q., 2005. Transgenic animal models of tauopathies. Biochim Biophys Acta. 1739, 251-259.

Leifer, D. and Kowall, N. W., 1992. Thy-1 in hippocampus: normal anatomy and neuritic growth in Alzheimer's disease. J Neuropathol Exp Neurol. 51, 133-141.

Liao, L., Cheng, D., Wang, J., Duong, D. M., Losik, T. G., Gearing, M., Rees, H. D., Lah, J. J., Levey, A. I. and Peng, J., 2004. Proteomic characterization of postmortem amyloid plaques isolated by laser capture microdissection. J Biol Chem. 279, 37061-37068.

Lubec, G., Nonaka, M., Krapfenbauer, K., Gratzer, M., Cairns, N. and Fountoulakis, M., 1999. Expression of the dihydropyrimidinase related protein 2 (DRP-2) in Down syndrome and Alzheimer's disease brain is downregulated at the mRNA and dysregulated at the protein level. J Neural Transm Suppl. 57, 161-177.

Lynch, C. and Mobley, W., 2000. Comprehensive theory of Alzheimer's disease. The effects of cholesterol on membrane receptor trafficking. Ann N Y Acad Sci. 924, 104-111.

Masliah, E., Mallory, M., Hansen, L., DeTeresa, R., Alford, M. and Terry, R., 1994. Synaptic and neuritic alterations during the progression of Alzheimer's disease. Neurosci Lett. 174, 67-72.

Meier-Ruge, W., Iwangoff, P. and Reichlmeier, K., 1984. Neurochemical enzyme changes in Alzheimer's and Pick's disease. Arch Gerontol Geriatr. 3, 161-165.

Meier-Ruge, W. A. and Bertoni-Freddari, C., 1997. Pathogenesis of decreased glucose turnover and oxidative phosphorylation in ischemic and trauma-induced dementia of the Alzheimer type. Ann N Y Acad Sci. 826, 229-241.

Minger, S. L., Honer, W. G., Esiri, M. M., McDonald, B., Keene, J., Nicoll, J. A., Carter, J., Hope, T. and Francis, P. T., 2001. Synaptic pathology in prefrontal cortex is present only with severe dementia in Alzheimer disease. J Neuropathol Exp Neurol. 60, 929-936.

Mitchelmore, C., Buchmann-Moller, S., Rask, L., West, M. J., Troncoso, J. C. and Jensen, N. A., 2004. NDRG2: a novel Alzheimer's disease associated protein. Neurobiol Dis. 16, 48-58.

Multhaup, G., Ruppert, T., Schlicksupp, A., Hesse, L., Beher, D., Masters, C. L. and Beyreuther, K., 1997. Reactive oxygen species and Alzheimer's disease. Biochem Pharmacol. 54, 533-539.

Nagy, J. I., Li, W., Hertzberg, E. L. and Marotta, C. A., 1996. Elevated connexin43 immunoreactivity at sites of amyloid plaques in Alzheimer's disease. Brain Res. 717, 173-178.

Parnetti, L., Lanari, A., Amici, S., Gallai, V., Vanmechelen, E. and Hulstaert, F., 2001. CSF phosphorylated tau is a possible marker for discriminating Alzheimer's disease from dementia with Lewy bodies. Phospho-Tau International Study Group. Neurol Sci. 22, 77-78.

Pei, J. J., Braak, H., An, W. L., Winblad, B., Cowburn, R. F., Iqbal, K. and Grundke-Iqbal, I., 2002. Up-regulation of mitogen-activated protein kinases ERK1/2 and MEK1/2 is associated with the progression of neurofibrillary degeneration in Alzheimer's disease. Brain Res Mol Brain Res. 109, 45-55.

Pepys, M. B., Rademacher, T. W., Amatayakul-Chantler, S., Williams, P., Noble, G. E., Hutchinson, W. L., Hawkins, P. N., Nelson, S. R., Gallimore, J. R., Herbert, J. and et al., 1994. Human serum amyloid P component is an invariant constituent of amyloid deposits and has a uniquely homogeneous glycostructure. Proc Natl Acad Sci U S A. 91, 5602-5606.

Perry, G., Friedman, R., Shaw, G. and Chau, V., 1987. Ubiquitin is detected in neurofibrillary tangles and senile plaque neurites of Alzheimer disease brains. Proc Natl Acad Sci U S A. 84, 3033-3036.

Porchet, R., Probst, A., Bouras, C., Draberova, E., Draber, P. and Riederer, B. M., 2003. Analysis of glial acidic fibrillary protein in the human entorhinal cortex during aging and in Alzheimer's disease. Proteomics. 3, 1476-1485.

Prinjha, R., Moore, S. E., Vinson, M., Blake, S., Morrow, R., Christie, G., Michalovich, D., Simmons, D. L. and Walsh, F. S., 2000. Inhibitor of neurite outgrowth in humans. Nature. 403, 383-384.

Qiao, H., Koya, R. C., Nakagawa, K., Tanaka, H., Fujita, H., Takimoto, M. and Kuzumaki, N., 2005. Inhibition of Alzheimer's amyloid-beta peptide-induced reduction of mitochondrial membrane potential and neurotoxicity by gelsolin. Neurobiol Aging. 26, 849-855.

Renkawek, K., Bosman, G. J. and Gaestel, M., 1993. Increased expression of heat-shock protein 27 kDa in Alzheimer disease: a preliminary study. Neuroreport. 5, 14-16.

Rezaie, P., Pontikis, C. C., Hudson, L., Cairns, N. J. and Lantos, P. L., 2005. Expression of cellular prion protein in the frontal and occipital lobe in Alzheimer's disease, diffuse Lewy body disease, and in normal brain: an immunohistochemical study. J Histochem Cytochem. 53, 929-940.

Rufenacht, P., Guntert, A., Bohrmann, B., Ducret, A. and Dobeli, H., 2005. Quantification of the A beta peptide in Alzheimer's plaques by laser dissection microscopy combined with mass spectrometry. J Mass Spectrom. 40, 193-201.

Schonberger, S. J., Edgar, P. F., Kydd, R., Faull, R. L. and Cooper, G. J., 2001. Proteomic analysis of the brain in Alzheimer's disease: molecular phenotype of a complex disease process. Proteomics. 1, 1519-1528.

Schubert, D., 2005. Glucose metabolism and Alzheimer's disease. Ageing Res Rev. 4, 240-257.

Selkoe, D. J., 2001. Alzheimer's disease: genes, proteins, and therapy. Physiol Rev. 81, 741-766.

Selkoe, D. J., Yamazaki, T., Citron, M., Podlisny, M. B., Koo, E. H., Teplow, D. B. and Haass, C., 1996. The role of APP processing and trafficking pathways in the formation of amyloid beta-protein. Ann N Y Acad Sci. 777, 57-64.

Selle, H., Lamerz, J., Buerger, K., Dessauer, A., Hager, K., Hampel, H., Karl, J., Kellmann, M., Lannfelt, L., Louhija, J., Riepe, M., Rollinger, W., Tumani, H., Schrader, M. and Zucht, H. D., 2005. Identification of novel biomarker candidates by differential peptidomics analysis of cerebrospinal fluid in Alzheimer's disease. Comb Chem High Throughput Screen. 8, 801-806.

Smith, S. K., Anderson, H. A., Yu, G., Robertson, A. G., Allen, S. J., Tyler, S. J., Naylor, R. L., Mason, G., Wilcock, G. W., Roche, P. A., Fraser, P. E. and Dawbarn, D., 2000. Identification of syntaxin 1A as a novel binding protein for presenilin-1. Brain Res Mol Brain Res. 78, 100-107.

Song, S. and Jung, Y. K., 2004. Alzheimer's disease meets the ubiquitin-proteasome system. Trends Mol Med. 10, 565-570.

Steiner, P., Kulangara, K., Sarria, J. C., Glauser, L., Regazzi, R. and Hirling, H., 2004. Reticulon 1-C/neuroendocrine-specific protein-C interacts with SNARE proteins. J Neurochem. 89, 569-580.

Stenius, K., Janz, R., Sudhof, T. C. and Jahn, R., 1995. Structure of synaptogyrin (p29) defines novel synaptic vesicle protein. J Cell Biol. 131, 1801-1809.

Strittmatter, S. M., 2002. Modulation of axonal regeneration in neurodegenerative disease: focus on Nogo. J Mol Neurosci. 19, 117-121.

Sugita, S., Janz, R. and Sudhof, T. C., 1999. Synaptogyrins regulate Ca2+-dependent exocytosis in PC12 cells. J Biol Chem. 274, 18893-18901.

Tsuji, T., Shiozaki, A., Kohno, R., Yoshizato, K. and Shimohama, S., 2002. Proteomic profiling and neurodegeneration in Alzheimer's disease. Neurochem Res. 27, 1245-1253.

Verma, R., Chauhan, C., Saleem, Q., Gandhi, C., Jain, S. and Brahmachari, S. K., 2004. A nonsense mutation in the synaptogyrin 1 gene in a family with schizophrenia. Biol Psychiatry. 55, 196-199.

Watson, D., Castano, E., Kokjohn, T. A., Kuo, Y. M., Lyubchenko, Y., Pinsky, D., Connolly, E. S., Jr., Esh, C., Luehrs, D. C., Stine, W. B., Rowse, L. M., Emmerling, M. R. and Roher, A. E., 2005. Physicochemical characteristics of soluble oligomeric Abeta and their pathologic role in Alzheimer's disease. Neurol Res. 27, 869-881.

Wessel, D. and Flugge, U. I., 1984. A method for the quantitative recovery of protein in dilute solution in the presence of detergents and lipids. Anal Biochem. 138, 141-143.

Wiltfang, J., Smirnov, A., Schnierstein, B., Kelemen, G., Matthies, U., Klafki, H. W., Staufenbiel, M., Huther, G., Ruther, E. and Kornhuber, J., 1997. Improved electrophoretic separation and immunoblotting of beta-amyloid (A beta) peptides 1-40, 1-42, and 1-43. Electrophoresis. 18, 527-532.

Wuhrer, M., Deelder, A. M. and Hokke, C. H., 2005. Protein glycosylation analysis by liquid chromatography-mass spectrometry. J Chromatogr B Analyt Technol Biomed Life Sci. 825, 124-133.

Yao, P. J., Morsch, R., Callahan, L. M. and Coleman, P. D., 1999. Changes in synaptic expression of clathrin assembly protein AP180 in Alzheimer's disease analysed by immunohistochemistry. Neuroscience. 94, 389-394.

Yew, D. T., Li, W. P., Webb, S. E., Lai, H. W. and Zhang, L., 1999. Neurotransmitters, peptides, and neural cell adhesion molecules in the cortices of normal elderly humans and Alzheimer patients: a comparison. Exp Gerontol. 34, 117-133.

Yoo, B. C., Kim, S. H., Cairns, N., Fountoulakis, M. and Lubec, G., 2001. Deranged expression of molecular chaperones in brains of patients with Alzheimer's disease. Biochem Biophys Res Commun. 280, 249-258.

Zhan, S. S., Beyreuther, K. and Schmitt, H. P., 1993. Quantitative assessment of the synaptophysin immuno-reactivity of the cortical neuropil in various neurodegenerative disorders with dementia. Dementia. 4, 66-74.

Zhao, H. and Nonet, M. L., 2001. A conserved mechanism of synaptogyrin localization. Mol Biol Cell. 12, 2275-2289.

ACKNOWLEDGEMENTS

We thank Fabienne Goepfert for assistance with Western blot analysis, Dr. Christian Czech and Dr. Fiona Grüninger for providing antibodies and copious discussions. Furthermore, we thank Claudia Richardson for general assistance and support. Finally, we thank Professor Theodor Güntert and Dr. Grayson Richards for critical review of the manuscript.

Table 1: Overview of proteins deregulated in AD.

Protein	Ratio AD / control tissue	Reference	Reported (De-)regulation
cell adhesion / neurite outgrowth			
Collagen α3 (VI) chain	only AD	(Liao et al., 2004)	n.d.[1]
Gap junction alpha-1 protein (Connexin-43)	1.22	Nagy et al. 1996	↑
Neural cell adhesion molecule 1 (180kD)	0.86	Yew et al. 1999	↔
Thy-1 membrane glycoprotein	0.65	Leifer et al. 1992	↓
Myelin-associated glycoprotein (MAG)	0.59	-	
Claudin-11 (Oligodendrocyte specific protein)	0.45	-	
Contactin associated protein 1 (Neurexin IV)	0.41	-	
Myelin oligodendrocyte glycoprotein (MOG)	0.38	-	
Dihydropyrimidinase related protein-5	0.29	(Lubec et al., 1999)	n.d.[2]
Contactin 1	0.7	-	
Contactin 2	0.28	-	
chaperones			
Hsp 27	1.59	Renkawek et al., 1993	↑
Hsp 75	1.48	-	
Hsp 90	1.43	Anthony et al., 2003	↑
Hsp 70.1	1.1	Yoo et al., 2001	↔
78 kDa glucose-regulated protein (GRP 78)	1	Yoo et al., 2001	↔
Hsp 60	0.68	Yoo et al., 2001	↓
T-complex protein 1	0.46	Schuller et al., 2000	↓
cytoskeleton			
Microtubule-associated protein tau	2.36	Mandelkow et al., 1994	↑
Plectin 1	1.3	-	
Neurofilament triplet H protein	1.03	Vickers et al., 1994	n.d.
Spectrin beta chain	0.97	Sihag et al., 1996	↑
Ankyrin 2	0.69	-	
Alpha-internexin	0.64	Dickson et al., 2005	n.d.
Gelsolin	0.6	Qiao et al., 2005	n.d.
Alpha adducin	0.59	-	
Microtubule-associated protein 1B	0.51	Hasegawa et al., 1990	n.d.
Microtubule-associated protein RP/EB family member 3	0.19	-	
inflammation			
GFAP	4.45	Styren et al., 1998	↑
Vimentin	1.44	Porchet et al., 2003	↑
Complement C3	only AD	McGeer et al., 1989	↑
Complement C4	only AD	McGeer et al., 1989	↑

[1] Liao and collegues detected elevated levels of collagen α1 (I) chain in amyloid plaques

[2] Lubec and collegues detected DRP-2 to be disregulated in AD

Table 1 (continued)

enzymes / regulators / channels			
Mitogen-activated protein kinase 3 (ERK 1)	only AD	Pei et al., 2002	↑
Protein-arginine deiminase type II	1.45	Ishigami et al., 2005	↑
Peroxiredoxin 1	1.26	Krapfenbauer et al. 2003	↔
Mitogen-activated protein kinase 1 (ERK 2)	0.86	Pei et al., 2002	↑
Peroxiredoxin 3	0.74	Krapfenbauer et al. 2003	↑
Isocitrate dehydrogenase	0.7	Hoyer, 1991	↓
Succinyl-CoA ligase	0.65	Hoyer, 1991	↓
Malate dehydrogenase, cytoplasmic	0.55	Hoyer, 1991	↓
Malate dehydrogenase, mitochondrial	0.51	Hoyer, 1991	↓
Succinate dehydrogenase	0.51	Hoyer, 1991	↓
Phosphofructokinase 1 (PFK-B)	0.49	Hoyer, 1991	↓
Peroxiredoxin 5	0.61	-	
Microsomal glutathione S-transferase 3	0.47	-	
Serine/threonine protein phosphatase 2A	0.45	Gong et al., 1995	n.d.
Superoxide dismutase [Mn]	decreased	Krapfenbauer et al., 2003	↔
membrane trafficking / synaptic proteins			
Synaptogyrin-1	1.73	-	
Synaptogyrin-3	increased	-	
Clathrin heavy chain 1	0.91	Nakamura et al., 1994	↔
Dynein	0.76	Liao et al., 2005	↑
Reticulon-3	0.74	Yan et al., 2004	n.d.
Synaptotagmin-1	0.62	Yoo et al., 2001	↓
Synaptotagmin-12	decreased	Yoo et al., 2001	↓
Clathrin coat assembly protein AP180	0.58	Yao et al., 1999	↓
Reticulon-4 (Nogo protein)	0.54	Strittmatter et al., 2002	n.d.
Reticulon-1	0.53	Yan et al., 2004	n.d.
Syntaxin-1A (HPC-1)	0.32	Minger et al., 2001	↓
Presynaptic density protein 95 (PSD-95)	0.3	Gylys et al., 2004	↓
proteolysis			
Ubiquitin	1.92	Iqbal et al. 1997	↑
others			
Amyloid Beta	only AD	Glenner & Wong, 1984	↑
Apolipoprotein E	2.33	Strittmatter et al., 1993	↑
Alpha-1-antichymotrypsin (ACT)	only AD	Abraham et al., 1988	↑
Alpha-synuclein	0.89	Iwai et al., 1996	n.d.
Matrin-3	0.49	-	
Major prion protein	0.43	Lantos et al., 2005	↓
NDRG2 protein	0.4	Mitchelmore et al., 2004	↑
Transgelin-3 (Neuronal protein NP25)	0.4	-	
Programmed cell death protein 8	0.34	-	

The ratio is indicative for the protein abundance in AD compared to control tissue. Proteins only present in AD are indicated. 'Increased' refers to protein level for proteins detected in only one of the control samples, 'decreased' indicates the protein level for proteins detected in only one of the AD cases. Arrows indicate change in protein levels found in AD in the respective references. n.d., not determined

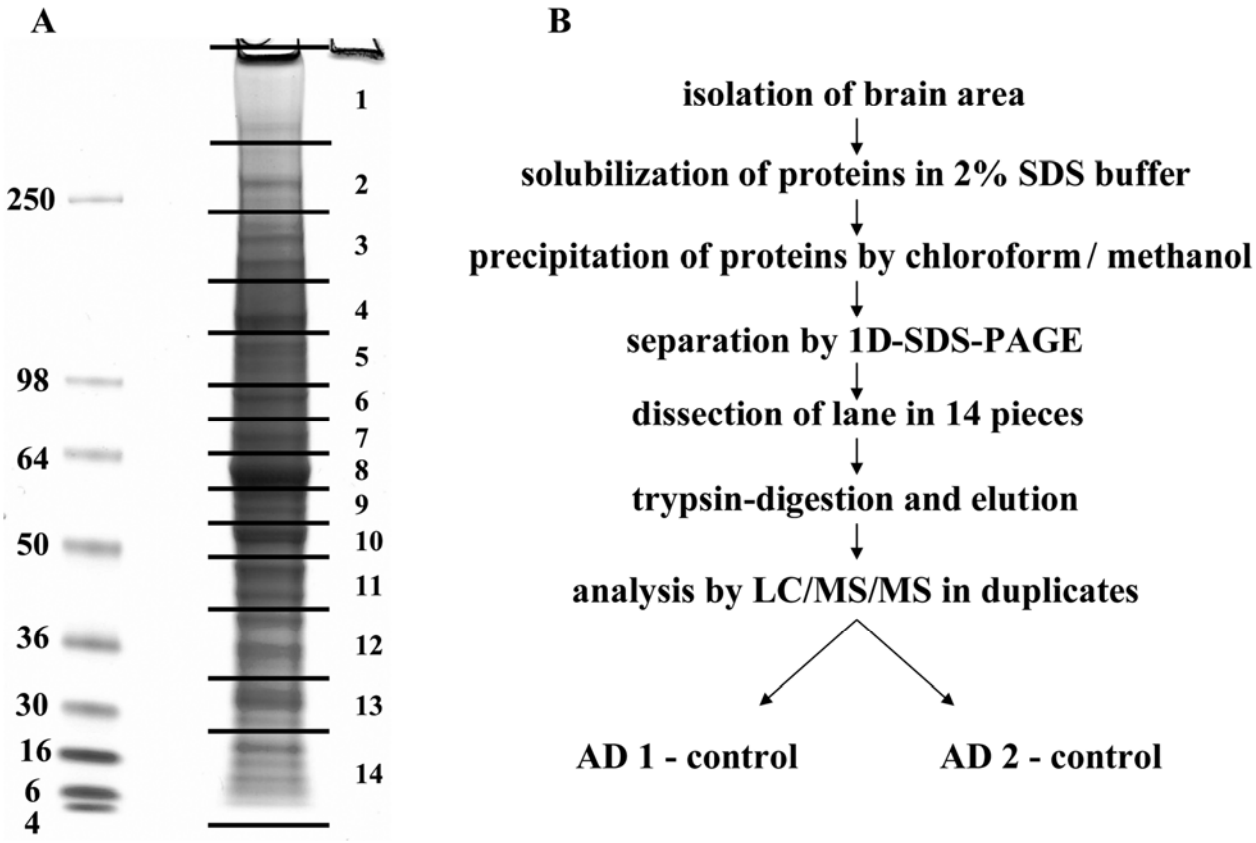

Fig. 1. Sample preparation for LC/MS/MS analysis of brain tissue.

(A) Solubilized protein sample of an AD case was run on an SDS gel followed by Coomassie Blue staining. The sample lane was cut into 14 pieces that were subjected to trypsin digestion and LC/MS/MS analysis. The left lane shows the molecular weight marker, the gel excision pattern is shown on the right. (B) Overview of the sample preparation procedure.

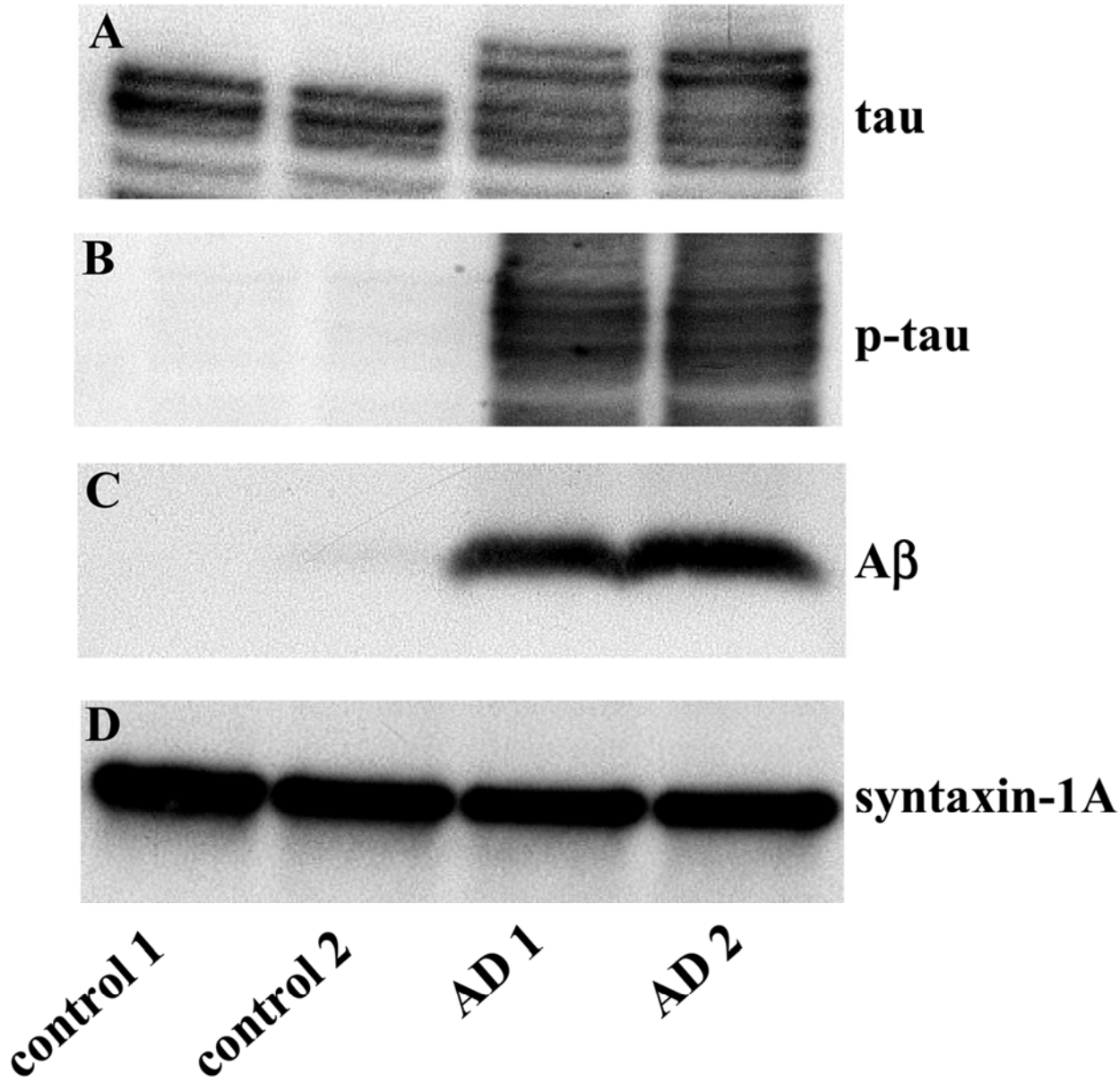

Fig. 2. Western blot analysis of brain homogenates.

Grey matter tissue from occipital association cortices was analyzed by Western blot analysis with tau (A), phospho-tau (p-tau) (B) and Aβ (C) antibodies. A substantial increase of the respective proteins in AD could be demonstrated. Densitometric analysis of syntaxin-1A revealed a decrease in both AD cases of ~ 15%.

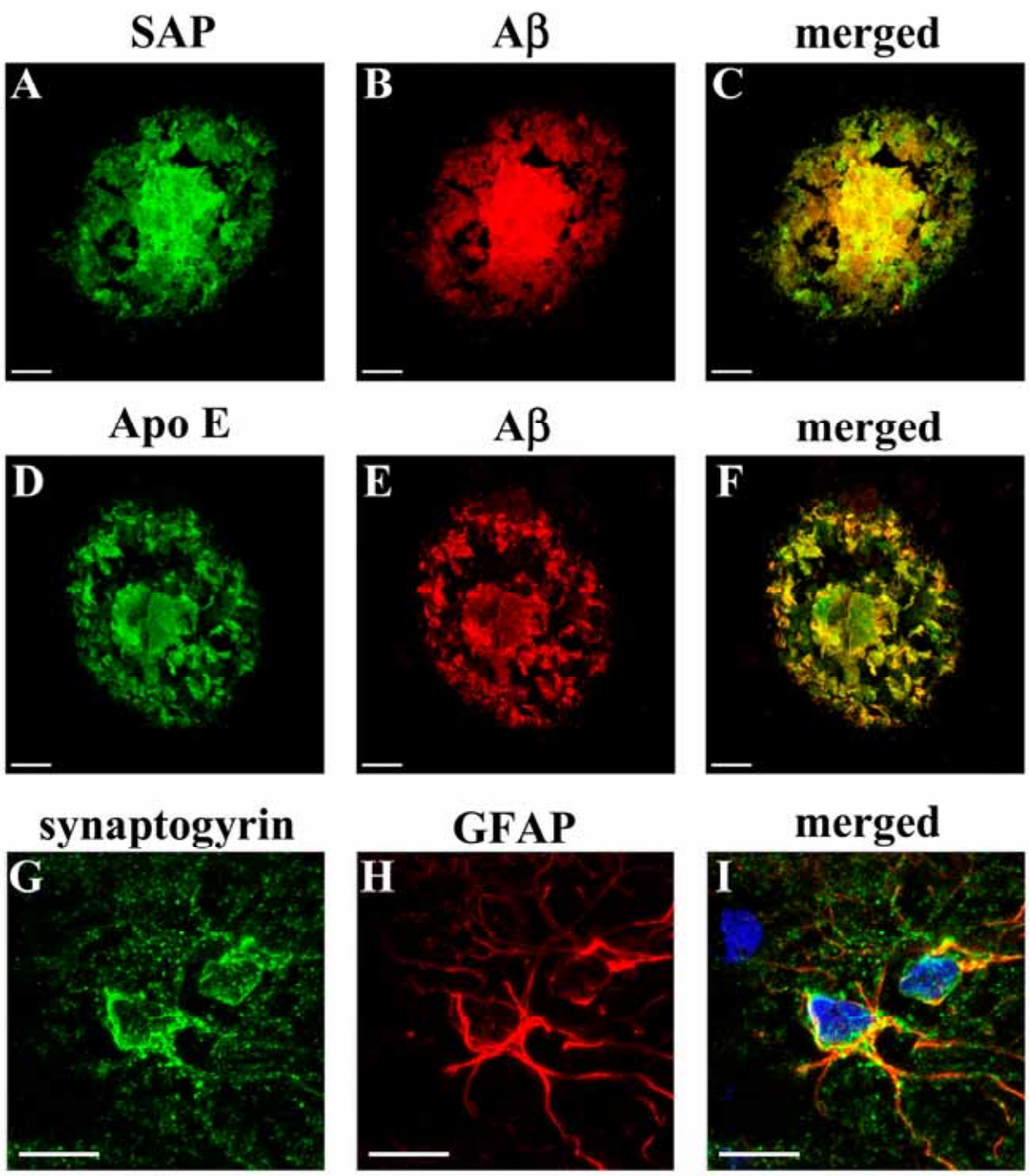

Fig. 3. Confocal microscopy of human AD grey matter sections of occipital association cortex.
Indirect immunofluorescence images were acquired by sequential scanning. The co-localization of Aβ present in cored senile plaques with SAP (A – C) and with apolipoprotein E (D – F) is clearly visible. Co-localization of synaptogyrin-1 with GFAP (G – I) was detected in the cytoplasm of astrocytes. The cell nucleus of astrocytes is revealed by nuclear counterstaining with DAPI. Scale bar in A – I: 10 μm

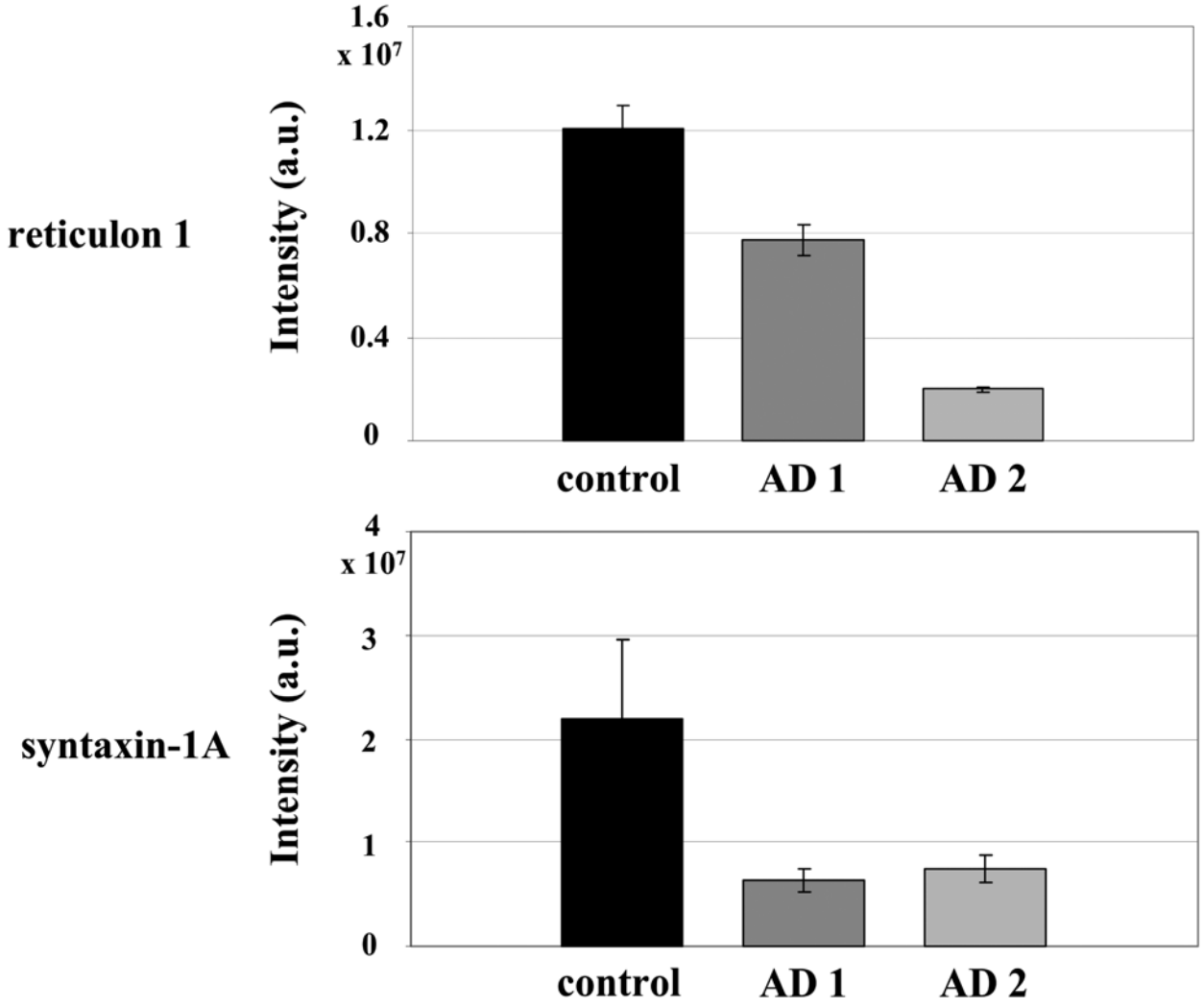

Fig. 4. Quantification of immunofluorescence signal by confocal laser scanning microscopy shown for reticulon-1 and syntaxin-1A.

Grey matter sections from AD occipital association cortex and control tissue were stained with reticulon-1 and syntaxin-1A antibodies. Fluorescence intensity is decreased for reticulon-1 and syntaxin-1A in AD brain compared to control tissue, consistent with the findings from the LC/MS/MS analysis.

CURRICULUM VITAE

I was born on the February 26, 1979 in San Francisco, USA as the son of Theodor and Regina Güntert-Hüssy. At the age of one year, I was transferred to Switzerland; here, I was brought up in Böckten, Baselland together with my younger brother Stefan, and went to primary school from 1986 – 1990. Thereafter, I visited the secondary school in Sissach (1990 – 1994, Progymnasiale Abteilung) and subsequently switched to the high school in Liestal (1994 – 1997). I graduated with the Matura Type E (economics) with a rating of 5.0. From 1998 – 2002, I studied at the Biocenter, University Basel and finished with a diploma in Biology II, with specialization in Neurobiology and a rating of 5.4. My Diploma Thesis was done on 'Laser Dissection Microscopy in the Comparison of Plaques in Human and Transgenic Mice' at F. Hoffmann-La Roche Ltd., Basel, where I conducted afterwards (2003 – 2006) also a Ph.D. thesis entitled "Characterization of Amyloid-β and Other Proteins Related to Alzheimer's Disease, their Role in Neurodegeneration and Biomarker Discovery" (supervised by Dr. B. Bohrmann).

During my studies (1998 – 2006) I attended lectures given by:
Prof. M. Rüegg, Prof. Y.-A. Barde, Prof. W. Gehring, Prof. U. Séquin, Prof., S. Arber, Prof. J. Engel, Prof. A. Engel, Prof. J. Seelig, Prof. M. Hall, Prof. H. Sigel, Prof. P. Philippsen, Prof. T. Kiefhaber, Prof. G. Cornelis, Prof. U.-A. Meyer, Prof. H.-P. Hauri, Prof. M. Affolter, Dr. M. Dürrenberger, Prof. U. Aebi, Prof. C. Dehio, Prof. S. Grzesiek, Prof. U. Jenal, Prof. P. Jenö, Prof. W. Keller, Prof. H. Reichert, Prof. A. Lüthi, Prof. J. Pieters, Prof. T. Schirmer, Prof. M. Spiess, Prof. T. Kaden, Prof. C. Schönenberger, Prof. A. Wiemken, Prof. H. Kraft, Prof. G.-R. Plattner, Prof. I. Sick, Prof. M. Jungen, Prof. K. Ballmer-Hofer, Prof. N. Schaeren-Wiemers, Dr. M. Page, Prof. M. Affolter, Prof. D. Monard